DIMETHYLSULFONIOPROPIONATE CATABOLISM AND PHYLOGENETICS IN THE ROSEOBACTER GROUP

by

TAO WANG

(Under the Direction of William B. Whitman)

ABSTRACT

Dimethylsulfoniopropionate (DMSP) is an abundant organosulfur compound in marine surface water that is processed by marine bacteria by cleavage and demethylation pathways. The demethylation pathway releases methanethiol, while the cleavage pathway produces acrylate and the climatically-active gas dimethylsulfide (DMS). When methanethiol is oxidized by the oxidase MtoX, it produces hydrogen peroxide (H_2O_2), leading to oxidative stress. Previous studies reported that DMSP and its cleavage products formed an antioxidant system in algae, corals, and some higher plants, all of which process DMSP by the cleavage pathway. To study how oxidative stress affects DMSP metabolism in bacteria, *Ruegeria pomeroyi* and its catalase deletion mutant were treated with H_2O_2 in a chemostat growing on glucose with or without DMSP. The presence of DMSP protected the mutant against H_2O_2. RNA-seq analysis indicated that under oxidative stress, the demethylation pathway was downregulated, but the cleavage pathway was upregulated. These results confirmed the antioxidant role of DMSP in bacteria and revealed oxidative stress is a factor regulating DMSP metabolism in *R. pomeroyi*.

DmdC is the 3-methylmercaptopropionyl-CoA (MMPA-CoA) dehydrogenase catalyzing the third reaction of the demethylation pathway. DmdC1 in *R. pomeroyi* was recombinantly

expressed and characterized for kinetic properties. Among the short chain acyl-CoAs tested, MMPA-CoA was the best substrate. DmdC1 was not affected by potential effectors at physiological concentrations, including DMSP, MMPA, ATP and ADP. These findings suggest that DmdC1 has only minimal adaptations for DMSP metabolism, supporting the hypothesis that it evolved relatively recently from a short chain acyl-CoA dehydrogenase involved in fatty acid oxidation.

The roseobacter group is a paraphyletic group within the family *Rhodobacteraceae* in the *Alphaproteobacteria*. Members in this group are abundant in marine environments and highly diverse physiologically and genetically. Recent research indicated that 16S rRNA gene sequence similarity is a poor marker for the phylogeny within this group. By whole-genome sequence-based analysis, most species in the genus *Loktanella* were moved into several novel genera. After reanalyzing the phylogeny, *Loktanella ponticola*, whose genome became available recently, and a newly isolated species *Lotanella acticola* were moved into the genus *Yoonia*.

INDEX WORDS: Dimethylsulfoniopropionate, DMSP, Dimethyl sulfide, DMS, Methanethiol, MeSH, *Ruegeria pomeroyi*, Oxidative stress, Hydrogen peroxide, Acyl-CoA dehydrogenases, 3-Methylmercaptopropionyl-CoA dehydrogenase, DmdC, Roseobacter group, *Alphaproteobacteria*, *Loktanella*, *Yoonia*

DIMETHYLSULFONIOPROPIONATE CATABOLISM AND PHYLOGENETICS IN THE ROSEOBACTER GROUP

by

TAO WANG

B.S., Wuhan University, P. R. CHINA, 2015

A Dissertation Submitted to the Graduate Faculty of The University of Georgia in Partial Fulfillment of the Requirements for the Degree

DOCTOR OF PHILOSOPHY

ATHENS, GEORGIA

2022

DIMETHYLSULFONIOPROPIONATE CATABOLISM AND PHYLOGENETICS IN THE ROSEOBACTER GROUP

by

TAO WANG

Major Professor:	William B. Whitman
Committee:	Mary Ann Moran
	Jorge C. Escalante-Semerena
	Timothy Hoover

Electronic Version Approved:

Ron Walcott
Dean of the Graduate School
The University of Georgia
May 2022

ACKNOWLEDGEMENTS

First, I would like to thank all my family and friends I have in the past years. No matter when I felt lonely or exhausted, I can always find someone. For my friends, I would like to thank Xiaomu Zhang and Bowen Meng especially. I and Xiaomu kept encouraging and supporting each other from undergraduate school, and we share a lot of experience and suggestions for our research. For Bowen, we knew each other during teaching and became good friend, he companied me a lot of time in Athens and helped me in research, language, and life.

I would like to thank my advisor, Dr. William B. Whitman, for helping me become a better scientist. His talent, passion, patience, and dedication to research inspired me when I performed my own studies. I still remembered many words he told me, and these will encourage me to use the knowledge I have to resolve the coming questions in my career. I would like to thank my doctoral committee, Dr. Mary Ann Moran, Dr. Jorge C. Escalante-Semerena, and Dr. Timothy Hoover for their constructive suggestions all these years. Besides, I also would like to thank Dr. Diana Downs, Dr. Xiaorong Lin, Dr. Robert J. Maier, and Dr. Vincent J. Starai for letting me use their chemicals and equipment, which made my experiment much easier.

I would like to thank the past members of the lab working on DMSP metabolism, which include Hannah A. Bullock, Joe S. Wirth, Suet Yee Chong, Hao Shi, and Qiuyuan Huang. From them, I learned the techniques and skills needed to complete my experiments and research. We also had good corporations for some projects. I would like to thank other past and present members of the lab including Feng Long, Zhe Lyu, Taiwo S. Akinyemi, Nana Shao, Yuehong Wu, Can Chen, José Orench, Amala Malladi, Courtney Grant, and Fizzah Khan.

I would like to thank the people helped me in learning RNA-seq data analysis, especially Christa Smith, who also taught me RNA extraction and quality control. In addition, my friend Yiao Jiang and Yu Sun gave me suggestions in data analysis and figure preparation.

Teaching is another important thing in my Ph. D. years. I would like to thank Dr. Francine Scott, Dr. Liz Ottesen, and Dr. Julie Grainy for mentoring and helping me for the courses I taught. Especially, I would like to thank Julie for nominating me for the Outstanding Teaching Assistant Award.

I would like to thank the members of my class, Aileen Ferraro, Allyson Loy, Anastacia Park, Andrew Wiggins, Andy Esterle, Clay Crippen, Jennifer Kurasz, Lauren Essler, Molly Bunkofske, Nathan Gluek, and Xiaoxuan Ge. We had good time in the beginning years taking courses together.

Finally, I would like to thank the staff of the Department of Microbiology, Andrea Barnett, Christie Haynes, Janice Stuart, Kim Brown, Nancy Perkins, and Sophia Fleming, for all the help and support.

TABLE OF CONTENTS

Page

ACKNOWLEDGEMENTS iv

LIST OF TABLES vii

LIST OF FIGURES ix

CHAPTER

1 INTRODUCTION AND LITERATURE REVIEW 1

2 OXIDATIVE STRESS REGULATES THE SWITCH OF DIMETHYLSULFONIOPROPIONATE METABOLISM FROM DEMETHYLATION TO CLEAVAGE IN *RUEGERIA POMEROYI* 29

3 SUBSTRATE SPECIFICITY OF THE 3-METHYLMERCAPTOPROPIONYL-COA DEHYDROGENASE (DMDC1) *FROM RUEGERIA POMEROYI* DSS-3 73

4 THE GENUS *LOKTANELLA* 91

5 THE GENUS *YOONIA* 118

6 CONCLUSIONS 154

APPENDICES

A CHAPTER 2 SUPPLEMENTARY INFORMATION 158

B CHAPTER 3 SUPPLEMENTARY INFORMATION 171

LIST OF TABLES

Page

Table 2-1 DMSP consumption and metabolic data of *R. pomeroyi* strains during chemostat growth on glucose or glucose and DMSP before and after H_2O_2 additions.....58

Table 2-2-Fold change of expression of selected oxidative stress responsive genes 60

Table 2-3 Fold change of expression of DMSP metabolism genes under each condition compared to wild-type with no additions or W transcriptome. 62

Table 2-4 Fold change of expression of selected sulfur metabolism genes under each condition compared to wild-type with no additions or W transcriptome 64

Table 2-5 DMSP consumption by *R. pomeroyi* during chemostat growth on glucose plus DMSP 66

Table 3-1 Substrate specificity and apparent kinetic constants for recombinant RPO_DmdC1 dehydrogenase.....87

Table 4-1 Selected characteristics of *Loktanella* species.....108

Table 4-2 Selected characteristics distinguishing of *Loktanella* species.....109

Table 4-3 Cellular fatty acids in the *Loktanella* species. 110

Table 4-4 Genome sequences for the *Loktanella* species 111

Table 4-5 Characteristics distinguishing of *Loktanella* from other, closely related genera 112

Table 5-1 Selected characteristics of *Yoonia* species 142

Table 5-2 Selected characteristics distinguishing of *Yoonia* species.....144

Table 5-3 Cellular fatty acids in the *Yoonia* species.....148

Table 5-4 Genome sequences for the *Yoonia* species 150

Table 5-5 Characteristics distinguishing of *Yoonia* from closely related genera 151

Table S2-1 Primers used for generating pCR2.1 deletion vector 159

Table S2-2 H_2O_2 stability in culture media 160

Table S2-3 Summary of sequencing data including the number of reads and indicators of their quality 161

Table S2-4 Comparison of replicates and determination of batch effects 162

Table S2-5 Number of differentially expressed genes in each comparison with adjusted p values <0.1 163

Table S2-6 Full list of genes selected for analyzing sulfur metabolism and oxidative stress 164

Table S3-1 Purification of the recombinant *R. pomeroyi* DSS-3 DmdC dehydrogenase from *E. coli* BL21(DE3) cells 172

Table S3-2 Electron acceptors of recombinant RPO_DmdC1 dehydrogenase 173

LIST OF FIGURES

Page

Figure 1-1 The pathways of DMSP biosynthesis 25

Figure 1-2 The pathways of DMSP metabolism common in bacteria.....27

Figure 2-1 DMSP metabolic pathways in *R. pomeroyi* DSS-3.....67

Figure 2-2 Experimental design for chemostat growth conditions.....69

Figure 2-3 Effect of growth conditions on the patterns of gene expression 70

Figure 2-4 Overview of sulfur metabolism in *R. pomeroyi* 71

Figure 2-5 Regulation network of oxidative stress on DMSP metabolism based on changes in gene expression.....72

Figure 3-1 Demethylation pathway in *R. pomeroyi* DSS-3 88

Figure 3-2 Phylogeny of DmdC homologues from *R. pomeroyi* DSS-3 and *R. subindices* ISM 9

Figure 3-3 Response of the recombinant RPO_DmdC1 dehydrogenase to pH.....90

Figure 4-1 16S rRNA gene-based phylogenetic tree of *Loktanella* species and their relatives 113

Figure 4-2 Core-gene-based phylogenetic tree of *Loktanella* species and its relatives.....115

Figure 5-1 Phylogeny of *Yoonia* and *Cognatiyoonia species*.....152

Figure 5-2 Pangenome analysis of *Yoonia* and *Cognatiyoonia species* 153

Figure S2-1 Chemostat design for H_2O_2 additions 168

Figure S2-2 Identification of oxidative stress responsive genes.....169

Figure S3-1 Purification of the recombinant RPO_DmdC1 expressed in *E. coli* BL21(DE3)....174

Figure S3-2 Inhibition of recombinant RPO_DmdC1 dehydrogenase activity by 0.4 M salts ...175

Figure S3-3 Role of potential effectors on RPO_DmdC dehydrogenase activity 176

CHAPTER 1

INTRODUCTION AND LITERATURE REVIEW

1. Dimethylsulfoniopropionate and its metabolism

Sulfur, the core of some amino acids and many cofactors, is an essential element for all of life. Sulfur is also involved in global climate through the movement of organic sulfur compounds, especially the volatile dimethylsulfide (DMS) (1, 2). Each year, 13-37 Tg of sulfur are delivered to the atmosphere in the form of DMS (3). As the largest natural sulfur source to the upper atmosphere, DMS plays an important role in the global sulfur cycle (4).

Most DMS is released biotically by the breakdown of dimethylsulfoniopropionate (DMSP), which is abundant in marine surface water (5). The majority of marine DMSP is produced by phytoplankton, especially the classes *Dinophyceae* (dinoflagellates) and *Prymnesiophyceae* (including the coccolithophores), algae, corals, and certain higher plants (6). It is estimated that up to 10 % of total carbon fixed in the ocean is used to biosynthesize DMSP, leading to a DMSP concentrations from less than 1 nM to micromolar levels in seawater, depending on the abundance of phytoplankton (7, 8).

The biosynthesis of DMSP in some representative organisms has been elucidated by isotope labelling experiments. There are three major pathways, which are named after their first reactions (Figure 1-1) (9-15). Among the main DMSP producers, the same pathway may be shared by very different taxa, and for closely related taxa the pathways used can be different (16). For example, based upon the presence of intermediates and annotated genes, it was proposed that green algae, diatoms, coccolithophores, and corals employ the transamination

pathway. In contrast, the angiosperms, which are taxonomically closely related to green algae, have unique pathways to synthesize DMSP. These results suggest that DMSP biosynthesis pathways have evolved independently (6, 16). Recent studies have shown that marine bacteria are significant producers of DMSP as well, especially in aphotic and high-pressure environments (17-19). Current evidence supports the hypothesis that marine bacteria can biosynthesize DMSP via more than one pathway (18, 19). However, although many of the intermediates have been identified, the genes encoding DMSP biosynthesis still remain largely unidentified among all DMSP producers (18). So far, only two bacterial genes, *dsyB* and *mmtN*, which encode 4-methylthio-2-hydroxybutyrate (MTHB) methyltransferase and S-adenosyl-methionine (SAM)-dependent methionine methyltransferase (MMT), respectively, have been identified experimentally (18, 19). These two genes may serve as markers for DMSP synthesis in bacteria. Homologs of *dsyB* and *mmtN* have also been identified in eukaryotic DMSP producers (19, 20). *DSYB*, the *dsyB*-like genes in eukaryotes, is widespread in phytoplankton and corals, and evolutionary analyses suggest that these eukaryotic *DSYB* genes originated in bacteria and were later passed to eukaryotes (20). In contrast, the plant-like MMT enzymes are very different from the bacterial MmtNs in length, amino acid sequence, and domains, suggesting that this DMSP biosynthetic pathway evolved independently in bacteria and plants (19).

One explanation of the origin of DMSP production is to balance the limitation of nutrients such as nitrogen with excess carbon and reducing equivalents (21). Although the intermediate steps are different, the three identified DMSP biosynthesis pathways all start with L-methionine (Figure 1-1) (6). The amino group of the L-methionine is removed either through deamination or transamination, where it can be used to produce glutamic acid or glutamine, respectively (11). In various DMSP producers, it is confirmed that nitrogen limitation can

stimulate DMSP production. Thus, the production of DMSP may allow cells to reallocate nitrogen for new amino acid biosynthesis and stimulate the continued sulfate reduction (6).

DMSP may have different roles in different organisms. The best known role of DMSP is as an organic osmolyte. Some DMSP producers can produce a significant amount of DMSP so that the intracellular DMSP concentration can reach molar levels (21). Increased salinity, especially under long term conditions, has been reported to stimulate the production or accumulation of DMSP in many organisms including algae, higher plants, and bacteria (13, 18, 22, 23). But unlike other common compatible solutes, such as betaine and proline, DMSP is constitutively maintained at a comparatively high intracellular level. The rate of DMSP production does not change significantly after a hyperosmotic shock. These indicate DMSP more likely acts as a buffer during initial periods of hyperosmotic shocks (21, 24). A cryoprotectant role is suggested by the higher intracellular DMSP concentrations in polar macroalgae compared to those in related species from temperature to tropical regions (25). In addition, polar macroalgae growing at 0 ºC have a higher intracellular DMSP content than those growing at 10 ºC. DMSP also stimulates the activities of malate dehydrogenase and lactate dehydrogenase at low temperature (25). Wolfe *et al.* reported algae *Emiliania huxleyi* can use DMSP as a predator deterrent (26). In their experiment, the protozoan predator exhibited strong preference on the *E. huxleyi* strain with low DMSP lyase activity. This was explained either by the signal role of DMS and acrylate generated during grazing, or the antimicrobial effect of accumulated acrylate (26, 27). In addition, DMSP can also act as an antioxidant, which will be discussed in detail later (28).

Currently, three different DMSP catabolic pathways have been discovered (Figure 1-2). The cleavage pathway carried out by algae, phytoplankton, higher plants, and bacteria, yields

DMS (4, 6, 29). The DMSP lyases involved in this pathway directly cleave DMSP, releasing acrylate, 3-hydroxypropionate, or acryloyl-CoA as products (30-38). Although many of these enzymes catalyze the same reaction, they are from different enzyme families and have different mechanisms (6). As the main DMSP consumers, bacteria can degrade DMSP in two additional pathways, the demethylation and the oxidation pathways (39, 40). In the demethylation pathway, a methyl group at the sulfur atom is first transferred from DMSP to tetrahydrofolate (THF) by DMSP demethylase (DmdA), forming 3-methylmercaptopropionate (MMPA) and methyl-THF. MMPA is then processed similarly to β-oxidation of fatty acids by DmdB (MMPA-CoA ligase), DmdC [3-methylmercaptopropionyl(MTA)-CoA dehydrogenase], and DmdD (MTA-CoA hydratase), and the sulfur atom is finally released as methanethiol (MeSH). MeSH can be efficiently assimilated by bacteria as a key intermediate to protein sulfur either by direct capture to form methionine or by lysis to sulfide for assimilation (41). In the newly identified oxidation pathway, DMSP is oxidized to dimethylsulfoxonium propionate (DMSOP) by microalgae and bacteria, but only bacteria can further make dimethylsulfoxide (DMSO) and acrylate from DMSOP (39). Currently, none of enzymes involved in the oxidation pathway have been identified.

Unlike MeSH, DMS can readily cross the cell membrane, and the sulfur from DMS is often not assimilated directly. Nevertheless, the majority of DMS released is still degraded by microorganisms in the sea (42-46). Many organisms have been reported to degrade DMS aerobically or anaerobically for carbon and energy (46, 47). Generally, there are two pathways to degrade DMS. In one pathway, DMS is oxidized to MeSH and formaldehyde by DMS monooxygenase or methyltransferases, which are mostly found in terrestrial organisms (43, 46). In the other pathway, DMS is oxidized to DMSO and then sulfate, which is common in marine

surface water (45). Studied marine bacteria, especially the members of *Alphaproteobacteria*, may transform DMS to either DMSO or MeSH (48, 49). In addition, DMS and DMSO can be interconverted though enzymatic reactions (46). Thus, regardless of the degradation pathway, DMSP can be an important source of sulfur, carbon, or energy for marine bacteria.

Despite being studied for nearly 40 years, there is still much to be learned regarding DMSP and its metabolism. Many enzymes involved in DMSP biosynthesis and metabolism, especially the oxidation pathways, are still unidentified. Even for some identified enzymes, such as DddD and DddL, their structures, catalytic mechanisms, biochemical properties, and regulation are still not well understood (50). In addition, many *Alphaproteobacteria* can utilize DMSP by both the cleavage and demethylation pathways, but the regulation and interaction between the two pathways are not completely studied. Obviously, sulfur demand is a key driver, but there could be other factors as both the pathways can produce toxic byproducts (51). Finally, bacteria are not isolated groups in marine environments; they interact with many organisms including other bacteria, phytoplankton, corals, and algae. Studies have shown that volatile compounds, such as DMS or dimethyl disulfide (DMDS), can act as signal molecules for communications among bacteria or even different kingdoms (52, 53). Thus, learning more about DMSP metabolism in these symbiotic relationships can lead to a better understand of marine ecosystems and potential applications in protecting environments.

2. Genus *Ruegeria* and model organism *Ruegeria pomeroyi*

The genus *Ruegeria* is a member of the class *Alphaproteobacteria*, family *Rhodobacteraceae*. This genus was originally proposed by Uchino et al. to describe a group of catalase- and peroxidase-positive, non-photosynthetic aerobic bacteria during the reclassification

of the genus *Agrobacterium* based on 16S rRNA gene sequence analysis (54). *Agrobacterium atlanticum* was reclassified as the type species *Ruegeria atlantica*. In the following two decades, many species were moved into or moved out of the genus *Ruegeria* (55-58). Recent studies indicate that 16S rRNA gene sequence similarity is a poor marker for the phylogeny of the roseobacter group, which includes *Ruegeria* (59). Thus, to accurately assign the members in this group, a whole genome sequence level analysis is required. So far, 18 species are remaining in *Ruegeria*, and whole genome sequences are available for all of them (57).

R. pomeroyi was originally isolated from Georgia coastal seawater by enrichment on DMSP and named *Silicibacter pomeroyi*. It was later reclassified into *Ruegeria* by Yi et al. (60, 61). While most *Ruegeria* species are non-motile, *R. pomeroyi* is motile via a polar flagellum. It grows between 10 to 40 ºC, with an optimum growth temperature of 30 ºC. Like other species of *Ruegeria*, *R. pomeroyi* requires sea salts to grow, and optimum growth occurs between 0.6-2.3% (w/v) NaCl. The two common media used to cultivate *R. pomeroyi* are half-strength yeast extract tryptone sea salts (1/2YTSS; DSMZ Medium 974) and marine basal medium (MBM) (60, 62).

R. pomeroyi is one of the earliest bacteria reported to degrade DMSP, with high activities via both the cleavage and demethylation pathways (48, 60). The demethylation pathway was first deciphered in *R. pomeroyi* (Figure 1-2), where there are multiple copies of some genes, *i.e.*, *dmdB* and *dmdC* (43, 62). For the cleavage pathway, four DMSP lyases *dddD*, *dddP*, *dddQ*, and *dddW* are present in *R. pomeroyi* (32-35). Beside the genes directly involved in DMSP metabolism, the large genome of *R. pomeroyi* encodes more than 4000 genes, suggesting that it has complex regulatory mechanisms that allow for growth under a range of conditions and large variety of substrates. An effective genetic tool for *R. pomeroyi* has also been developed (40). In

addition, there are many genomic, transcriptomic, and proteomic studies on *R. pomeroyi*, which greatly improves the understand of metabolic networks in this organism (63-65).

Thus, *R. pomeroyi* is a useful model organism used for studying the regulation of DMSP catabolism. The availability of DMSP itself can affect the ratio of DMS and MeSH produced. With an increased DMSP concentrations, *R. pomeroyi* upregulates both of the pathways to produce more DMS and MeSH, but the percentage of DMSP cleaved also increases (51, 66). A widely accepted explanation is that the catabolism of DMSP will first fulfill the sulfur demand via the demethylation pathway. At certain DMSP concentration, the sulfur demand is met, and the activity of the cleavage pathway increases to release the excess organic sulfur via DMS (41, 51). The assimilation of DMSP sulfur and methyl carbon for methionine and cysteine biosynthesis was also studied in *R. pomeroyi* recently through isotope labeling experiments (66).

Acrylate is the byproduct of DMSP lyases. When acrylate is processed by PrpE, a propionate-CoA ligase, the downstream metabolite acryloyl-CoA is highly toxic as it can react with essential macromolecules such as nucleic acids (67, 68). The gene *acuI* encodes a reductase transforming acryloyl-CoA to propionyl-CoA, detoxifying this reactive electrophilic molecule (69, 70). This protective function may explain why in many bacteria, *acuI*-like genes are distributed near the cleavage *ddd* genes (69). Interestingly, in *R. pomeroyi acuI* is located next to *dmdA*, and these genes are co-regulated (69). Treatment with acrylate will lead to a significant increase of MeSH production when *R. pomeroyi* grows on DMSP (71). The same result was obtained in chemostat as well (personal observation). These results indicate that the two DMSP catabolic pathways are interrelated in *R. pomeroyi*.

Salinity is another environmental factor regulating the ratio of DMS and MeSH production, and many studies have shown that low salinity results in a greater DMS production

in some marine habitats (72-74). The same conclusion and enhanced MeSH production with high salinity was confirmed by Salgado *et al.* in *R. pomeroyi* (75). Although there is no clear explanation available for this observation yet, it may be related to the function of DMSP as an intracellular osmolyte.

According to the latest core gene analysis completed by Cao *et al.*, *R. pomeroyi* and *Ruegeria marina* formed a distinct group from the majority of other *Ruegeria* species (57). This result portends a reclassification of *R. pomeroyi* into a novel genus in the future.

3. Oxidative stress and antioxidant mechanisms

The imbalance between the oxidants and antioxidants in favor of the oxidants is called oxidative stress, potentially leading to cellular damage (76). This imbalance is usually caused by an increase of reactive oxygen species (ROS) or reactive nitrogen species (RNS) or a decrease in the antioxidant network (77). ROS is a collective term that includes both oxygen radicals and certain nonradical oxidizing agents (78, 79). ROS can be produced either endogenously or exogenously (80). Endogenous production of ROS usually occurs in normal enzymatic redox reactions, such as oxidative phosphorylation and photosynthesis, while exogenous sources of ROS could be ionizing radiation and oxidative chemicals (81). Oxidative stress is a common stress in marine environments. In marine surface water, solar radiation, especially ultraviolet, can lead to photochemical oxidation of dissolved organic matter, producing ROS (82).

ROS can attack numerous cellular components, including DNA, proteins, lipids, and iron-sulfur clusters (78). In humans, the accumulation of damage to these macromolecules may be a cause of aging, where tissues and organs loss their functions over time (83). These damages can further lead to severe diseases, such as cancer and neurological disease (84). As a result, in

the past decades, oxidative stress has become a popular research topic. Aerobic organisms have evolved many ways to protect themselves from the damage of oxidative stress. Antioxidant defenses include both enzymatic and non-enzymatic mechanisms (85, 86). For enzymatic antioxidant defense, a variety of enzymes, including superoxide dismutase (SOD), catalase, and peroxidase, are produced to directly reduce ROS levels by transforming them to harmless molecules. Non-enzymatic defenses involve low-molecular-weight reductive compounds, such as glutathione and ascorbic acid, that scavenge ROS. The stress genes are also activated to remove or repair the damage of macromolecules when facing oxidative stress (86). Oxidative stress or ROS can also be beneficial for organisms as important signals, which can regulate many cellular activities (87). For example, Hansel *et al*. (88) reported that levels of extracellular superoxide were tightly regulated by *R. pomeroyi* to maintain a normal growth cycle in batch culture.

The role of DMSP as an antioxidant was originally proposed by Sunda *et al*. (28). They experimentally confirmed that DMSP, DMS, acrylate, dimethylsulfoxide (DMSO), and methane sulfinic acid (MSNA) are strong scavengers of the hydroxyl radical (·OH) (28). As DMS and acrylate are about 20 to 60 times more reactive to ·OH than DMSP and the uncharged DMS can freely diffuse across the membrane, they hypothesized that when there is oxidative stress, DMSP synthesis and the cleavage pathways should be substantially upregulated. This hypothesis was supported by experiments in algae, where several different types of oxidative stressors were applied. Similar results were then reported in most DMSP-producers including higher plants, coral holobionts, and phytoplankton (89-92). However, the studies of the antioxidant role of DMSP in bacteria is largely missing, where DMSP metabolism is much more complex. As the presence of oxidative stress could lead to a higher DMS production, further study on this could

potentially expand our understanding about the biogeochemistry of sulfur cycle and the global climate.

References

1. Charlson RJ, Lovelock JE, Andreae MO, Warren SG. 1987. Oceanic phytoplankton, atmospheric sulphur, cloud albedo and climate. Nature 326:655-661.
2. Lovelock JE, Maggs R, Rasmussen R. 1972. Atmospheric dimethyl sulphide and the natural sulphur cycle. Nature 237:452-453.
3. Ksionzek KB, Lechtenfeld OJ, McCallister SL, Schmitt-Kopplin P, Geuer JK, Geibert W, Koch BP. 2016. Dissolved organic sulfur in the ocean: Biogeochemistry of a petagram inventory. Science 354:456-459.
4. Andreae MO. 1990. Ocean-atmosphere interactions in the global biogeochemical sulfur cycle. Mar Chem 30:1-29.
5. Kiene RP, Linn LJ, Bruton JA. 2000. New and important roles for DMSP in marine microbial communities. J Sea Res 43:209-224.
6. Bullock HA, Luo H, Whitman WB. 2017. Evolution of dimethylsulfoniopropionate metabolism in marine phytoplankton and bacteria. Front Microbiol 8:637.
7. Yoch DC. 2002. Dimethylsulfoniopropionate: its sources, role in the marine food web, and biological degradation to dimethylsulfide. Appl Environ Microbiol 68:5804-5815.
8. van Duyl FC, Gieskes WW, Kop AJ, Lewis WE. 1998. Biological control of short-term variations in the concentration of DMSP and DMS during a *Phaeocystis* spring bloom. J Sea Res 40:221-231.
9. Kocsis MG, Nolte KD, Rhodes D, Shen T-L, Gage DA, Hanson AD. 1998. Dimethylsulfoniopropionate biosynthesis in *Spartina alterniflora*: Evidence that S-methylmethionine and dimethylsulfoniopropylamine are intermediates. Plant Physiol 117:273-281.

10. Gage DA, Rhodes D, Nolte KD, Hicks WA, Leustek T, Cooper AJ, Hanson AD. 1997. A new route for synthesis of dimethylsulphoniopropionate in marine algae. Nature 387:891-894.

11. Rhodes D, Gage DA, Cooper AJ, Hanson AD. 1997. S-Methylmethionine conversion to dimethylsulfoniopropionate: evidence for an unusual transamination reaction. Plant Physiol 115:1541-1548.

12. Raina J-B, Tapiolas DM, Forêt S, Lutz A, Abrego D, Ceh J, Seneca FO, Clode PL, Bourne DG, Willis BL. 2013. DMSP biosynthesis by an animal and its role in coral thermal stress response. Nature 502:677-680.

13. Hanson AD, Rivoal J, Paquet L, Gage DA. 1994. Biosynthesis of 3-dimethylsulfoniopropionate in Wollastonia biflora (L.) DC.(evidence that S-methylmethionine is an intermediate). Plant Physiol 105:103-110.

14. Uchida A, Ooguri T, Ishida T, Kitaguchi H, Ishida Y. 1996. Biosynthesis of dimethylsulfoniopropionate in Crypthecodinium cohnii (Dinophyceae), p 97-107, *In* Kiene RP, Visscher PT, Keller MD, Kirst GO (ed), Biological and Environmental Chemistry of DMSP and Related Sulfonium Compounds. Springer US, Boston, MA.

15. Kettles NL, Kopriva S, Malin G. 2014. Insights into the regulation of DMSP synthesis in the diatom *Thalassiosira pseudonana* through APR activity, proteomics and gene expression analyses on cells acclimating to changes in salinity, light and nitrogen. PloS One 9:e94795.

16. Dickschat JS, Rabe P, Citron CA. 2015. The chemical biology of dimethylsulfoniopropionate. Org Biomol Chem 13:1954-1968.

17. Zheng Y, Wang J, Zhou S, Zhang Y, Liu J, Xue C-X, Williams BT, Zhao X, Zhao L, Zhu X-Y. 2020. Bacteria are important dimethylsulfoniopropionate producers in marine aphotic and high-pressure environments. Nat Commun 11:1-12.

18. Curson AR, Liu J, Martínez AB, Green RT, Chan Y, Carrión O, Williams BT, Zhang S-H, Yang G-P, Page PCB. 2017. Dimethylsulfoniopropionate biosynthesis in marine bacteria and identification of the key gene in this process. Nat Microbiol 2:1-9.

19. Williams BT, Cowles K, Martínez AB, Curson AR, Zheng Y, Liu J, Newton-Payne S, Hind AJ, Li C-Y, Rivera PPL. 2019. Bacteria are important dimethylsulfoniopropionate producers in coastal sediments. Nat Microbiol 4:1815-1825.

20. Curson AR, Williams BT, Pinchbeck BJ, Sims LP, Martínez AB, Rivera PPL, Kumaresan D, Mercadé E, Spurgin LG, Carrión O. 2018. DSYB catalyses the key step of dimethylsulfoniopropionate biosynthesis in many phytoplankton. Nat Microbiol 3:430-439.

21. Stefels J. 2000. Physiological aspects of the production and conversion of DMSP in marine algae and higher plants. J Sea Res 43:183-197.

22. Cosquer A, Pichereau V, Pocard J-A, Minet J, Cormier M, Bernard T. 1999. Nanomolar levels of dimethylsulfoniopropionate, dimethylsulfonioacetate, and glycine betaine are sufficient to confer osmoprotection to *Escherichia coli*. Appl Environ Microbiol 65:3304-3311.

23. Kirst G, Thiel C, Wolff H, Nothnagel J, Wanzek M, Ulmke R. 1991. Dimethylsulfoniopropionate (DMSP) in icealgae and its possible biological role. Mar Chem 35:381-388.

24. Kirst GO. 1996. Osmotic adjustment in phytoplankton and macroalgae, p 121-129. *In* Kiene RP, Visscher PT, Keller MD, Kirst GO (ed), Biological and Environmental Chemistry of DMSP and Related Sulfonium Compounds. Springer US, Boston, MA.

25. Karsten U, Kück K, Vogt C, Kirst G. 1996. Dimethylsulfoniopropionate production in phototrophic organisms and its physiological functions as a cryoprotectant, p 143-153, *In* Kiene RP, Visscher PT, Keller MD, Kirst GO (ed), Biological and Environmental Chemistry of DMSP and Related Sulfonium Compounds. Springer US, Boston, MA.

26. Wolfe GV, Steinke M, Kirst GO. 1997. Grazing-activated chemical defence in a unicellular marine alga. Nature 387:894-897.

27. Fredrickson KA, Strom SL. 2009. The algal osmolyte DMSP as a microzooplankton grazing deterrent in laboratory and field studies. J Plankton Res 31:135-152.

28. Sunda W, Kieber D, Kiene R, Huntsman S. 2002. An antioxidant function for DMSP and DMS in marine algae. Nature 418:317-320.

29. Taylor BF, Visscher PT. 1996. Metabolic pathways involved in DMSP degradation, p 265-276, *In* Kiene RP, Visscher PT, Keller MD, Kirst GO (ed), Biological and Environmental Chemistry of DMSP and Related Sulfonium Compounds. Springer US, Boston, MA.

30. Li C-Y, Wang X-J, Chen X-L, Sheng Q, Zhang S, Wang P, Quareshy M, Rihtman B, Shao X, Gao C. 2021. A novel ATP dependent dimethylsulfoniopropionate lyase in bacteria that releases dimethyl sulfide and acryloyl-CoA. Elife 10:e64045.

31. Todd JD, Rogers R, Li YG, Wexler M, Bond PL, Sun L, Curson AR, Malin G, Steinke M, Johnston AW. 2007. Structural and regulatory genes required to make the gas dimethyl sulfide in bacteria. Science 315:666-669.

32. Todd JD, Kirkwood M, Newton-Payne S, Johnston AW. 2012. DddW, a third DMSP lyase in a model Roseobacter marine bacterium, *Ruegeria pomeroyi* DSS-3. ISME J 6:223-226.

33. Todd JD, Curson ARJ, Kirkwood M, Sullivan MJ, Green RT, Johnston AWB. 2011. DddQ, a novel, cupin-containing, dimethylsulfoniopropionate lyase in marine roseobacters and in uncultured marine bacteria. Environ Microbiol 13:427-438.

34. Curson A, Rogers R, Todd J, Brearley C, Johnston A. 2008. Molecular genetic analysis of a dimethylsulfoniopropionate lyase that liberates the climate-changing gas dimethylsulfide in several marine α-proteobacteria and *Rhodobacter sphaeroides*. Environ Microbiol 10:757-767.

35. Todd J, Curson A, Dupont C, Nicholson P, Johnston A. 2009. The *dddP* gene, encoding a novel enzyme that converts dimethylsulfoniopropionate into dimethyl sulfide, is widespread in ocean metagenomes and marine bacteria and also occurs in some Ascomycete fungi. Environ Microbiol 11:1376-1385.

36. Curson AR, Sullivan MJ, Todd JD, Johnston AW. 2011. DddY, a periplasmic dimethylsulfoniopropionate lyase found in taxonomically diverse species of Proteobacteria. ISME J 5:1191-1200.

37. Peng M, Chen X-L, Zhang D, Wang X-J, Wang N, Wang P, Todd JD, Zhang Y-Z, Li C-Y. 2019. Structure-function analysis indicates that an active-site water molecule participates in dimethylsulfoniopropionate cleavage by DddK. Appl Environ Microbiol 85:e03127-18.

38. Alcolombri U, Ben-Dor S, Feldmesser E, Levin Y, Tawfik DS, Vardi A. 2015. Identification of the algal dimethyl sulfide-releasing enzyme: A missing link in the marine sulfur cycle. Science 348:1466-1469.

39. Thume K, Gebser B, Chen L, Meyer N, Kieber DJ, Pohnert G. 2018. The metabolite dimethylsulfoxonium propionate extends the marine organosulfur cycle. Nature 563:412-415.

40. Reisch CR, Stoudemayer MJ, Varaljay VA, Amster IJ, Moran MA, Whitman WB. 2011. Novel pathway for assimilation of dimethylsulphoniopropionate widespread in marine bacteria. Nature 473:208-211.

41. Kiene RP, Linn LJ, Gonzalez J, Moran MA, Bruton JA. 1999. Dimethylsulfoniopropionate and methanethiol are important precursors of methionine and protein-sulfur in marine bacterioplankton. Appl Environ Microbiol 65:4945-4558.

42. Kiene RP, Bates TS. 1990. Biological removal of dimethyl sulphide from sea water. Nature 345:702-705.

43. Reisch CR, Moran MA, Whitman WB. 2011. Bacterial catabolism of dimethylsulfoniopropionate (DMSP). Front Microbiol 2:172.

44. Spiese CE, Le T, Zimmer RL, Kieber DJ. 2015. Dimethylsulfide membrane permeability, cellular concentrations and implications for physiological functions in marine algae. J Plankton Res 38:41-54.

45. Vila-Costa M, Del Valle DA, González JM, Slezak D, Kiene RP, Sánchez O, Simó R. 2006. Phylogenetic identification and metabolism of marine dimethylsulfide-consuming bacteria. Environ Microbiol 8:2189-2200.

46. Kappler U, Schäfer H. 2014. Transformations of dimethylsulfide, p 279-313. *In* Kroneck PMH, Torres MES (eds), The Metal-Driven Biogeochemistry of Gaseous Compounds in the Environment. Metal Ions in Life Sciences, vol 14. Springer, Dordrecht.

47. Fuse H, Takimura O, Murakami K, Yamaoka Y, Omori T. 2000. Utilization of dimethyl sulfide as a sulfur source with the aid of light by *Marinobacterium* sp. strain DMS-S1. Appl Environ Microbiol 66:5527-5532.

48. González JM, Kiene RP, Moran MA. 1999. Transformation of sulfur compounds by an abundant lineage of marine bacteria in the α-subclass of the class *Proteobacteria*. Appl Environ Microbiol 65:3810-3819.

49. Visscher PT, Taylor BF. 1993. Aerobic and anaerobic degradation of a range of alkyl sulfides by a denitrifying marine bacterium. Appl Environ Microbiol 59:4083-4089.

50. Do H, Hwang J, Lee SG, Lee JH. 2021. Enzymes and their reaction mechanisms in dimethylsulfoniopropionate cleavage and biosynthesis of dimethylsulfide by marine bacteria. Journal of Marine Life Science 6:1-8.

51. Gao C, Fernandez VI, Lee KS, Fenizia S, Pohnert G, Seymour JR, Raina J-B, Stocker R. 2020. Single-cell bacterial transcription measurements reveal the importance of dimethylsulfoniopropionate (DMSP) hotspots in ocean sulfur cycling. Nat Commun 11:1942.

52. Weisskopf L, Schulz S, Garbeva P. 2021. Microbial volatile organic compounds in intra-kingdom and inter-kingdom interactions. Nat Rev Microbiol 19:391-404.

53. Jackson RL, Gabric AJ, Cropp R, Woodhouse MT. 2020. Dimethylsulfide (DMS), marine biogenic aerosols and the ecophysiology of coral reefs. Biogeosciences 17:2181-2204.

54. Uchino Y, Hirata A, Yokota A, Sugiyama J. 1998. Reclassification of marine *Agrobacterium* species: proposals of *Stappia stellulata* gen. nov., comb. nov., *Stappia aggregata* sp. nov., nom. rev., *Ruegeria atlantica* gen. nov., comb. nov., *Ruegeria gelatinovora* comb. nov., *Ruegeria algicola* comb. nov., and *Ahrensia kieliense* gen. nov., sp. nov., nom. rev. J Gen Appl Microbiol 44:201-210.

55. Wirth JS, Whitman WB. 2019. *Ruegeria*, p 1-25. *In* Trujillo ME, Dedysh S, DeVos P, Hedlund B, Kämpfer P, Rainey FA and Whitman WB (ed), Bergey's Manual of Systematics of Archaea and Bacteria. John Wiley & Sons, Inc.

56. Hördt A, López MG, Meier-Kolthoff JP, Schleuning M, Weinhold LM, Tindall BJ, Gronow S, Kyrpides NC, Woyke T, Göker M. 2020. Analysis of 1,000+ type-strain genomes substantially improves taxonomic classification of *Alphaproteobacteria*. Front Microbiol 11:468.

57. Cao W-R, Shang D-D, Liu B-T, Hu Y-H, Sun X-K, Sun Y-Y, Jiang M-Y, Du Z-J. 2021. *Ruegeria haliotis* sp. nov., isolated from the gut of the abalone *Haliotis rubra*. Curr Microbiol 78:2151-2159.

58. Baek J, Kim J-H, Sukhoom A, Kim W. 2020. *Ruegeria sediminis* sp. nov., isolated from tidal flat sediment. Int J Syst Evol Microbiol 70:3055-3061.

59. Breider S, Scheuner C, Schumann P, Fiebig A, Petersen J, Pradella S, Klenk HP, Brinkhoff T, Goker M. 2014. Genome-scale data suggest reclassifications in the *Leisingera-Phaeobacter* cluster including proposals for *Sedimentitalea* gen. nov. and *Pseudophaeobacter* gen. nov. Front Microbiol 5:416.

60. González JM, Covert JS, Whitman WB, Henriksen JR, Mayer F, Scharf B, Schmitt R, Buchan A, Fuhrman JA, Kiene RP, Moran MA. 2003. *Silicibacter pomeroyi* sp. nov. and

Roseovarius nubinhibens sp. nov., dimethylsulfoniopropionate-demethylating bacteria from marine environments. Int J Syst Evol Microbiol 53:1261-1269.

61. Yi H, Lim YW, Chun J. 2007. Taxonomic evaluation of the genera *Ruegeria* and *Silicibacter*: a proposal to transfer the genus *Silicibacter* Petursdottir and Kristjansson 1999 to the genus *Ruegeria* Uchino et al. 1999. Int J Syst Evol Microbiol 57:815-819.

62. Reisch CR, Moran MA, Whitman WB. 2008. Dimethylsulfoniopropionate-dependent demethylase (DmdA) from *Pelagibacter ubique* and *Silicibacter pomeroyi*. J Bacteriol 190:8018-8024.

63. Rivers AR, Smith CB, Moran MA. 2014. An updated genome annotation for the model marine bacterium *Ruegeria pomeroyi* DSS-3. Stand Genomic Sci 9:1-9.

64. Krayushkina D, Timmins-Schiffman E, Faux J, May DH, Riffle M, Harvey HR, Nunn BL. 2019. Growth phase proteomics of the heterotrophic marine bacterium *Ruegeria pomeroyi*. Sci Data 6:1-6.

65. Bürgmann H, Howard EC, Ye W, Sun F, Sun S, Napierala S, Moran MA. 2007. Transcriptional response of *Silicibacter pomeroyi* DSS-3 to dimethylsulfoniopropionate (DMSP). Environ Microbiol 9:2742-2755.

66. Wirth JS, Wang T, Huang Q, White RH, Whitman WB. 2020. Dimethylsulfoniopropionate sulfur and methyl carbon assimilation in *Ruegeria* species. mBio 11:e00329-20.

67. Asao M, Alber BE. 2013. Acrylyl-coenzyme A reductase, an enzyme involved in the assimilation of 3-hydroxypropionate by *Rhodobacter sphaeroides*. J Bacteriol 195:4716-4725.

68. Reisch CR, Crabb WM, Gifford SM, Teng Q, Stoudemayer MJ, Moran MA, Whitman WB. 2013. Metabolism of dimethylsulphoniopropionate by *Ruegeria pomeroyi* DSS-3. Mol Microbiol 89:774-791.

69. Todd JD, Curson AR, Sullivan MJ, Kirkwood M, Johnston AW. 2012. The *Ruegeria pomeroyi acuI* gene has a role in DMSP catabolism and resembles *yhdH* of *E. coli* and other bacteria in conferring resistance to acrylate. PloS One 7:e35947.

70. Herrmann G, Selmer T, Jessen HJ, Gokarn RR, Selifonova O, Gort SJ, Buckel W. 2005. Two beta-alanyl-CoA: ammonia lyases in *Clostridium propionicum*. FEBS J 272:813-821.

71. Landa M, Burns AS, Durham BP, Esson K, Nowinski B, Sharma S, Vorobev A, Nielsen T, Kiene RP, Moran MA. 2019. Sulfur metabolites that facilitate oceanic phytoplankton–bacteria carbon flux. ISME J 13:2536-2550.

72. Visscher PT, Baumgartner LK, Buckley DH, Rogers DR, Hogan ME, Raleigh CD, Turk KA, Des Marais DJ. 2003. Dimethyl sulphide and methanethiol formation in microbial mats: potential pathways for biogenic signatures. Environ Microbiol 5:296-308.

73. Yang G, Li C, Sun J. 2011. Influence of salinity and nitrogen content on production of dimethylsulfoniopropionate (DMSP) and dimethylsulfide (DMS) by *Skeletonema costatum*. Chin J Oceanol Limnol 29:378-386.

74. Magalhães C, Salgado P, Kiene R, Bordalo A. 2012. Influence of salinity on dimethyl sulfide and methanethiol formation in estuarine sediments and its side effect on nitrous oxide emissions. Biogeochemistry 110:75-86.

75. Salgado P, Kiene R, Wiebe W, Magalhães C. 2014. Salinity as a regulator of DMSP degradation in *Ruegeria pomeroyi* DSS-3. J Microbiol 52:948-954.

76. Sies H. 1997. Oxidative stress: oxidants and antioxidants. Exp Physiol 82:291-295.

77. López-Alarcón C, Denicola A. 2013. Evaluating the antioxidant capacity of natural products: A review on chemical and cellular-based assays. Anal Chim Acta 763:1-10.

78. Bayr H. 2005. Reactive oxygen species. Crit Care Med 33:S498-S501.

79. Liou G-Y, Storz P. 2010. Reactive oxygen species in cancer. Free Radic Res 44:479-496.

80. Krumova K, Cosa G. 2016. Overview of reactive oxygen species, p 1-21. *In* Nonell S, Flors C (ed), Singlet Oxygen: Applications in Biosciences and Nanosciences, vol 1. Royal Society of Chemistry.

81. Lesser MP. 2006. Oxidative stress in marine environments: biochemistry and physiological ecology. Annu Rev Physiol 68:253-278.

82. Mopper K, Kieber DJ. 2000. Marine photochemistry and its impact on carbon cycling. p 101-129. *In* Mora SD, Demers S, Vernet M (ed), The effects of UV radiation in the marine environment. Cambridge University Press.

83. Liguori I, Russo G, Curcio F, Bulli G, Aran L, Della-Morte D, Gargiulo G, Testa G, Cacciatore F, Bonaduce D. 2018. Oxidative stress, aging, and diseases. Clin Interv Aging 13:757-772.

84. Pizzino G, Irrera N, Cucinotta M, Pallio G, Mannino F, Arcoraci V, Squadrito F, Altavilla D, Bitto A. 2017. Oxidative stress: harms and benefits for human health. Oxid Med Cell Longev 2017.

85. Birben E, Sahiner UM, Sackesen C, Erzurum S, Kalayci O. 2012. Oxidative stress and antioxidant defense. World Allergy Organ J 5:9-19.

86. Davies KJ. 2000. Oxidative stress, antioxidant defenses, and damage removal, repair, and replacement systems. IUBMB life 50:279-289.

87. Poli G, Leonarduzzi G, Biasi F, Chiarpotto E. 2004. Oxidative stress and cell signalling. Curr Med Chem 11:1163-1182.

88. Hansel CM, Diaz JM, Plummer S. 2019. Tight regulation of extracellular superoxide points to its vital role in the physiology of the globally relevant *Roseobacter* clade. mBio 10:e02668-18.

89. Deschaseaux ES, Jones GB, Deseo MA, Shepherd KM, Kiene R, Swan H, Harrison PL, Eyre BD. 2014. Effects of environmental factors on dimethylated sulfur compounds and their potential role in the antioxidant system of the coral holobiont. Limnol Oceanogr 59:758-768.

90. Husband JD, Kiene RP, Sherman TD. 2012. Oxidation of dimethylsulfoniopropionate (DMSP) in response to oxidative stress in *Spartina alterniflora* and protection of a non-DMSP producing grass by exogenous DMSP+ acrylate. Environ Exp Bot 79:44-48.

91. Jones GB, King S. 2015. Dimethylsulphoniopropionate (DMSP) as an indicator of bleaching tolerance in scleractinian corals. J Mar Sci Eng 3:444-465.

92. Harada H, Kiene RP. 2011. Assessment and characteristics of DMSP lyase activity in seawater and phytoplankton cultures. Publ Seto Mar Biol Lab 41:1-16.

93. Lyon BR, Lee PA, Bennett JM, DiTullio GR, Janech MG. 2011. Proteomic analysis of a sea-ice diatom: salinity acclimation provides new insight into the dimethylsulfoniopropionate production pathway. Plant Physiol 157:1926-1941.

94. Kitaguchi H, Uchida A, Ishida Y. 1999. Purification and characterization of L-methionine decarboxylase from *Crypthecodinium cohnii*. Fish Sci 65:613-617.

95. Tan D, Crabb WM, Whitman WB, Tong L. 2013. Crystal structure of DmdD, a crotonase superfamily enzyme that catalyzes the hydration and hydrolysis of methylthioacryloyl-CoA. PloS One 8:e63870.

96. Schuller DJ, Reisch CR, Moran MA, Whitman WB, Lanzilotta WN. 2012. Structures of dimethylsulfoniopropionate-dependent demethylase from the marine organism *Pelagabacter ubique*. Protein Sci 21:289-298.

97. Shao X, Cao HY, Zhao F, Peng M, Wang P, Li CY, Shi WL, Wei TD, Yuan Z, Zhang XH. 2019. Mechanistic insight into 3-methylmercaptopropionate metabolism and kinetical regulation of demethylation pathway in marine dimethylsulfoniopropionate-catabolizing bacteria. Mol Microbiol 111:1057-1073.

98. Li C-Y, Wei T-D, Zhang S-H, Chen X-L, Gao X, Wang P, Xie B-B, Su H-N, Qin Q-L, Zhang X-Y. 2014. Molecular insight into bacterial cleavage of oceanic dimethylsulfoniopropionate into dimethyl sulfide. Proc Natl Acad Sci U S A 111:1026-1031.

99. Li C-Y, Zhang D, Chen X-L, Wang P, Shi W-L, Li P-Y, Zhang X-Y, Qin Q-L, Todd JD, Zhang Y-Z. 2017. Mechanistic insights into dimethylsulfoniopropionate lyase DddY, a new member of the cupin superfamily. J Mol Biol 429:3850-3862.

100. Schnicker NJ, De Silva SM, Todd JD, Dey M. 2017. Structural and biochemical insights into dimethylsulfoniopropionate cleavage by cofactor-bound DddK from the prolific marine bacterium *Pelagibacter*. Biochemistry 56:2873-2885.

101. Wang P, Chen XL, Li CY, Gao X, Zhu Dy, Xie BB, Qin QL, Zhang XY, Su HN, Zhou BC. 2015. Structural and molecular basis for the novel catalytic mechanism and evolution

of DddP, an abundant peptidase-like bacterial Dimethylsulfoniopropionate lyase: a new enzyme from an old fold. Mol Microbiol 98:289-301.

Figure 1-1. The pathways of DMSP biosynthesis. The methylation pathway (left) is used by higher plants (*Spartina alterniflora*) and bacteria containing *mmtN* (16, 19). The green arrow represents alternative reactions found in *Wollastonia biflora* (13). The transamination pathway (middle) has been found in algae (*Ulva intestinalis*), diatoms (*Fragilariopsis cylindrus*, *Melosira nummuloides*), prymnesiophytes (*Emiliania huxleyi*), prasinophytes (*Tetraselmis sp.*), and algae that contain DSYB and bacteria that contain DsyB (10, 18, 20, 93). The decarboxylation pathway (right) is found in the dinoflagellate *Crypthecodinium cohnii* (94). The dotted line and structure in bracket represent predicted but unconfirmed steps and intermediates. Enzymes involved are labeled in blue. Abbreviation: SMM, S-methyl-methionine; MTOB, 4-methylthio-2-oxobutyrate; MTHB, 4-methylthio-2-hydroxybutyrate; DMSHB, 4-dimethylsulfonio-2-hydroxybutyrate; MTPA, 3-methylthiopropylamine; AdoMet, S-Adenosylmethionine; AdoHcy, S-Adenosyl-L-homocysteine; MMT, methionine methyltransferase; SDC, SMM decarboxylase; DOX, DMSP-amine oxidase; DDH, DMSP-aldehyde dehydrogenase; DsyB/DSYB, MTHB methyltransferase.

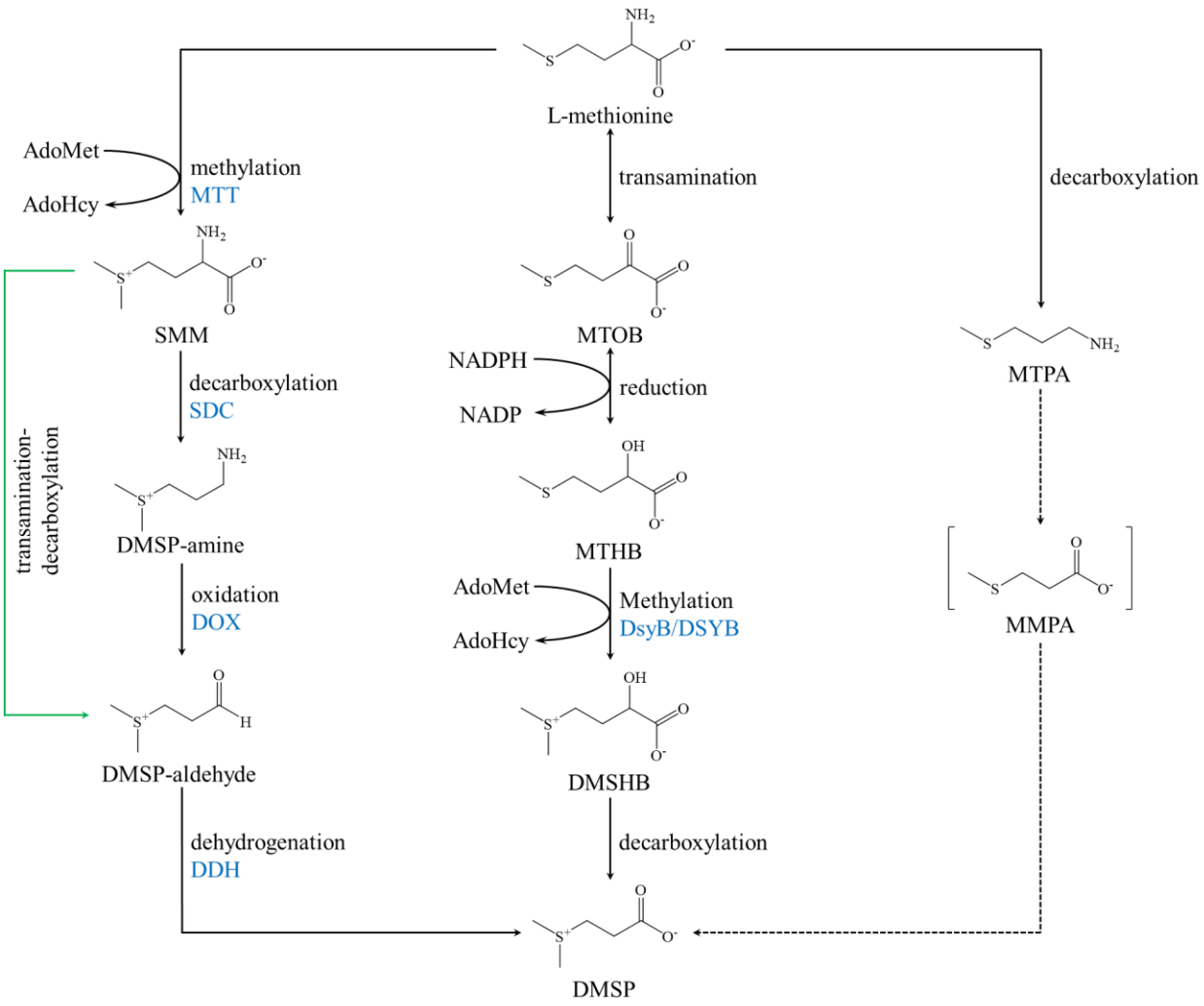
L-methionine
AdoMet
AdoHcy
methylation
MTT
transamination
decarboxylation
SMM
MTOB
MTPA
decarboxylation
SDC
NADPH
NADP
reduction
transamination-
decarboxylation
DMSP-amine
MTHB
MMPA
oxidation
DOX
AdoMet
AdoHcy
Methylation
DsyB/DSYB
DMSP-aldehyde
DMSHB
dehydrogenation
DDH
decarboxylation
DMSP

Figure 1-2. The pathways of DMSP metabolism common in bacteria. Three pathways of DMSP metabolism and their enzymes are indicated. Not all enzymes or pathways are found in all bacteria. For the demethylation pathway, many bacteria are missing DmdD, which is replaced by AcuH. Among the DMSP lyases, DddD and DddX release 3-hydroxypropionate and acryloyl-CoA, respectively. DddK/L/Q/W/Y belong to the cupin family (20). DddD belongs to type III acyl CoA transferase family. DddP is in the metallopeptidase family. DddX belongs to the ACD super family. Alma1 is a DMSP lyse encoded by algae, and it belongs to the aspartate racemase family (not shown). The X-ray crystal structures of DmdA/B/C/D, DddK/P/Q/X/Y have been solved (30, 37, 95-101). Currently, the enzyme(s) in the oxidation pathway have not been identified. Abbreviation: THF, Tetrahydrofolate; DMSO, dimethylsulfoxide.

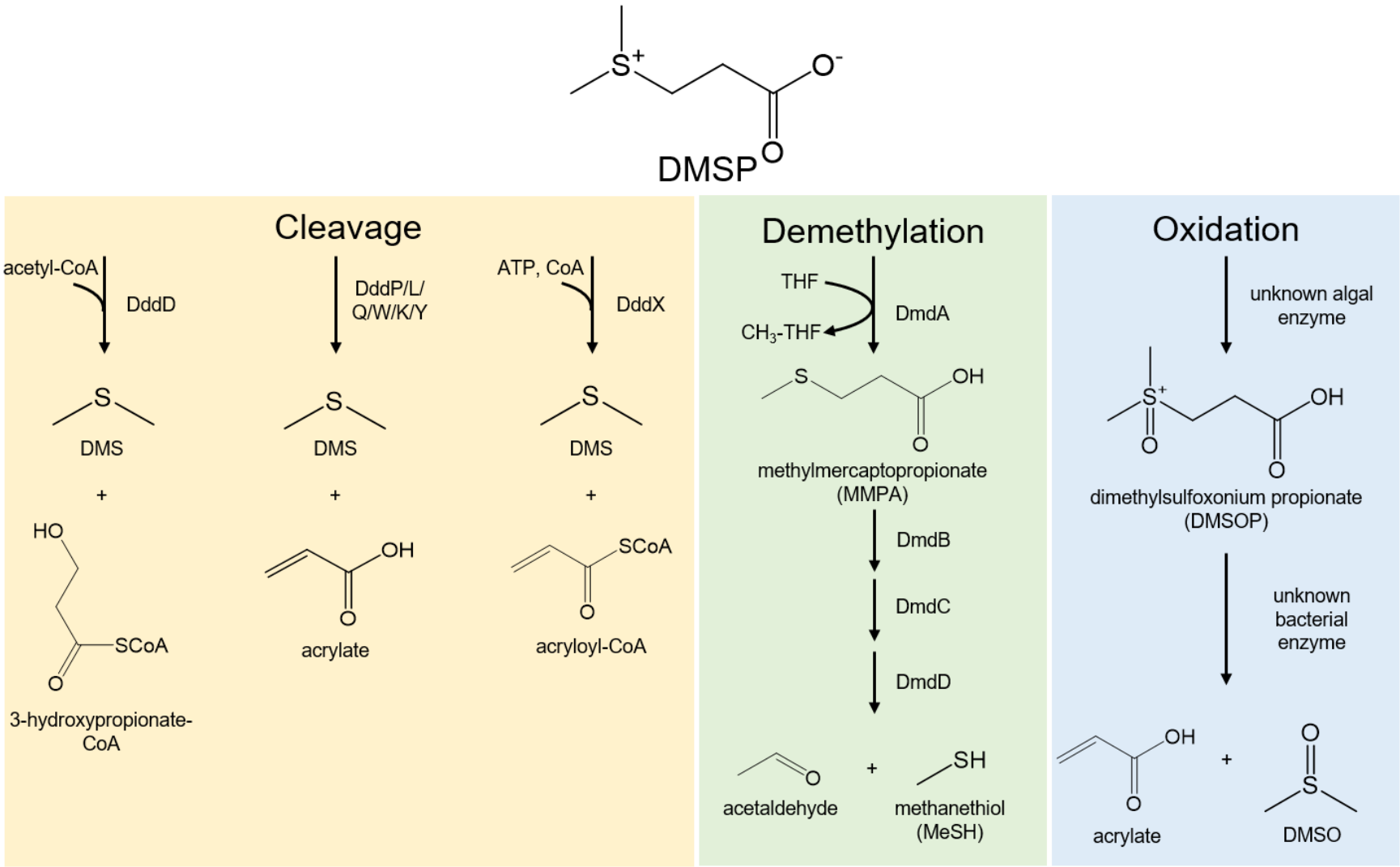
DMSP
Cleavage
acetyl-CoA
DddD
DMS
+
HO
SCoA
O
3-hydroxypropionate-CoA
DddP/L/
Q/W/K/Y
DMS
+
OH
O
acrylate
ATP, CoA
DddX
DMS
+
SCoA
O
acryloyl-CoA
Demethylation
THF
CH3-THF
DmdA
OH
methylmercaptopropionate
(MMPA)
DmdB
DmdC
DmdD
acetaldehyde
+
SH
methanethiol
(MeSH)
Oxidation
unknown algal
enzyme
OH
dimethylsulfoxonium propionate
(DMSOP)
unknown
bacterial
enzyme
OH
acrylate
+
DMSO

CHAPTER 2

OXIDATIVE STRESS REGULATES THE SWITCH OF DIMETHYLSULFONIOPROPIONATE METABOLISM FROM DEMETHYLATION TO CLEAVAGE IN *RUEGERIA POMEROYI*[1]

[1]Wang T, Huang Q, Burns A, Moran M.A., Whitman W.B. To be submitted to Nature Communications.

Abstract

Dimethylsulphoniopropionate (DMSP) is one of the most abundant low molecular weight organic compounds in marine surface water and a source of the dimethyl sulfide (DMS), the largest natural sulfur source to the upper atmosphere. Marine bacteria either mineralize DMSP largely through the demethylation pathway or transform it to DMS through the cleavage pathway. The factors that regulate which pathway is utilized are not fully understood. In chemostat experiments, the marine roseobacter *Ruegeria pomeroyi* DSS-3 was exposed to oxidative stress either during growth with H_2O_2 or a mutation of the *katG* gene, which encodes catalase, one of the major enzymes protective of oxidative stress. During growth with DMSP, the expression of genes responsive to oxidative stress was greatly reduced. During oxidative stress, the expression of the genes of encoding the demethylation pathway were reduced and expression of those encoding the cleavage pathway increased. Contrary to the sulfur demand hypothesis, under the same conditions only a small portion of the DMSP metabolized was utilized to provide sulfur for the cells. These observations are consistent with a hypothesis where oxidative stress controlled the switch in DMSP metabolism from demethylation to DMS production via the cleavage pathway.

Introduction

Dimethylsulphoniopropionate (DMSP) is an ubiquitous low molecular weight organic compound in marine surface water produced mainly by marine algae, plants, corals, and bacteria (1, 2). DMSP is an osmolyte in many of these organisms and often found in very high intracellular concentrations. In addition, it may act as an antioxidant, predator deterrent, and cryoprotectant (3-5). DMSP is also an important precursor of the volatile compound dimethyl sulfide (DMS) (6). The emission of DMS is the largest natural sulfur source to the upper atmosphere, participates in the formation of cloud condensation nuclei, and is hypothesized to connect biotic activities and the global climate (7, 8).

The transformation of DMSP to DMS is accomplished through the cleavage pathway by algae, phytoplankton, higher plants, and bacteria (9-11). So far, nine enzymes are known to have this activity, although they are from various enzyme families, have different catalytic mechanisms, and form different products, such as acrylate, acryloyl-CoA, or 3-hydroxypropionate-CoA (12). Bacteria possess at least two additional DMSP degradation pathways (13, 14). In the demethylation pathway, DMSP is processed by four enzymes, yielding MeSH as the final product. MeSH can be directly captured for methionine biosynthesis or degraded to hydrogen sulfide for sulfur assimilation (15, 16). This pathway is an important source of reduced sulfur for bacteria, which may help explain why most DMSP is processed through the demethylation pathway (17). Wirth *et al*. 2020 reported that even at a low concentration of 0.3 μM, DMSP is still the preferred sulfur source even in the presence of seawater levels of 14 mM sulfate. In the oxidation pathway, DMSP is first oxidized to dimethylsulfoxonium propionate (DMSOP) by both marine algae and bacteria. Bacteria can then

metabolize DMSOP to dimethylsulfoxide (DMSO) and acrylate (14). However, the enzymes involved in this pathway are currently not known.

The enzyme catalyzing MeSH oxidation is MtoX (15). One byproduct of this reaction is hydrogen peroxide (H_2O_2), a reactive oxygen species (ROS). The accumulation of ROS can potentially lead to oxidative stress, causing damage of cellular components including lipids, proteins, and DNA. Compared to other ROS, H_2O_2 is not very reactive and relatively stable. Because it is not charged, it can easily cross the cellular membrane (18). A major route of damage caused by H_2O_2 is through the Fenton reaction with free intracellular ferrous ions and other transition metal ions yielding the much more reactive hydroxyl radical (19). H_2O_2 is also common in marine surface water, where it is produced by solar radiation (20). The estimated concentration of H_2O_2 can reach 0.1 μM in marine surface water.

The antioxidant role of DMSP was first reported by Sunda *et al*. in 2002 (21). They found that DMSP rapidly reacts with hydroxyl radicals and serves as a cellular scavenger. Moreover, the DMSP cleavage products acrylate and DMS as well as the DMS oxidation products dimethylsulphoxide (DMSO) and methane sulfinic acid (MSNA) are also strong ROS scavengers. Thus, these molecules form an effective antioxidant system when DMSP and its degradation products are present. Many studies have confirmed this antioxidant role of DMSP in algae, corals, and plants (22-25). However, there are few studies involving this process in bacteria, the major DMSP consumers (26-28).

Bacterial metabolism of dissolved DMSP plays a major role in DMS evolution, with high levels of degradation by the demethylation pathway preventing DMS formation by the cleavage pathway or the ‘bacterial switch’ hypothesis (29). However, the factors controlling the switch are poorly understood. Possibilities that have been identified include bacterial sulfur demand (6, 29,

30) and requirements for osmolytes (6, 31). In addition, oxidative stress has been proposed to play a role. ROS are common in marine environments, being generated by algae during photosynthesis as well as abiotically by photoreactions with dissolved organic matter. A role for ROS could explain the effect of ultraviolet light stress on DMS production (32, 33) and the correlation between expression of the genes encoding the demethylation pathway and catalase in *R. pomeroyi* and field populations of the roseobacter HTCC2255 (26). To directly examine the role of oxidative stress in the bacterial switch, the relative expression of the genes encoding the demethylation and cleavage pathways was examined in chemostat cultures of *Ruegeria pomeroyi*. *R. pomeroyi* DSS-3, a member of the *Rhodobacteraceae* family of the class *Alphaproteobacteria*, is one of the most studied model organisms for DMSP catabolism. It possesses high activity for both cleavage and demethylation pathways (Figure 2-1) (16, 30, 34). In these experiments, oxidative stress was controlled by exposure to H_2O_2 in wild type and a mutant with the gene encoding catalase deleted (*ΔkatG*), and the effects on transcription of the genes for DMSP metabolism was evaluated.

Results and discussion

Establishment of chemostat conditions

One goal of the planned studies was to examine the relationship between oxidative stress and DMSP metabolism under conditions comparable to what might be found in nature, ie. slow growth and low DMSP concentrations. For this reason, conditions were sought where the response to non-lethal concentrations of H_2O_2 could be determined during chemostat growth in both wild-type and a *ΔkatG* mutant. In preliminary experiments in the absence of DMSP, 150 µM H_2O_2 rapidly killed chemostat cultures of the *ΔkatG* mutant, but the wild type tolerated at

least 3 mM H_2O_2. At 100 µM and 1 mM H_2O_2, chemostat cultures of the mutant and wild type, respectively, were able to achieve steady state growth, and these conditions were chosen for further study.

R. pomeroyi DSS-3 was previously cultivated in chemostats with a seawater-based minimum medium with 68 µM Fe(III)EDTA, an iron source required for growth. However, Fe(III)EDTA and other metal ions catalyze the degradation of H_2O_2 (35). To improve the stability of H_2O_2 throughout these experiments, a second reservoir was added to the chemostat system so that the H_2O_2 solution could be stored separately from the medium containing Fe(III)EDTA (Figure S2-1). In addition, to lower the rate of abiotic H_2O_2 decomposition during growth in the chemostat, the Fe(III)EDTA concentration was lowered. In a series of batch tests for growth on glucose, 5 µM Fe(III)EDTA supported good growth while reducing H_2O_2 decomposition, and this concentration was chosen for further studies.

Abiotic chemostat controls were performed to test the stability of DMSP and H_2O_2 under these conditions. In water alone, both DMSP and H_2O_2 were stable, and their concentrations did not change significantly after 11 days of incubation at 30 ºC. In the chemostat medium, about 40-50 % of the H_2O_2 added was consumed abiotically, presumably due to a reaction with the remaining Fe(III)EDTA and other metal ions (Table S2-2). In contrast, when DMSP was added, the concentration of H_2O_2 in the outflow increased by about 10 % of the total. Likewise, the DMSP concentration declined by 7-8 % regardless of the concentration of H_2O_2. Neither DMS nor MeSH was detected in the headspace. The reaction of H_2O_2 with Fe(III)EDTA is a radical chain reaction involving the hydroxyl radical in the chain propagation step. Because DMSP is a hydroxyl radical scavenger, it's presence may have blocked the chain reaction and lessened H_2O_2 degradation.

Chemostat growth and enzyme activities

The media for chemostat cultures contained 2 mM glucose plus or minus 0.20 mM DMSP. Under these conditions, 99 % or more of both substrates were consumed (Table 2-1; (16)). The addition of DMSP resulted in a small increase in growth yield for wild-type but not the *ΔkatG* cultures. The further addition of H_2O_2 had little if any effect on the growth yields.

The addition of H_2O_2 to the wild-type cultures had a dramatic effect on the catalase specific activity, which rapidly increased nearly two-fold within the first day of exposure (data not shown). After three days, the catalase activity reached the maximum level and remained stable (Table 1). This result was consistent with a major role for catalase in the oxidative stress response and its increased expression by ROS. When DMSP was present in the absence of H_2O_2, the catalase specific activity was reduced by about 40 % (Table 2-1). Because DMSP inhibited the abiotic degradation of H_2O_2 in this media, this result suggested that DMSP was able to mitigate oxidation stress independent of its effect on H_2O_2 concentrations. Upon the addition of H_2O_2, the catalase specific activity reached the same high level with or without DMSP (Table 2-1). Presumably the high levels of exogenous H_2O_2 saturated the protective effect of DMSP.

For the Δ*katG* mutant, the observed catalase specific activity was about 4 μmol min^{-1} mg^{-1}, or about one-third of the wild-type levels. As *katG* was the only catalase gene in *R. pomeroyi*, the catalase activity of the Δ*katG* mutant presumably reflected the activity of endogenous peroxidases or other enzymes. The specific activity did not increase upon the addition H_2O_2, a further indication that this activity was not KatG (Table 2-1). This activity was not sufficient to consume all of the H_2O_2 added to the medium, even though the amount of H_2O_2 was only one-tenth of that added to wild-type cultures. Remarkably, addition of DMSP to the Δ*katG* culture led to a decrease in the levels of H_2O_2 (Table 2-1). Since DMSP inhibited the abiotic

consumption of H_2O_2, the drop in extracellular H_2O_2 implied that DMSP stimulated a cell-dependent consumption of H_2O_2.

Transcriptional response to DMSP and oxidative stress

To further elucidate the interaction between DMSP metabolism and oxidative stress in *R. pomeroyi* , the transcriptional response was examined in 24 cDNA libraries representing eight conditions, both wild type and Δ*katG* during growth on glucose, glucose plus DMSP, glucose plus H_2O_2, and glucose plus both DMSP and H_2O_2 (Figure 2-2). A total of 9.569 to 14.848 million (M) uniquely mapped clean reads were obtained for each library (Table S2-3). The reads of all 4457 genes were counted by featureCounts and then processed by DESeq2. Replicates were also examined for differences due to batch effects, *i.e.*, different chemostat runs, methods of RNA preparation, or sequencing runs. However, no evidence was found for systematic biases due to batch effects (see Methods). In addition, the inclusion of the replicate WD1 severely reduced the number of differentially expressed genes (DEGs) calculated. For that reason, it was removed from subsequent analyses.

In principal components analysis of the entire transcriptome, a strong signal was present for growth with DMSP (Figure 2-3A). In addition, a smaller response of the Δ*katG* mutant to H_2O_2 was detected. To identify the physiological bases for these responses, the transcription of groups of functionally related genes were examined further.

Identification of oxidative stress responsive genes

To examine the relationship between oxidative stress and DMSP metabolism, genes responsive to oxidative stress were first identified. While the oxidative stress response in *R. pomeroyi* has not been studied in detail, oxidative stress has been documented in some related proteobacteria in the family *Rhodobacteraceae*, such as *Rhodobacter sphaeroides* (36, 37), and the OxyR regulon

is a well-studied group of oxidative response genes whose function is conserved in proteobacteria (38). In addition, up-regulation of genes encoding repair of DNA, proteins and lipids is often associated with oxidative stress. Thus, the genome was searched for homologs to oxidative responsive genes from other proteobacteria, and 84 candidates were identified. Their response to the presence of H_2O_2 in both the wild-type and the Δ*katG* mutant was then examined to determine their role in *R. pomeroyi* (Figure S2-2). Many of these candidates had a complex or no response to the oxidative stressors used and were not suitable indicators. As an example, *R. pomeroyi* possessed four homologs to the *Escherichia coli oxyR*, which encodes a transcription factor involved in the oxidative stress response in proteobacteria. However, the abundance of transcripts from one of them (SPO_RS20725) was very low and considered unreliable for that reason. The abundance of transcripts of two others, SPO_RS11345 and SPO_RS16785, did not respond to the addition of H_2O_2 in either the wild-type or the Δ*katG* mutant in the absence of DMSP and were not considered further. Lastly, the abundance of transcripts of only one, SPO_RS10675, was affected by the mutation or growth on H_2O_2. By these criteria, this gene as well as 17 others were chosen as indicators of oxidative stress in *R. pomeroyi* (Table 2-2).

Expression of the oxidative stress responsive genes was affected by growth in the presence of DMSP and H_2O_2 as well as the Δ*katG* mutation. In principal components analysis, the transcription of the oxidative stress responsive genes in cultures grown with DMSP were clearly distinguished from those grown without. Smaller effects were also seen for growth with H_2O_2 and between the wild-type and the Δ*katG* mutant. The expression of *katG* in the wild type increased nearly two-fold upon the addition of H_2O_2, comparable to the increase in specific activity during growth with H_2O_2. Expression of seven of the indicator genes increased in the mutant compared to the wild type (Table 2-2, Figure 2-5B). These included the genes for DNA

and Fe-S cluster repair in the *ruv* and *suf* operons, respectively. The low expression of these repair genes in wild type even with H_2O_2 addition suggested that the wild type strain was well protected against H_2O_2 exposure. Lastly, expression of Gpx, an important enzyme reducing hydroperoxides including lipid hydroperoxide (39), and *ruvC*, a gene involved in DNA repair, further increased in the mutant upon the addition of H_2O_2. These increases were evidence for the high susceptibility of the mutant to H_2O_2.

The addition of DMSP had strong effects on the expression of the oxidative stress responsive genes , especially in the mutant (Table 2-2). During growth of the mutant with DMSP, there was a two to eight-fold reduction in the expression of many of the oxidative stress responsive genes in both the presence and absence of H_2O_2. The results with the wild type were similar although fewer genes were affected. These results indicated that DMSP or the intermediates or products of its metabolism were largely protective of oxidative stress.

Interaction between oxidative stress and DMSP metabolism

In the absence of DMSP, the DMSP metabolic genes are only transcribed at low levels (40). This low level or basal expression in both the wild type and mutant was unaffected during growth with H_2O_2 (Figure 2-2C). Upon growth with DMSP, expression of genes encoding both the demethylation and cleavage pathways increased (Table 2-3, Figure 2-5). Among the demethylation genes, the largest increases were in the expression of *mtoX*, *dmdD*, *dmdC1*, and *dmdC3*. Among the cleavage genes, the largest increases were in *dddW* and *dddD*. The addition of H_2O_2 lowered the expression of the genes encoding the demethylation pathway in both the mutant and wild type. In contrast, the expression of *dddW* and *dddD* of the cleavage pathway both increased in the wild type (Table 2-3). Likewise, compared with wild type, the mutant had significantly higher expression of *dddW* and *dddD* but lower expression of *mtoX*. Thus,

oxidative stress lowered the expression of the genes of the demethylation pathway and increased expression of the genes of the cleavage pathway (Figure 2-5).

Response of sulfur metabolism to DMSP and oxidative stress

DMSP is a preferred sulfur source for *R. pomeroyi* even when the concentration is much lower than that of sulfate (16), and growth with DMSP dramatically changed the pattern of expression of the sulfur metabolism genes (Figure 2-2D). DMSP sulfur is incorporated via the demethylation pathway where both sulfide and methane thiol are intermediates for biosynthesis of the sulfur-containing amino acids (Figure 2-4). When grown only on glucose, sulfate was the only sulfur source available, and the expression of the genes involved in sulfate assimilation was high in both the wild type and the mutant. Upon the addition of DMSP, the expression of the sulfate assimilation genes was greatly reduced, as expected if DMSP was the primary sulfur source (Table 2-4). Expression of *metY,* which encodes an alternative route of biosynthesizing methionine from methanethiol, also declined (Table 2-4). Similarly, expression of 5-methyltetrahydrofolate-homocysteine methyltransferase (MTR), cysteine synthase A (*cysK*), and serine O-acetyltransferase (*cysE*) declined during growth on DMSP (Table 2-4). Possibly when intracellular methanethiol and sulfide are abundant, less of these enzymes is required to satisfy the requirement for biosynthesis of methionine and cysteine. Increases in oxidative stress either in the mutant or by the addition of H_2O_2 did not cause major changes in the expression of the genes encoding sulfate assimilation. This result shows that under oxidative stress, DMSP would likely remain the primary sulfur source.

Previous studies have shown that during growth with DMSP as the sole carbon source, the expression of the *sox* genes for sulfur oxidation were upregulated (41). The *sox* genes of *R. pomeroyi* are mainly present in a single cluster as *soxVWXYZABCDEF*, encoding enzymes

oxidizing various inorganic sulfur compounds (42, 43). When grown with DMSP, the expression of *soxC* and *soxD* increased significantly in both the wild-type and mutant (Table 2-4). These genes encode the enzyme $Sox(CD)_2$, which plays an important role in sulfur oxidation. Likewise, expression of *soxV*, a membrane protein involved in sulfur oxidation, also increased. These increases in expression would facilitate metabolism of sulfide during DMSP demethylation. However, the increases in their expression as well as that of many of the other *sox* genes was lower in the *ΔkatG* mutant than wildtype (Table 2-4). This pattern was consistent with the decreased expression of the genes encoding the demethylation pathway in the mutant. Likewise, SoeCBA is a cytoplasmic sulfite dehydrogenase (44) whose expression increased during growth with DMSP in the mutant but only in the wild type when H_2O_2 was also present (Table 2-4 and data not shown). Presumably, the increased expression of *soeCBA* was a response to increased sulfite formed from sulfide under oxidative stress. Similarly, the expression of *megL* encoding methionine gamma-lyase greatly increased upon exposure to H_2O_2 in both the wild-type and the mutant. This enzyme may play a role in metabolism of methionine sulfoxide, a common oxidation product of methionine, and may be protective of oxidative stress (45, 46).

Conclusions

In the mixed substrate chemostat used in these experiments, conditions were chosen to simulate those that might be found in nature, *i.e.*, the DMSP concentration was maintained at a low value of about 2 µM, the growth rate was slow with a doubling time of 24 hours, and the cell density remained constant. In addition, the rates of DMSP consumption and DMS and MeSH production were similar in both the wild-type and the mutant in the presence and absence of H_2O_2. Thus, in spite of the changes in the transcriptome, DMSP metabolism was not affected by the levels of

oxidative stress induced by these manipulations. Many studies have reported a low correlation between the abundance of mRNAs and proteins, indicating the importance of posttranscription regulation, translational regulation, degradation, and other regulatory processes (47). Thus, changes in gene expression and enzyme levels will only effect metabolism if they change the levels of key, rate-limiting enzymes. Nevertheless, the transcriptome still provides insights into the factors sensed by the cells and used to control metabolism.

The demand for reduced sulfur has also been proposed to be a major regulatory strategy for DMSP metabolism in *R. pomeroyi*. However, under the conditions used here, the sulfur demand would account for only a small fraction of the DMSP consumed by the demethylation pathway. For instance, in the chemostat with 2 µM DMSP, the rate of DMSP consumption by wild-type cells is 19.8 nmol min^{-1}, 0.45 nmol min^{-1} of which is consumed by the cleavage pathway and 19.3 nmol min^{-1} of which is consumed by the demethylation pathway. In contrast, the sulfur demand is about 3.4 nmol min^{-1} or about 18% of the activity of the demethylation pathway. Thus, the rate of demethylation far exceeds the sulfur demand at these concentrations. Similar results have been found at other DMSP concentrations in carbon-limited chemostats (Table 2-5). Even at lower extracellular DMSP concentrations of 0.3 µM, only 36% of the demethylation activity was needed to satisfy the sulfur demand, and at 61 µM only 1% of the demethylation activity was needed (Wirth et al., 2020). Lastly, under both 0.3 and 2 µM DMSP, the rate of DMS production was nearly the same, implying that the cleavage activity was independent of the relative sulfur demand and sulfur demand played no more than a minor role in the regulation of DMSP metabolism at these concentrations.

There is a complex interaction between DMSP metabolism and oxidative stress in *R. pomeroyi.* In response to DMSP, expression of the indicators of oxidative stress are down

regulated (Figure 2-5B), suggesting that DMSP is largely protective. In response to oxidative stress, the DMSP transcriptome shifts from the demethylation to the cleavage pathway (Figure 2-5). Like many marine roseobacters, *R. pomeroyi* is adapted to live associated with marine phytoplankton (48). Phytoplankton, including diatoms, dinoflagellates, and coccolithophores, produce both DMSP and ROS, such as superoxide and H_2O_2 (11, 49, 50). Thus, it is likely that when *R. pomeroyi* grows in the phycosphere, it is exposed to higher concentrations of both DMSP and H_2O_2 than found in open seawater (51), and cells must balance the response to both compounds. In this context, the cleavage pathway produces the strong ROS scavengers acrylate and DMS and not the oxidant H_2O_2 like the demethylation pathway, so it would be favored during oxidative stress.

Under the experimental conditions chosen here, both the expression of the *katG* gene and the catalase activity declined during growth with DMSP. In contrast, Varaljay *et al*. (2015) observed an increase in *katG* expression when *R. pomeroyi* was exposed to DMSP. However, the concentration of DMSP was 80 µM, which was much higher than the concentration used in this study. Presumably, the higher levels of DMSP may have led to increased demethylation activity and higher production of intracellular H_2O_2. The levels of H_2O_2 and not DMSP may have then regulated *katG* expression, a conclusion consistent with increases in KatG activity observed here during growth with H_2O_2.

These results are consistent with the hypothesis that, at the concentrations of DMSP investigated, oxidative stress is one of the factors controlling the bacterial switch between the demethylation and cleavage pathways in *R. pomeroyi* (Figure 2-5A). In this model, demethylation activity increases with increasing concentrations of DMSP and with it the intracellular concentration of H_2O_2 increased. The higher levels of H_2O_2 lead to increases in

oxidative stress, which then provides the signal for increased expression of the cleavage pathway, which not only reduces further H_2O_2 production but also produces more efficient scavengers for ROS, such as acrylate and DMS. Evidence to support this model include the following. 1) The cleavage pathway only become significant in cultures during growth at very high concentrations of DMSP. This result seems to preclude the sulfur demand hypothesis. Moreover, it is generally consistent with the observations of Gao *et al*. (2020), who reported that the relative expression of a cleavage pathway gene increases at high DMSP concentrations. 2) Growth on DMSP reduces the expression of oxidative stress responsive genes, suggesting that DMSP protects against oxidative stress. 3) Oxidative stress induced by the addition of H_2O_2 or the *katG* mutation reduces the expression of the demethylation genes and increases the expression of the cleavage genes.

Other regulatory schemata are also likely to play roles in oxidative stress response in *R. pomeroyi*. For instance, acrylate, the product of the cleavage pathway, is both toxic and a strong a scavenger of hydroxyl radicals. Its toxicity seems to be the basis of a complex interaction between the two DMSP catabolic pathways. *dmdA* , the first gene of the demethylation pathway, and *acuI*, which encodes the reduction of acrylyl-CoA to propionyl-CoA, share an operon that is co-regulated by both DMSP and acrylate (52, 53). Loss of a functional *acuI* abolishes *R. pomeroyi*'s ability to grow on DMSP or acrylate as sole carbon sources. This indicates that acrylate or acryloyl-CoA accumulated via the cleavage pathway are highly toxic and need to be removed even though this pathway only processes a small portion of the DMSP (16, 54). Moreover, addition of even small amounts of acrylate to cultures leads to a higher production of MeSH and DMSP demethylation activity (27). Thus, this regulatory network may serve to limit the cleavage pathway and DMS production.

Methods

Construction of catalase deletion stain (Δ*katG*)

A deletion mutant of *katG* was constructed by homologous recombination as described previously (55). Briefly, 1 kb regions up- and downstream of the *katG* gene in the *R. pomeroyi* genome and *tetAR* cassette from pRK415 were cloned into pCR2.1 using sequence and ligation-independent cloning (SLIC) (56) and electroporated into competent *R. pomeroyi* cells using a BTX Electro Cell Manipulator 630 under the following conditions: 1.8 kV, 24 μF, 200 Ω. Recombinant clones were selected on tetracycline-amended (20 μg/ml) 1/2YTSS medium (DSMZ medium 974), and the *katG* deletion was verified via PCR and sequencing. Primers used are listed in Table S2-1.

Chemostat cultivation

R. pomeroyi DSS-3 was routinely cultivated at 30 ºC on a carbon-limited chemostat. Two reservoirs were used to prevent the degradation of H_2O_2 caused by Fe(III)EDTA and other metal ions in the medium (Figure S2-1). One reservoir contained 160 mM HEPES (pH 6.8), 10 μM Fe(III)EDTA, 0.2% (v/v) trace mineral solution, and 0.2% (v/v) vitamin solution in general salts solution (16, 31, 57). Another reservoir contained 1.16 mM KH_2PO_4 solution. The two reservoirs were connected by a single pump and the flowrate was 0.05 ml/min, for a combined flow rate at the chemostat of 0.1 ml/min and leading to the final Fe(III)EDTA concentration of 5 μM. Chemostat experiments were initiated with inoculation of a glycerol stock culture of *R. pomeroyi* into 1/2YTSS broth (DSMZ 974) with 20 μg/ml tetracycline for *ΔkatG* strain in a shaking incubator at 30 ºC. After 24 hours, 1 ml of the starter culture was inoculated into the empty chemostat vessel, and the addition of fresh medium was started. The medium was supplemented

with sufficient glucose or glucose plus DMSP for final concentrations of 2 mM glucose and 0.2 mM DMSP. The chemostat was allowed to fill to its maximum volume of 144 ml at a rate of 0.1 ml/min. Air was bubbled into the chemostat at 3 ml/min. For cultures with DMSP, methanethiol and DMS present in the headspace of the chemostats and DMSP remaining in the outflow were measured daily. To add H_2O_2 into the chemostat, 2 mM or 0.2 mM H_2O_2 was applied to the phosphate solution for wild type or *ΔkatG* strains, respectively, when the culture reached steady state. At the end of each experiment, contamination of the chemostat was checked by microscopy as well as sequencing the PCR amplified 16S rRNA genes. The 16S rRNA genes were amplified with universal primers 27F (5′-AGAGTTTGATCCTGGCTCAG-3′) and 1492R (5′-TACGGYTACCTTGTTACGACTT-3′) containing 4 µl 5× Phusion HF or GC Buffer, 0.4 µl 10 mM dNTPs, 10 pmol of primer 27F, 10 pmol of primer 1492R, 200 ng genomic DNA extracted using Quick-DNA Fungal/Bacterial Miniprep Kit (Zymo Research), and 0.2 µl Phusion® High-Fidelity DNA Polymerase (New England Biolabs) brought up to a final volume of 20 µl with nuclease-free water. The reactions were performed on C1000 Touch Thermal Cycler (Bio-Rad) thermocycler under these conditions: 5 min at 98 °C, followed by 30 cycles of 30 s at 98 °C, 30 s at 55 °C and 90 s at 72 °C, and a final extension step at 72 °C for 10 min. According to the sequencing result, no contamination was founded for all chemostats.

The abiotic chemostat controls followed the same procedure for the H_2O_2 addition except that a starter culture was not added. The carbon sources were 2 mM glucose or 2 mM glucose plus 0.25 mM DMSP. After two volume changes, H_2O_2 was applied to the phosphate solution. The H_2O_2 and DMSP in the outflow were measured twice daily.

Measurement of MeSH, DMS and outflow DMSP

DMS and methanethiol were measured as previously described (16, 41). Briefly, 1 ml of the headspace gas was injected onto an SRI-8610-C gas chromatograph with a Chromosil 330 column, N_2 carrier gas at a flow rate of 60 ml/min, an oven temperature of 60°C, and a flame photometric detector. Under these conditions, methanethiol and DMS had retention times of approximately 1.30 min and 1.60 min, respectively. Standard curves generated from known amounts of DMS and methanethiol were used to convert peak areas to amounts of DMS and methanethiol in the gas phase. The DMS and methanethiol concentrations in the aqueous phase were then calculated by using the distribution coefficient for 10 ppm DMS (K_i=8.830) or MeSH (K_i=7.107) at 30°C in artificial seawater (58).

Outflow DMSP was measured by mixing 1 ml of chemostat outflow with 1 ml of 4 M NaOH in a crimp sealed 10 ml vial to hydrolyze DMSP to DMS (actual volume is 11.5 ml). 1 ml of headspace gas was analyzed after 0.5 h incubation at 30 °C. The DMSP in the outflow was calculated based on the injected DMS and the distribution coefficient mentioned above.

Quantification of H_2O_2

For measuring H_2O_2 in uninoculated medium, the absorbance at 240 nm of the diluted H_2O_2 solution was measured with a 1.16 mM KH_2PO_4 solution as the control. The concentration of H_2O_2 was calculated from the molar extinction coefficient of 43.6 $M^{-1}cm^{-1}$ at 240 nm.

For measuring H_2O_2 in the chemostat outflow, the FOX1 reaction was used with sorbitol to increase sensitivity (59). Chemostat outflow was collected on ice for 15 minutes to minimize the catalase activity during the collection. To completely inactivate catalase and adjust the sample pH, 975 µl of the outflow was acidified with 25 µl 1 M H_2SO_4. It was then centrifuged at 5,000 g for 5 min to remove the cellular debris. A series of 0-50 µM H_2O_2 standard samples was prepared by diluting fresh 1 mM H_2O_2 in sterile medium acidified as above. 200 µl of FOX1

reagent [100 μM xylenol orange, 250 μM $(NH_4)_2Fe(SO_4)_2$, 100 mM sorbitol in 25 mM H_2SO_4] was mixed with 20 μl of each sample in duplicate for the standard or triplicate for the chemostat outflow. After incubating at room temperature for 20 minutes, the absorbance at 595 nm was read in a plate reader (BioTek Synergy Mx).

Catalase assay

To measure the enzyme activity of chemostat culture, the fresh outflow was collected and assayed immediately. Cell dry weight was calculated from the absorbance at 660 nm by the equation: dry weight (μg/ml) = $364.74A_{660} + 6.7A_{660} \times A_{660}$. The protein was estimated as 55% of the cell dry weight. The assays were set as described by Chance and Maehly with modification (60).

Briefly, culture was directly mixed with equal volume of 0.05% (v/v) H_2O_2 in 50 mM potassium phosphate buffer (pH 7.0). The absorbance at 240 nm was monitored for 3 minutes at 30 °C. The H_2O_2 concentration was calculated from the molar extinction coefficient of 43.6 $M^{-1}cm^{-1}$ at 240 nm.

RNA extraction and sequencing

The chemostat outflow for RNA extraction was collected in pre-chilled 5% (w/v) phenol-ethanol solution on ice to stabilize mRNA. After 4 hours, the collections were centrifuged at 5,000 g for 20 minutes at 4 ºC. Cell pellets were either stored at -80 ºC or processed for RNA extraction immediately. For each condition, three samples were collected. Total RNA extraction and DNA digestion were performed using the Zymo BIOMICS RNA Miniprep kit (Zymo Research) with elongated bead beating. The quality of purified total RNA was then checked with agarose gel electrophoresis, Qubit RNA HS assays (Invitrogen) and nanodrop. Some samples were further purified with the RNA Clean & Concentrator kit (Zymo Research). The eligible samples were

sent to Novogene for the subsequent steps. Ribosomal RNA was removed using the Ribo-Zero kit. Strand-specific cDNA libraries were prepared and sequenced using an Illumina NovaSeq 6000 Sequencing System with a read length of PE150.

Bioinformatic analysis

Raw data was trimmed by Trim galore to remove adapters and reads with quality scores lower than 20 (61). Reads were mapped to the *R. pomeroyi* DSS-3 genome using Bowtie2 (Version 2.4.2) and counted using featureCounts (Version 2.0.1) (62, 63). Differential expression of genes between each condition was calculated using DESeq2 (Version 3.12) in R (Version 4.0.5) with *apeglm* type shrinkage of log2 fold changes (64, 65). When comparing different conditions to the wild type with no additions or the W transcriptome, 23 samples without WD1 were processed by DESeq2 together and each condition was chosen to be the experimental condition with wild type with no additions as the control condition. A shrinkage estimator was not used.

A total of 9.569 to 14.848 million (M) uniquely mapped clean reads were obtained for the subsequent analyses (Table S2-3). The average Q30 was 94.06%, and the lowest was 93.08%. The average GC content was 64.09 mol %, which was close to the genome GC content of 64.1 mol %. The average overall alignment rate without sample K1 was 98.87 % with a range of 95.21-100 %. K1 had a low overall alignment rate of 82.22 %, and it was found to have a 16.32 % overall alignment rate to the *Escherichia coli* genome (K-12 substr. MG1655). As no contamination was found throughout growth, this contamination appeared to have occurred during the downstream processing of the sample and should not have affected the reliability of the *R. pomeroyi* reads, which were included in the subsequent analyses.

The reads of all 4457 genes were counted by featureCounts and then processed by DEseq2. The PCA (Figure 2-3) shows that among all of the conditions, often one replicate did

not cluster with the other replicates. One possible reason leading to these differences could be batch effects during sample processing. For example, some samples failed the quality check for library construction so that additional replicate samples were prepared from different chemostat runs. Similarly, some replicates were sequenced at different times. These 'batch' effects may have contributed to the observed differences between the replicates. To look for batch effects, the distances between replicates were calculated from the regularized-logarithm transformations (rlog) of the raw counts of all 24 samples (Table S2-4). For 14 replicates, there were no batch differences in their processing, and the average difference (± standard deviation) was 35±18. Six replicates differed only in the sequencing run, and the average difference was 42±18. Lastly, four replicates differed in both the chemostat run and RNA purification procedure, and the average difference was 48±10. Because the differences were not significantly different between replicates processed in different batches, the batch effects were likely to be small.

Upon calculation of the differential expressed genes (DEGs) for each of the comparisons in Figure 2-2, it was found thar the number of DEGs was greatly reduced for comparisons including replicate WD1. When WD1 was dropped in subsequent analyses, the number of DEGs was comparable to other comparisons even though only two replicates were used for the WD condition.

For principal component analysis, all 23 samples were normalized together first by DESeq2. The results were calculated and plotted by DESeq2 by the normalized counts of selected genes.

References

1. Reisch CR, Moran MA, Whitman WB. 2011. Bacterial catabolism of dimethylsulfoniopropionate (DMSP). Front Microbiol 2:172.
2. Curson AR, Liu J, Martínez AB, Green RT, Chan Y, Carrión O, Williams BT, Zhang S-H, Yang G-P, Page PCB. 2017. Dimethylsulfoniopropionate biosynthesis in marine bacteria and identification of the key gene in this process. Nat Microbiol 2:17009.
3. Cosquer A, Pichereau V, Pocard J-A, Minet J, Cormier M, Bernard T. 1999. Nanomolar levels of dimethylsulfoniopropionate, dimethylsulfonioacetate, and glycine betaine are sufficient to confer osmoprotection to *Escherichia coli*. Appl and Environ Microbiol 65:3304-3311.
4. Wolfe GV, Steinke M, Kirst GO. 1997. Grazing-activated chemical defence in a unicellular marine alga. Nature 387:894-897.
5. Karsten U, Kück K, Vogt C, Kirst G. 1996. Dimethylsulfoniopropionate production in phototrophic organisms and its physiological functions as a cryoprotectant, p 143-153, *In* Kiene RP, Visscher PT, Keller MD, Kirst GO (ed), Biological and Environmental Chemistry of DMSP and Related Sulfonium Compounds. Springer US, Boston, MA.
6. Kiene RP, Linn LJ, Bruton JA. 2000. New and important roles for DMSP in marine microbial communities. J Sea Res 43:209-224.
7. Charlson RJ, Lovelock JE, Andreae MO, Warren SG. 1987. Oceanic phytoplankton, atmospheric sulphur, cloud albedo and climate. Nature 326:655-661.
8. Kettle A, Andreae M. 2000. Flux of dimethylsulfide from the oceans: A comparison of updated data sets and flux models. J Geophys Res Atmos 105:26793-26808.

9. Taylor BF, Visscher PT. 1996. Metabolic pathways involved in DMSP degradation, p 265-276, *In* Kiene RP, Visscher PT, Keller MD, Kirst GO (ed), Biological and Environmental Chemistry of DMSP and Related Sulfonium Compounds. Springer US, Boston, MA.

10. Andreae MO. 1990. Ocean-atmosphere interactions in the global biogeochemical sulfur cycle. Mar Chem 30:1-29.

11. Bullock HA, Luo H, Whitman WB. 2017. Evolution of dimethylsulfoniopropionate metabolism in marine phytoplankton and bacteria. Front Microbiol 8:637.

12. Li C-Y, Wang X-J, Chen X-L, Sheng Q, Zhang S, Wang P, Quareshy M, Rihtman B, Shao X, Gao C. 2021. A novel ATP dependent dimethylsulfoniopropionate lyase in bacteria that releases dimethyl sulfide and acryloyl-CoA. Elife 10:e64045.

13. Howard EC, Henriksen JR, Buchan A, Reisch CR, Burgmann H, Welsh R, Ye W, Gonzalez JM, Mace K, Joye SB. 2006. Bacterial taxa that limit sulfur flux from the ocean. Science 314.

14. Thume K, Gebser B, Chen L, Meyer N, Kieber DJ, Pohnert G. 2018. The metabolite dimethylsulfoxonium propionate extends the marine organosulfur cycle. Nature 563:412-415.

15. Eyice Ö, Myronova N, Pol A, Carrión O, Todd JD, Smith TJ, Gurman SJ, Cuthbertson A, Mazard S, Mennink-Kersten MA. 2018. Bacterial SBP56 identified as a Cu-dependent methanethiol oxidase widely distributed in the biosphere. ISME J 12:145-160.

16. Wirth JS, Wang T, Huang Q, White RH, Whitman WB. 2020. Dimethylsulfoniopropionate sulfur and methyl carbon assimilation in *Ruegeria* species. mBio 11:e00329-20.

Kiene RP. 1996. Production of methanethiol from dimethylsulfoniopropionate in marine surface waters. Mar Chem 54:69-83.

18. Gutteridge JM. 1994. Biological origin of free radicals, and mechanisms of antioxidant protection. Chem Biol Interact 91:133-140.

19. Imlay JA, Chin SM, Linn S. 1988. Toxic DNA damage by hydrogen peroxide through the Fenton reaction *in vivo* and *in vitro*. Science 240:640-642.

20. Mopper K, Kieber DJ. 2000. Marine photochemistry and its impact on carbon cycling. p101-129. *In* Mora SD, Demers S, Vernet M (ed), The effects of UV radiation in the marine environment. Cambridge University Press.

21. Sunda W, Kieber D, Kiene R, Huntsman S. 2002. An antioxidant function for DMSP and DMS in marine algae. Nature 418:317-320.

22. Van Alstyne KL, Sutton L, Gifford S-A. 2020. Inducible versus constitutive antioxidant defenses in algae along an environmental stress gradient. Mar Ecol Prog Ser 640:107-115.

23. Deschaseaux ES, Jones GB, Deseo MA, Shepherd KM, Kiene R, Swan H, Harrison PL, Eyre BD. 2014. Effects of environmental factors on dimethylated sulfur compounds and their potential role in the antioxidant system of the coral holobiont. Limnol Oceanogr 59:758-768.

24. Husband JD, Kiene RP, Sherman TD. 2012. Oxidation of dimethylsulfoniopropionate (DMSP) in response to oxidative stress in *Spartina alterniflora* and protection of a non-DMSP producing grass by exogenous DMSP + acrylate. Environ Exp Bot 79:44-48.

25. Jones GB, King S. 2015. Dimethylsulphoniopropionate (DMSP) as an indicator of bleaching tolerance in scleractinian corals. J Mar Sci Eng 3:444-465.

Varaljay VA, Robidart J, Preston CM, Gifford SM, Durham BP, Burns AS, Ryan JP, Marin III R, Kiene RP, Zehr JP. 2015. Single-taxon field measurements of bacterial gene regulation controlling DMSP fate. ISME J 9:1677-1686.

27. Landa M, Burns AS, Durham BP, Esson K, Nowinski B, Sharma S, Vorobev A, Nielsen T, Kiene RP, Moran MA. 2019. Sulfur metabolites that facilitate oceanic phytoplankton-bacteria carbon flux. ISME J 13:2536-2550.

28. Bullock HA, Reisch CR, Burns AS, Moran MA, Whitman WB. 2014. Regulatory and Functional diversity of methylmercaptopropionate coenzyme A ligases from the dimethylsulfoniopropionate demethylation pathway in *Ruegeria pomeroyi* DSS-3 and other proteobacteria. J Bacteriol 196:1275-1285.

29. Simó R. 2001. Production of atmospheric sulfur by oceanic plankton: biogeochemical, ecological and evolutionary links. Trends Ecol Evol 16:287-294.

30. González JM, Kiene RP, Moran MA. 1999. Transformation of sulfur compounds by an abundant lineage of marine bacteria in the α-subclass of the class *Proteobacteria*. Appl Environ Microbiol 65:3810-3819.

31. Reisch CR, Moran MA, Whitman WB. 2008. Dimethylsulfoniopropionate-dependent demethylase (DmdA) from *Pelagibacter ubique* and *Silicibacter pomeroyi*. J Bacteriol 190:8018-8024.

32. Slezak D, Kiene RP, Toole DA, Simó R, Kieber DJ. 2007. Effects of solar radiation on the fate of dissolved DMSP and conversion to DMS in seawater. Aquat Sci 69:377-393.

33. Levine NM, Varaljay VA, Toole DA, Dacey JW, Doney SC, Moran MA. 2012. Environmental, biochemical and genetic drivers of DMSP degradation and DMS production in the Sargasso Sea. Environ Microbiol 14:1210-1223.

34. González JM, Covert JS, Whitman WB, Henriksen JR, Mayer F, Scharf B, Schmitt R, Buchan A, Fuhrman JA, Kiene RP, Moran MA. 2003. *Silicibacter pomeroyi* sp. nov. and *Roseovarius nubinhibens* sp. nov., dimethylsulfoniopropionate-demethylating bacteria from marine environments. Int J Syst Evol Microbiol 53:1261-1269.

35. Walling C, Partch RE, Weil T. 1975. Kinetics of the decomposition of hydrogen peroxide catalyzed by ferric ethylenediaminetetraacetate complex. Proc Natl Acad Sci U S A 72:140-142.

36. Zeller T, Moskvin OV, Li K, Klug G, Gomelsky M. 2005. Transcriptome and physiological responses to hydrogen peroxide of the facultatively phototrophic bacterium *Rhodobacter sphaeroides*. J Bacteriol 187:7232-7242.

37. Zeller T, Mraheil MA, Moskvin OV, Li K, Gomelsky M, Klug G. 2007. Regulation of hydrogen peroxide-dependent gene expression in *Rhodobacter sphaeroides*: regulatory functions of OxyR. J Bacteriol 189:3784-3792.

38. Chiang SM, Schellhorn HE. 2012. Regulators of oxidative stress response genes in *Escherichia coli* and their functional conservation in bacteria. Arch Biochem Biophys 525:161-169.

39. Kurutas EB. 2015. The importance of antioxidants which play the role in cellular response against oxidative/nitrosative stress: current state. Nutr J 15:1-22.

40. Gao C, Fernandez VI, Lee KS, Fenizia S, Pohnert G, Seymour JR, Raina J-B, Stocker R. 2020. Single-cell bacterial transcription measurements reveal the importance of dimethylsulfoniopropionate (DMSP) hotspots in ocean sulfur cycling. Nat Commun 11:1942.

41. Reisch CR, Crabb WM, Gifford SM, Teng Q, Stoudemayer MJ, Moran MA, Whitman WB. 2013. Metabolism of dimethylsulphoniopropionate by *Ruegeria pomeroyi* DSS-3. Mol Microbiol 89:774-791.

42. Friedrich CG, Bardischewsky F, Rother D, Quentmeier A, Fischer J. 2005. Prokaryotic sulfur oxidation. Curr Opin Microbiol 8:253-259.

43. Rother D, Henrich H-Jr, Quentmeier A, Bardischewsky F, Friedrich CG. 2001. Novel genes of the *sox* gene cluster, mutagenesis of the flavoprotein SoxF, and evidence for a general sulfur-oxidizing system in *Paracoccus pantotrophus* GB17. J Bacteriol 183:4499-4508.

44. Dahl C, Franz B, Hensen D, Kesselheim A, Zigann R. 2013. Sulfite oxidation in the purple sulfur bacterium *Allochromatium vinosum*: identification of SoeABC as a major player and relevance of SoxYZ in the process. Microbiology 159:2626-2638.

45. Morozova E, Bazhulina N, Anufrieva N, Mamaeva D, Tkachev Y, Streltsov S, Timofeev V, Faleev N, Demidkina T. 2010. Kinetic and spectral parameters of interaction of Citrobacter freundii methionine γ-lyase with amino acids. Biochem (Mosc) 75:1272-1280.

46. Morozova E, Kulikova V, Yashin D, Anufrieva N, Anisimova N, Revtovich S, Kotlov M, Belyi Y, Pokrovsky V, Demidkina T. 2013. Kinetic parameters and cytotoxic activity of recombinant methionine γ-lyase from *Clostridium tetani*, *Clostridium sporogenes*, *Porphyromonas gingivalis* and *Citrobacter freundii*. Acta Naturae 5:92-98.

47. Vogel C, Marcotte EM. 2012. Insights into the regulation of protein abundance from proteomic and transcriptomic analyses. Nat Rev Genet 13:227-232.

48. Moran MA, Buchan A, González JM, Heidelberg JF, Whitman WB, Kiene RP, Henriksen JR, King GM, Belas R, Fuqua C. 2004. Genome sequence of *Silicibacter pomeroyi* reveals adaptations to the marine environment. Nature 432:910-913.

49. Diaz JM, Plummer S, Tomas C, Alves-de-Souza C. 2018. Production of extracellular superoxide and hydrogen peroxide by five marine species of harmful bloom-forming algae. J Plankton Res 40:667-677.

50. Zinser ER. 2018. The microbial contribution to reactive oxygen species dynamics in marine ecosystems. Environ Microbiol Rep 10:412-427.

51. Seymour JR, Amin SA, Raina J-B, Stocker R. 2017. Zooming in on the phycosphere: the ecological interface for phytoplankton-bacteria relationships. Nat Microbiol 2:1-12.

52. Bürgmann H, Howard EC, Ye W, Sun F, Sun S, Napierala S, Moran MA. 2007. Transcriptional response of *Silicibacter pomeroyi* DSS-3 to dimethylsulfoniopropionate (DMSP). Environmental microbiology 9:2742-2755.

53. Kirkwood M. 2012. Genetic analysis of DMSP metabolism in the marine Roseobacter clade. Doctoral thesis, University of East Anglia

54. Todd JD, Curson AR, Sullivan MJ, Kirkwood M, Johnston AW. 2012. The *Ruegeria pomeroyi acuI* gene has a role in DMSP catabolism and resembles *yhdH* of *E. coli* and other bacteria in conferring resistance to acrylate. PloS One 7:e35947.

55. Reisch CR, Stoudemayer MJ, Varaljay VA, Amster IJ, Moran MA, Whitman WB. 2011. Novel pathway for assimilation of dimethylsulphoniopropionate widespread in marine bacteria. Nature 473:208-211.

56. Li MZ, Elledge SJ. 2007. Harnessing homologous recombination in vitro to generate recombinant DNA via SLIC. Nat Methods 4:251-256.

57. Sarmiento FB, Leigh JA, Whitman WB. 2011. Genetic systems for hydrogenotrophic methanogens. Methods Enzymol 494:43-73.

58. Przyjazny A, Janicki W, Chrzanowski W, Staszewski R. 1983. Headspace gas chromatographic determination of distribution coefficients of selected organosulphur compounds and their dependence on some parameters. J Chromatogr 280:249-260.

59. Wolff SP. 1994. Ferrous ion oxidation in presence of ferric ion indicator xylenol orange for measurement of hydroperoxides. Methods Enzymol 233:182-189.

60. Chance B, Maehly A. 1955. Assay of catalases and peroxidases. Methods Enzymol 2:764-775.

61. Krueger F, James F, Ewels P, Afyounian E, Schuster-Boeckler B. 2021. FelixKrueger/TrimGalore: v0.6.7 - DOI via Zenodo. doi:10.5281/zenodo.5127899.

62. Langmead B, Salzberg SL. 2012. Fast gapped-read alignment with Bowtie 2. Nat Methods 9:357-359.

63. Liao Y, Smyth GK, Shi W. 2014. featureCounts: an efficient general purpose program for assigning sequence reads to genomic features. Bioinformatics 30:923-930.

64. Zhu A, Ibrahim JG, Love MI. 2019. Heavy-tailed prior distributions for sequence count data: removing the noise and preserving large differences. Bioinformatics 35:2084-2092.

65. Love MI, Huber W, Anders S. 2014. Moderated estimation of fold change and dispersion for RNA-seq data with DESeq2. Genome biology 15:1-21.

Table 2-1. DMSP consumption and metabolic data of *R. pomeroyi* strains during chemostat growth on glucose or glucose and DMSP before and after H_2O_2 additions. [1]

Parameter	Unit	Wild type		*ΔkatG*	
		Glucose	Glucose + DMSP	Glucose	Glucose + DMSP
Inflow glucose	nmol min^{-1}	200	200	200	200
Inflow DMSP	nmol min^{-1}	0	20	0	20
Before adding H_2O_2 [2]					
OD600	NA	0.30±0.00	0.36±0.01	0.33±0.01	0.33±0.01
Cell dry weight [3]	μg/ml	110±0	133±2	121±2	122±3
MeSH produced	nmol min^{-1}	NA	0.04±0.01	NA	0.06±0.01
DMS produced	nmol min^{-1}	NA	0.45±0.02	NA	0.45±0.08
Outflow DMSP	nmol min^{-1}	NA	0.20±0.01	NA	0.18±0.01
Catalase activity[4]	μmol min^{-1} mg^{-1}	11.4±0.5	6.9±0.2	4.4±0.3	1.8±0.4
After adding H_2O_2 [5]					
Inflow H_2O_2 [6]	μM	975	1045	110	107
OD600	NA	0.31±0.01	0.30±0.00	0.35±0.01	0.34±0.01
Cell dry weight	μg/ml	112±2	112±1	129±3	126±2
Outflow H_2O_2	μM	<1	<1	5.8±1.3	<1
MeSH produced	nmol min^{-1}	NA	0.06±0.01	NA	0.05±0.01
DMS produced	nmol min^{-1}	NA	0.50±0.05	NA	0.38±0.06
Outflow DMSP	nmol min^{-1}	NA	0.19±0.02	NA	0.24±0.04
Catalase activity	μmol min^{-1} mg^{-1}	24.3±0.4	24.0±0.5	1.8±0.8	3.0±0.4

[1]The 95% confidence intervals are based on three measurements unless indicated otherwise. NA: not applicable.

[2]The data reported are the means (n=6) of results for the last two days of steady state before the addition of H_2O_2 except for the OD600, where n=4. All cultures had a background H_2O_2 concentrations of less than 1 μM.

[3]Cell dry weights were calculated from the absorbance at 660 nm by the equation: dry weight = $364.74A_{660} + 6.7A_{660} \times A_{660}$.

[4]For catalase specific activity, 55% of the cell dry weight was assumed to be protein. Catalase activity was measured on whole cultures collected from the chemostat outflow, and the average of three determinations are reported.

[5]After adding H_2O_2, all the parameters were measured three times daily. The data reported are the means (n=9) of results for day 3 to day 5 after adding H_2O_2 except for OD600, where n=6.

[6]The inflow H_2O_2 is calculated from the concentration measured in the reservoir.

Table 2-2. Fold change of expression of selected oxidative stress responsive genes. Abbreviations for growth conditions are defined in Figure 2-2. Each comparison was made to the wild-type with no additions or W transcriptome. Conditions in parentheses are controls for each comparison. NA: cannot be compared due to the gene deletion.

Genes	Locus tag[1]	Annotations	WH	WD	WDH	K	KH	KD	KDH
katG	20080	catalase-peroxidase	2.120*	0.703	0.936	NA	NA	NA	NA
soxR	04980	redox-sensitive transcriptional activator	0.614	0.909	0.620	0.630	0.452	0.497	0.233**
soxS	04985	regulatory protein	0.935	3.218**	2.699**	0.855	0.949	1.394	2.021**
sodB	11860	Fe-Mn family superoxide dismutase	0.992	0.567	0.227**	0.686	0.769	0.451*	0.154**
oxyR	10675	H_2O_2-inducible genes activator	1.029	0.588	1.013	2.596**	2.153**	0.862	1.212
lexA	10920	SOS response genes repressor	0.851	0.391*	0.297**	2.871*	1.791	0.330**	0.203**
GPx	18990	glutathione peroxidase	1.072	1.655	1.786*	3.228**	19.504**	1.722*	2.167**
recA	10320	recombinase	0.701	0.595	0.357**	2.320	2.113	0.436*	0.162**
mutT	00305	8-oxo-dGTP diphosphatase	1.202	1.225	1.087	1.544	1.528**	1.323	1.061
ruvB	15785	Holliday junction DNA helicase	1.054	1.085	1.567**	2.136**	1.873**	1.223	1.620**
ruvA	15790	Holliday junction DNA helicase	1.063	0.965	1.488**	2.147**	2.156**	1.223	1.697**
ruvC	15795	crossover junction endodeoxyribonuclease	1.412	1.460	3.448**	2.637*	5.608**	2.808**	4.431**
uvrA	11250	excinuclease ABC subunit A	0.922	1.218	0.839	1.823	1.814**	0.825	0.511**
uvrB	02750	excinuclease ABC subunit B	1.033	1.324	1.110	1.280	1.430**	0.951	0.883
uvrD	05950	excinuclease ABC subunit C	0.760	0.672	0.590**	1.362	1.093	0.528**	0.386**
sufD	10235	Fe-S cluster assembly protein	1.069	0.548	0.422**	1.554	1.494	0.446**	0.427**

sufC	10240	Fe-S cluster assembly ATPase	1.317	1.179	0.890	2.150**	3.068**	0.987	0.744
sufB	10265	Fe-S cluster assembly protein	0.950	1.033	0.836	2.093	3.431**	0.971	0.415**

[1]all locus tags have the prefix SPO_RS

*: adjusted p value <0.1.

**: adjusted p value <0.05.

Table 2-3. Fold change of expression of DMSP metabolism genes under each condition compared to wild-type with no additions or W transcriptome. Abbreviations for growth conditions are defined in Figure 2-2.

Genes	Locus tag[1]	Annotations	WH	WD	WDH	K	KH	KD	KDH
demethylation pathway genes									
dmdA	09710	DMSP demethylase	1.347	2.309**	2.100**	1.277	1.066	2.406**	1.847**
dmdB1	10375	MMPA-CoA ligase	1.027	1.070	0.712	1.154	0.876	0.726	0.346**
dmdB2	03420	MMPA-CoA ligase	1.147	1.195	1.277	1.583*	0.867	1.234	1.421**
dmdC1	19300	MMPA-CoA dehydrogenase	0.910	3.422**	2.849**	1.180	1.819	3.719**	2.084**
dmdC2	01515	MMPA-CoA dehydrogenase	1.487	2.605	1.601	3.223	1.038	1.418	0.475
dmdC3	14785	MMPA-CoA dehydrogenase	1.114	3.957**	2.449*	2.127	0.967	2.099	0.734
dmdD	19305	MTA-CoA hydratase	1.476	4.966**	2.217**	1.038	2.012	3.535**	1.720
acuH	00755	enoyl -CoA hydratase	1.021	0.991	0.539	0.747	1.063	0.692	0.261**
mtoX	21180	methanethiol oxidase	1.004	39.371**	13.000**	1.091	1.021	15.110**	4.171**
cleavage pathway genes									
dddD	08640	DMSP lyase	0.911	1.105	2.480**	1.000	1.390	2.958**	4.846**
dddP	11655	DMSP lyase	0.744	1.004	1.069	0.700	0.709*	1.006	1.081
dddQ	22175	DMSP lyase	1.098	1.079	1.586*	0.911	0.828	1.257	1.874**
dddW	02290	DMSP lyase	2.169	4.304**	14.979**	1.943	8.304**	12.113**	20.800**
acuI	09715	NADPH-dependent acryloyl-CoA reductase	1.114	1.693	1.356	1.010	1.248	1.474	1.420
other DMSP pathway genes									

adlH	00490	aldehyde dehydrogenase	1.364	1.077	1.082	1.092	0.855	0.827	1.042
prpE	14880	propionyl-CoA synthetase	1.974	1.101	0.736	1.546	0.861	0.843	0.543**

*: adjusted p value <0.1.

**: adjusted p value <0.05.

[1]all locus tags have the prefix SPO_RS.

Table 2-4. Fold change of expression of selected sulfur metabolism genes under each condition compared to wild-type with no additions or W transcriptome. Abbreviations for growth conditions are defined in Figure 2-2.

Genes	Locus tag[1]	Annotations	WH	WD	WDH	K	KH	KD	KDH
		sulfate reduction genes							
cysJI	13360	sulfite reductase	1.538	0.029**	0.056**	1.132	2.018	0.046**	0.088**
cysH	13365	phosophoadenylyl-sulfate reductase	1.290	0.030**	0.079**	0.987	1.227	0.054**	0.094**
SAT	04535	bifunctional sulfate adenylyltransferase/adenylylsulfate kinase	2.084	0.535	0.506	1.516	2.424	0.603	0.442
		sulfur oxidation *sox* enzyme system							
soxV	04990	sulfur oxidation V protein	1.310	5.607**	21.655**	1.046	7.365**	14.899**	31.372**
soxW	04995	thioredoxin	0.662	0.849	0.585*	0.901	0.450**	0.483**	0.310**
soxX	05000	L-cysteine S-thiosulfotransferase	0.710	1.890*	1.347	1.055	0.369**	0.474**	0.398**
soxY	05005	sulfur oxidation Y protein	0.550	1.068	0.666	0.770	0.262**	0.325**	0.326**
soxZ	05010	sulfur oxidation Z protein	0.620	0.999	0.462*	0.704	0.216**	0.171**	0.073**
soxA	05015	L-cysteine S-thiosulfotransferase	0.645	1.088	0.651	0.828	0.303**	0.344**	0.284**
soxB	05020	S-sulfosulfanyl-L-cysteine sulfohydrolase	0.682	2.754**	2.302**	0.845	0.409**	1.029	1.387
soxC	05025	sulfur oxidation molybdopterin C protein	0.695	10.367**	10.058**	0.960	1.536	3.637**	5.234**
soxD	05030	S-disulfanyl-L-cysteine oxidoreductase	0.759	5.763**	5.591**	0.926	1.104	2.239**	3.523**
soxE	05035	diheme cytochrome C	0.984	1.516	1.186	0.705	0.447**	0.692	0.829
soxF	05040	sulfide-cytochrome-c reductase	0.500**	0.733	0.638*	0.598	0.352**	0.319**	0.364**
		quinone-reducing molybdenum sulfite dehydrogenase SoeABC							

soeC	17005	sulfite dehydrogenase subunit C	1.456	1.805	6.018**	0.981	2.885**	4.516**	8.861**
soeB	17010	sulfite dehydrogenase subunit B	0.856	1.208	1.664*	1.118	1.245	1.423	2.160**
soeA	17015	sulfite dehydrogenase subunit A	1.067	1.205	3.568**	1.633	4.533**	3.150**	5.716**
		methionine and cysteine metabolism genes							
metY	07295	O-acetyl-L-homoserine sulfhydrylase	1.379	0.879	0.456**	0.834	0.706	0.578**	0.317**
metZ	06880	O-succinyl-L-homoserine sulfhydrylase	1.385	0.704	1.019	0.929	2.006	1.098	1.499
megL	21430	methionine gamma-lyase	1.235	4.841*	38.284**	1.242	14.694**	27.219**	58.386**
MTR	09575	5-methyltetrahydrofolate-homocysteine methyltransferase	0.736	0.515*	0.336**	1.086	0.560**	0.368**	0.203**
cysQ	00195	3'(2'),5'-bisphosphate nucleotidase	1.228	1.330	0.947	0.746	1.265	1.236	0.628
cysK	11395	cysteine synthase A	1.211	0.367**	0.193**	0.929	1.392	0.184**	0.104**
cysE	11400	serine O-acetyltransferase	0.960	0.773	0.410**	0.947	0.704	0.426**	0.166**

*: adjusted p value <0.1.

**: adjusted p value <0.05.

[1]all locus tags have the prefix SPO_RS.

Table 2-5. DMSP consumption by *R. pomeroyi* during chemostat growth on glucose plus DMSP. [1]

Parameter	units	100 µM[2]	200 µM	5000 µM[2]
Inflow DMSP	nmol min^{-1}	10	20	500
DMSP concentration	µM	0.3	2.0	61
DMSP metabolized	nmol min^{-1}	10.0	19.8	494
Demethylation activity	nmol min^{-1}	9.6	19.3	35.3
Cleavage activity	nmol min^{-1}	0.4	0.5	93.6

[1]Chemostats where carbon-limited and fed 200 nmol min^{-1} (or 2 mM) glucose plus the indicated amounts of DMSP. Dilution rates were 1 da^{-1} in minimal medium as described in Table 1 and the methods.

[2]Calculated from the data in Table 1 of Wirth et al. (2020). The chemostats were run under the same conditions as this study but with 68 µM Fe(III)EDTA.

Figure 2-1. DMSP metabolic pathways in *R. pomeroyi* DSS-3. Genes: *dmdA* (SPO_RS09710), *dmdB* (SPO_RS10375, SPO_RS03420), *dmdC* (SPO_RS19300, SPO_RS01515, SPO_RS14785), *dmdD* (SPO_RS19305), *acuH*(SPO_RS00755), *adlH* (SPO_RS00490), *mtoX* (SPO_RS21180), *dddD* (SPO_RS08640), *dddP* (SPO_RS11655), *dddQ* (SPO_RS22175), *dddW* (SPO_RS02290), *prpE* (SPO_RS14880), and *acuI* (SPO_RS09715).

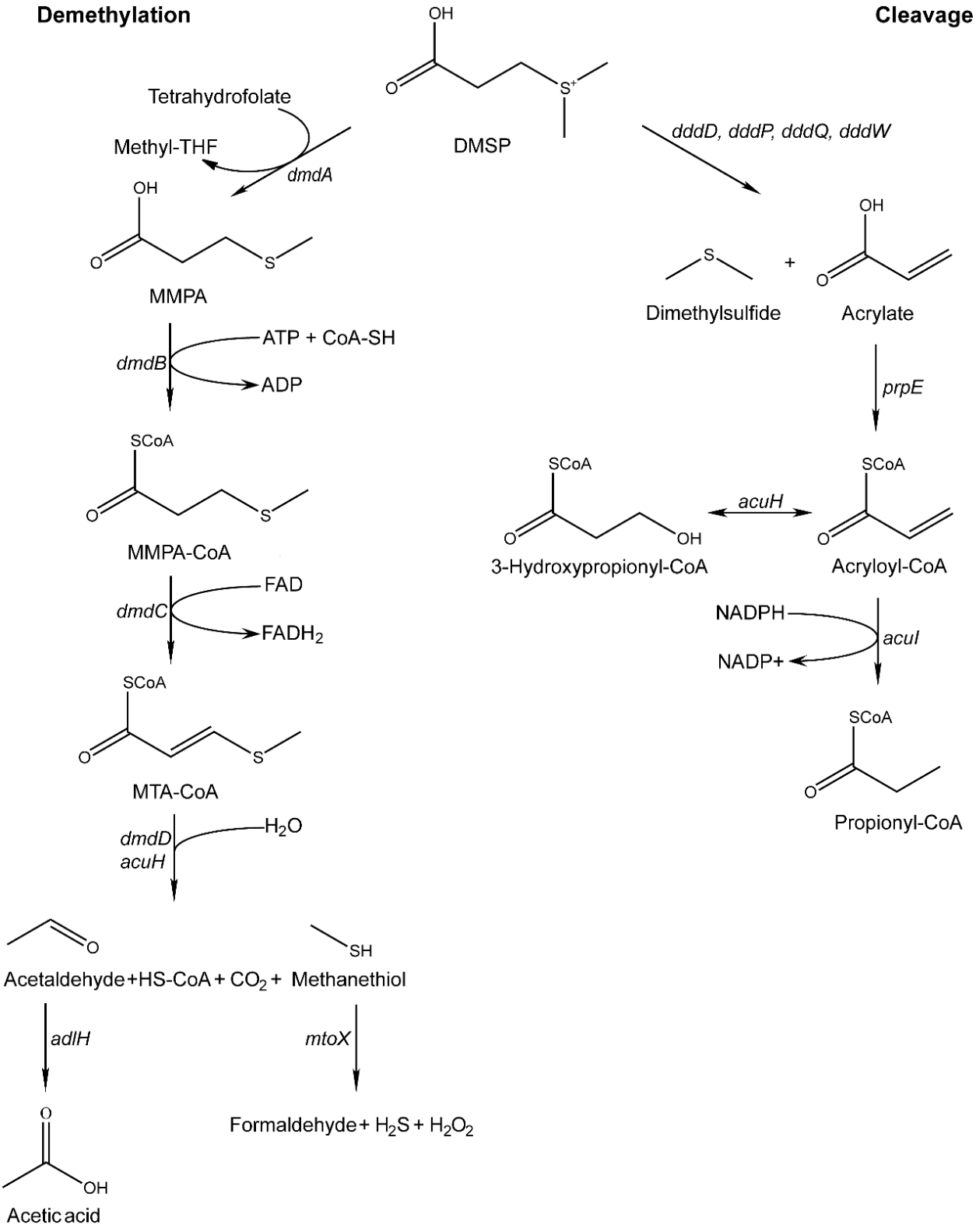
Demethylation
Cleavage
DMSP
Tetrahydrofolate
Methyl-THF
dmdA
MMPA
dmdB
ATP + CoA-SH
ADP
MMPA-CoA
dmdC
FAD
FADH2
MTA-CoA
dmdD
acuH
H2O
Acetaldehyde
+HS-CoA
+ CO2
+ Methanethiol
adlH
mtoX
Acetic acid
Formaldehyde + H2S + H2O2
dddD, dddP, dddQ, dddW
Dimethylsulfide
Acrylate
prpE
3-Hydroxypropionyl-CoA
acuH
Acryloyl-CoA
NADPH
NADP+
acuI
Propionyl-CoA

Figure 2-2. Experimental design for chemostat growth conditions. The arrows indicate the possible comparisons between selected conditions. Abbreviations for the growth conditions are indicated in parentheses. WT: wild type *R. pomeroyi* DSS-3; *ΔkatG*: the catalase deletion mutant.

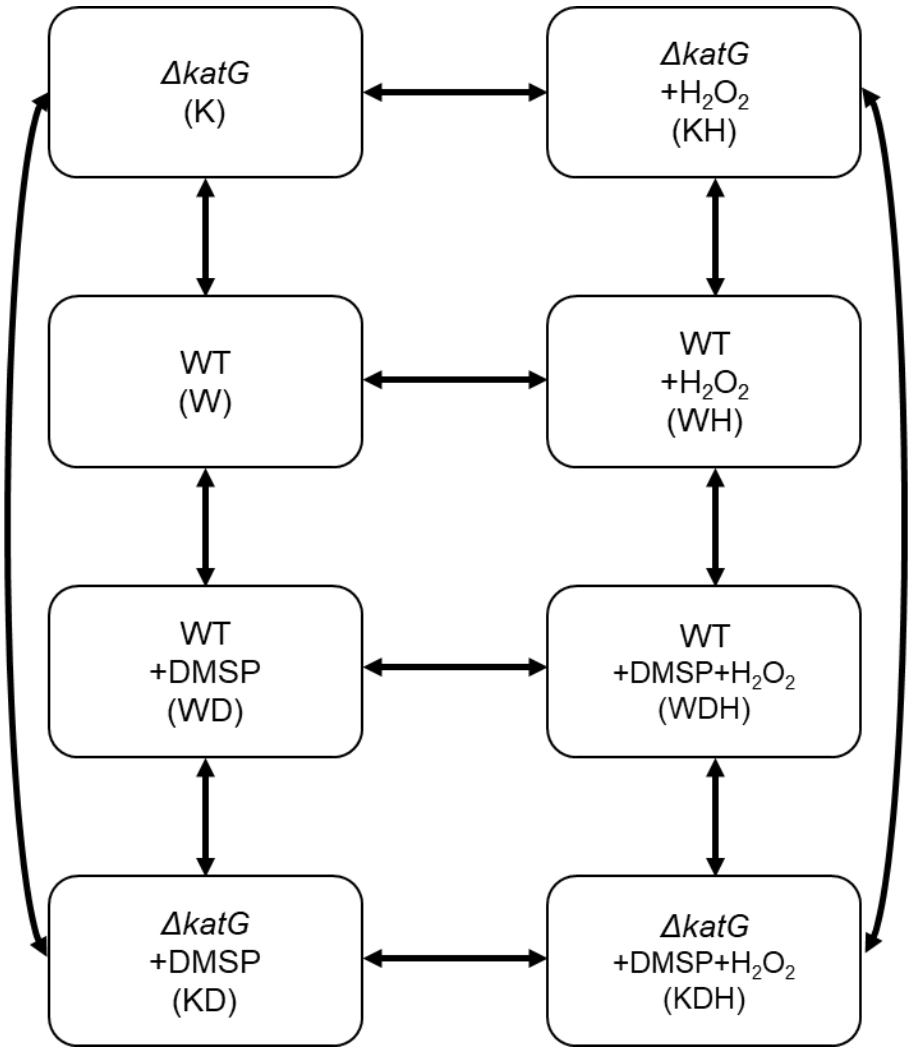

Figure 2-3. Effect of growth conditions on the patterns of gene expression. Principal component analyses for RNAseq results of each sample except for WD1. Abbreviations are defined in Figure 2-2. A, the entire genome; B, oxidative stress genes listed in table 2-2 (katG was not included because it is absent in the mutant); C, DMSP metabolism genes listed in table 2-3; D, sulfur metabolism genes listed in table 2-4.

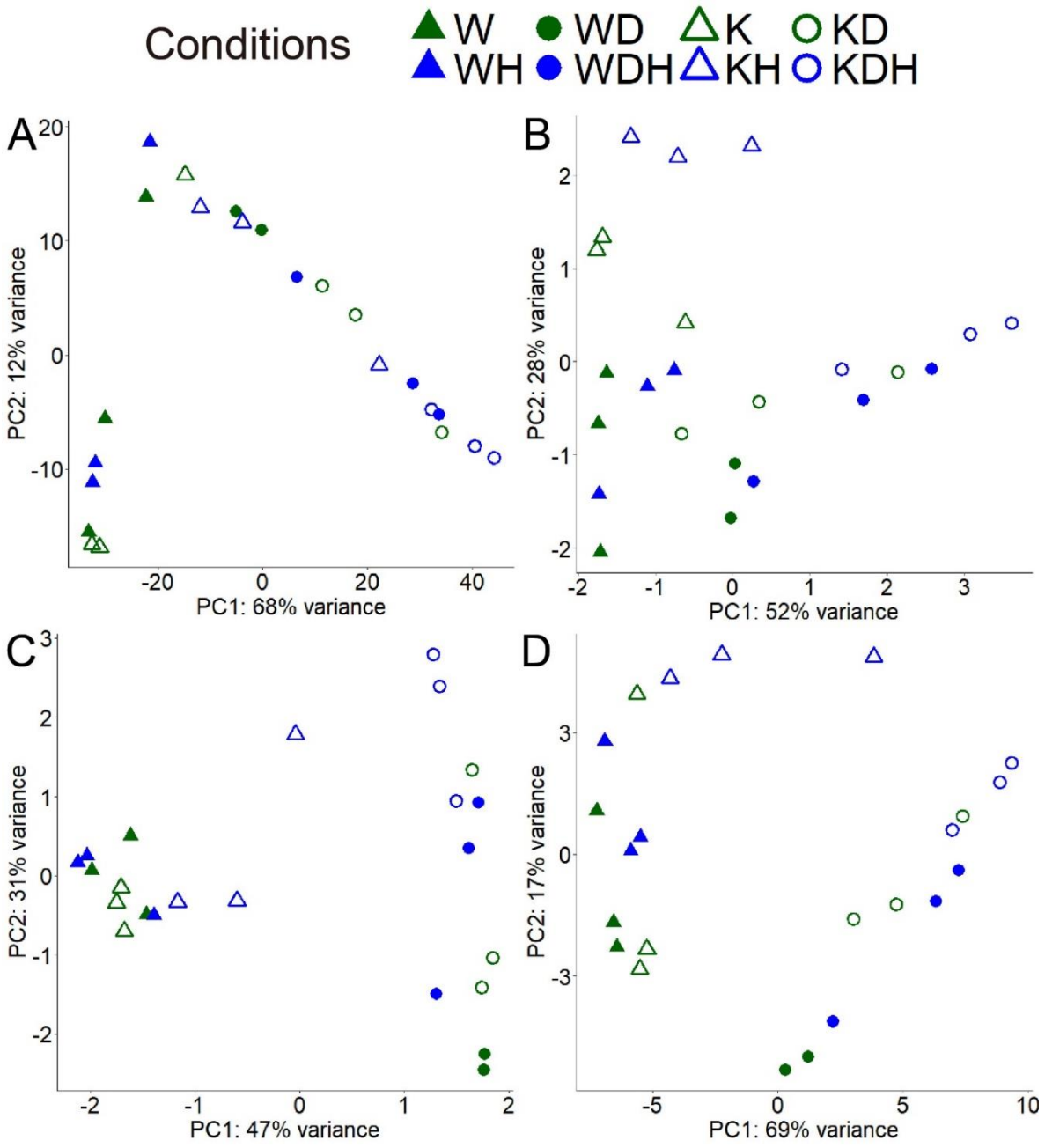

Figure 2-4. Overview of sulfur metabolism in *R. pomeroyi*. Sulfide can be used for biosynthesizing cysteine or methionine by CysK or MetZ and MTR, respectively. In chemostats, sulfide can be produced either by reducing sulfate or oxidizing MeSH released by DMSP demethylation. MeSH can also be directly incorporated for methionine biosynthesis by MetY. For locus tags, see table 2-3 and table 2-4.

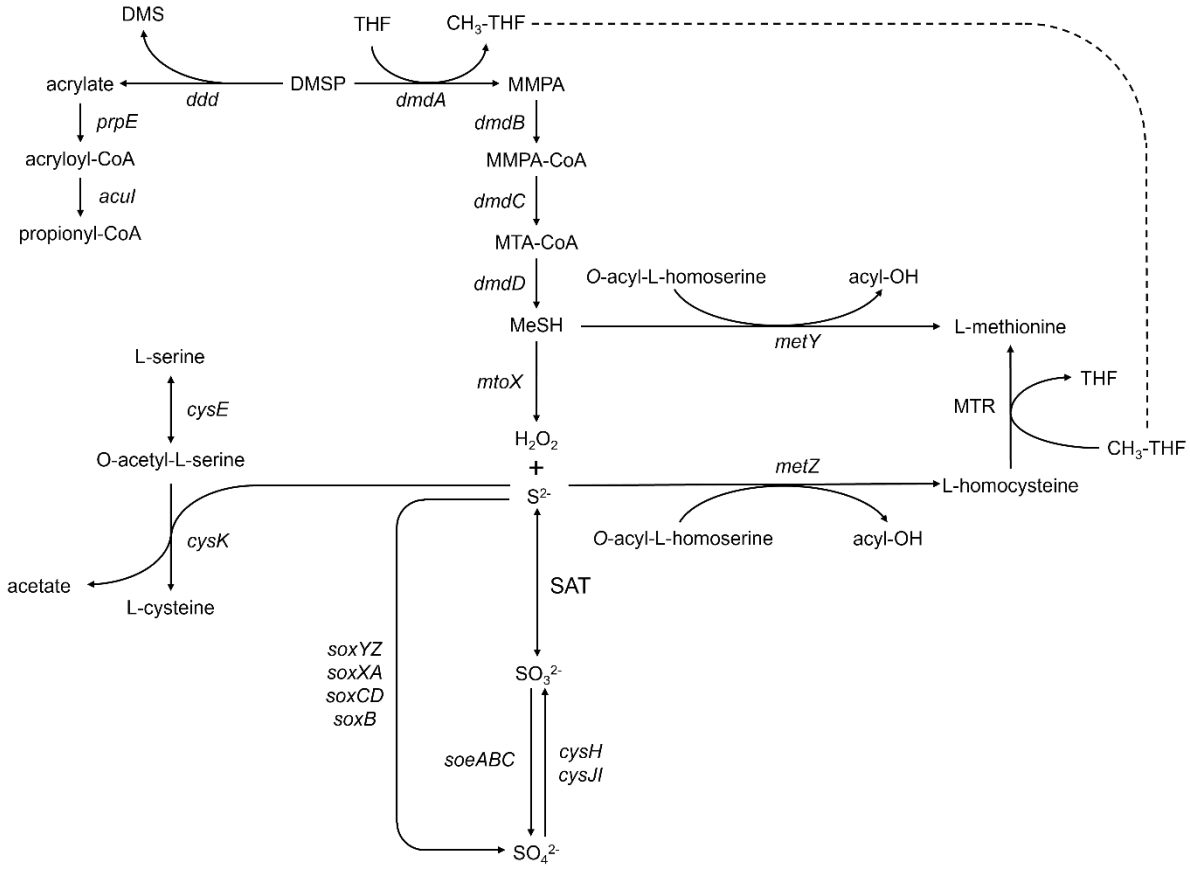

Figure 2-5. Regulation network of oxidative stress on DMSP metabolism based on changes in gene expression. The increasing expression of oxidative stress genes from W, WH, K and KH when DMSP was not present indicated the increasing oxidative stress among the conditions. The log2fold changes of selected genes were calculated compared to wild-type with no additions (the W transcriptome). A. Proposed regulation network; B. Averaged log2fold change of the oxidative stress genes listed in table 2-2; C. Averaged log2fold change of the demethylation pathway genes listed in table 2-3; D. Averaged log2fold change of the cleavage pathway genes listed in table 2-3.

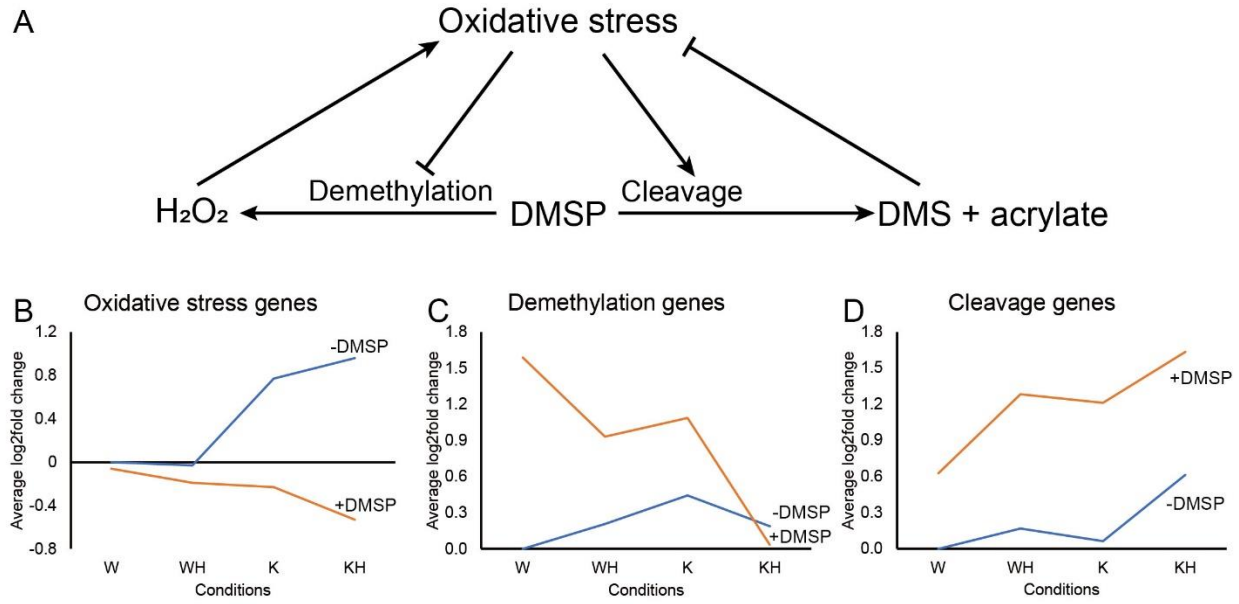

CHAPTER 3

SUBSTRATE SPECIFICITY OF THE 3-METHYLMERCAPTOPROPIONYL-COA DEHYDROGENASE (DMDC1) FROM *RUEGERIA POMEROYI* DSS-3[1]

[1]Wang T, Shi H and Whitman W.B. 2021. *Applied and Environmental Microbiology*. AEM. 01729-21.

Reprinted here with permission of the publisher.

Abstract

The acyl-coenzyme A (CoA) dehydrogenase family enzyme DmdC catalyzes the third step in the dimethylsulfoniopropionate (DMSP) demethylation pathway, the oxidation of 3-methylmercaptopropionyl-CoA (MMPA-CoA) to 3-methylthioacryloyl-CoA (MTA-CoA). To study its substrate specificity, the recombinant DmdC1 from *Ruegeria pomeroyi* was characterized. In addition to MMPA-CoA, the enzyme was highly active with short chain acyl-CoAs, with K_m values for MMPA-CoA, butyryl-CoA, valeryl-CoA, caproyl-CoA, heptanoyl-CoA, caprylyl-CoA and isobutyryl-CoA of 36, 19, 7, 11, 14, 10, and 149 μM, respectively, and k_{cat} values of 1.48, 0.40, 0.48, 0.73, 0.46, 0.23 and 0.01 sec^{-1}, respectively. Among these compounds, MMPA-CoA was the best substrate. The high affinity of DmdC1 for its substrate supports the model for kinetic regulation of the demethylation pathway. In contrast to DmdB, which catalyzes the formation of MMPA-CoA from MMPA, CoA and ATP, DmdC1 was not affected by physiological concentrations of potential effectors, such as DMSP, MMPA, ATP and ADP. Thus, compared to the other enzymes of the DMSP demethylation pathway, DmdC1 has only minimal adaptations for DMSP metabolism compared to other enzymes in the same family with similar substrates, supporting the hypothesis that it evolved relatively recently from a short chain acyl-CoA dehydrogenase involved in fatty acid oxidation.

Importance

We report the kinetic properties of DmdC1 from the model organism *R. pomeroyi* and close an important gap in the literature. While the crystal structure of this enzyme was recently solved and its mechanism of action described (Shao et al. 2020), its substrate specificity and sensitivity to potential effectors was never examined. We show that DmdC1 has a high affinity for other short chain acyl-CoAs in addition to MMPA-CoA, which is the natural substrate in DMSP metabolism

and is not affected by the potential effectors tested. This evidence supports the hypothesis that DmdC1 possesses few adaptations to DMSP metabolism and likely evolved relatively recently from a short chain acyl-CoA dehydrogenase involved in fatty acid oxidation. This work is important because it expands our understanding about the adaptation of marine bacteria to the increased availability of DMSP about 250 million years ago.

Introduction

Dimethylsulfoniopropionate (DMSP) is a ubiquitous low molecular compound in marine surface water produced by phytoplankton, algae, bacteria, corals, and higher plants (1-4). About 10% of DMSP is degraded to the volatile compound dimethylsulfide (DMS) (5). DMS is the major natural sulfur source to the atmosphere, where it can be oxidized to sulfate and methanesulfonate (6). According to the CLAW hypothesis, these products and DMS itself act as cloud condensation nuclei, promoting the albedo effect and lowering global temperatures. Marine bacteria metabolize DMSP by three competing pathways, the cleavage, demethylation and oxidation pathways (7, 8). Only the cleavage pathway directly yields DMS (9, 10). In contrast, most of DMSP is processed by the demethylation pathway, which involves four enzymes, DMSP demethylase DmdA (E.C. 2.1.1.269), MMPA-CoA ligase DmdB (E.C. 6.2.1.44), MMPA-CoA dehydrogenase DmdC (E.C. 1.3.8.-),, and MTA-CoA hydratase DmdD (E.C. 4.2.1.155) or the DmdD ortholog, AcuH (EC:4.2.1.17) (Figure 3-1) (5, 7). The final products of this pathway are methanethiol (MeSH), carbon dioxide, and acetaldehyde. The reduced sulfur in MeSH can be assimilated into biomass directly or oxidized to formaldehyde and hydrogen sulfide by MtoX (1, 11). Thus, DMSP is not only an important sulfur source for marine organisms, but it is also an integral part of the global sulfur cycle.

DMSP may have first become abundant in seawater about 250 million years ago when the highly active DMSP producers, dinoflagellates and coccolithophores, became abundant and coinciding with the first predicted episode of roseobacter genome expansion (12, 13). Thus, it has been proposed that the individual steps of the demethylation pathway in the roseobacters may have evolved at that time by recruitment of existing enzymes through specific adaptations to novel functions (9). For instance, the first enzyme of the pathway DmdA shares structural

similarity especially near the tetrahydrofolate-binding site but low sequence identity to the ubiquitous glycine cleavage T-protein (GcvT) (7, 14, 15). In spite of these similarities, DmdA possesses a catalytic mechanism distinct from GvcT as well as a high substrate specificity for DMSP. Likewise, the last enzyme in the pathway DmdD is a member of the crotonase superfamily and possesses a similar structure and activity site residues with other enoyl-CoA hydratases (16). However, it also possesses a high affinity and catalytic efficiency for its physiological substrate MTA-CoA, and greatly reduced activity for crotonyl-CoA, a good substrate for other enoyl-CoA hydratases. Similarly, the enzymes catalyzing the middle steps of the pathway, DmdB and DmdC, possess sequence and structural similarly to acyl-CoA ligases and acyl-CoA dehydrogenases, respectively, widely used in fatty acid metabolism (17). Although DmdB shares a similar mechanism and overlapping substrate specificity with other acyl-CoA ligases, the enzymes from marine bacteria have acquired sensitivities to effectors such as DMSP that may allow regulation of the demethylation pathway (18). Likewise, many properties of DmdC are similar to those of other acyl-CoA dehydrogenases (17). Enzymes in this family catalyze the initial step of fatty acid β-oxidation using flavin adenine dinucleotide (FAD) as a required cofactor and have a glutamate residue at the active site, resulting in the formation of a double bond at the α and β positions of various CoA-conjugated substrates (19). However, its substrate specificity and sensitivity to potential effectors has not been evaluated. To address these questions, the recombinant DmdC1 from *Ruegeria pomeroyi* was studied further.

Results and Discussion

Phylogenetic analysis of dmdC homologues. The roseobacters contain a large number of genes with significant sequence similarity to *dmdC* and other acyl-CoA dehydrogenases genes. For example, the genomes of *R. pomeroyi* DSS-3 and *Roseovarius nubinhibens* ISM encode at least

10 acyl-CoA dehydrogenase family enzymes including DmdC (Figure 3-2). While the function of most of these enzymes is not known, the DmdCs form a distinct clade consistent with a specific role in DMSP catabolism. Moreover, *R. pomeroyi* possesses three closely related DmdC enzymes, named DmdC1, DmdC2 and DmdC3, all of which are more closely related to each other than other acyl-CoA dehydrogenases (Figure 3-2). In contrast, *R. nubinhibens* encodes homologs to DmdC2 and DmdC3 but not DmdC1 (9).

Purification of RPO_DmdC1 dehydrogenase. Previously, it was found that a *dmdC1* deletion mutant of *R. pomeroyi* had reduced DmdC activity in cell-free extracts and failed to grow with MMPA as the sole carbon source (7). To examine the properties of this physiologically important enyzme further, the recombinant RPO_DmdC1 dehydrogenase was purified. Induction of the recombinant enzyme expression in *Escherichia coli* BL21(DE3) led to the appearance of new protein band with a M_r of ~60 kDa (Figure S3-1). This protein was purified 8.7-fold to electrophoretic homogeneity using a three-step chromatographic procedure (Table S3-1). No obviously contaminating proteins were detected by SDS-PAGE in the final preparation, and purity was estimated to be >85%. The purified RPO_DmdC1 dehydrogenase had a specific activity of 0.785 μmol min^{-1} mg^{-1} in the standard assay at pH 7.5. For storage, the purified enzyme was mixed with 30% (vol/vol) glycerol, 1 mM dithiothreitol (DTT), and 0.1 mM EDTA. Under these conditions, it was stable at -20 ˚C for at least 2 months.

Properties of RPO_DmdC1 dehydrogenase. The M_r of purified RPO_DmdC1 dehydrogenase determined by SDS-PAGE was 61.2 kDa and close to the molecular weight predicted from the amino acid sequence, which was 62.9 kDa. The native enzyme eluted as a single peak on a gel filtration column with a M_r of 130.5 kDa, indicating that it was a homodimer. Similarly, the DmdC3 from *R. nubinhibens* ISM also forms a homodimer (17).

DmdC is a member of the acyl-CoA dehydrogenase family of proteins, which frequently couple the oxidation of acyl-CoA compounds to the reduction of an acceptor flavoprotein, although some enzymes can reduce free FAD (19). MTA-CoA formation from MMPA-CoA by RPO_DmdC1 dehydrogenase was only detected in the presence of the artificial electron acceptors phenazine methosulfate (PMS) plus 2,6-dichloroindophenol sodium (DCPIP) or PMS plus iodonitrotetrazolium violet (INT) (Table S3-2). No activity was detected with DCPIP, FAD, FMN, or $NADP^+$ alone. This result suggests that this enzyme is coupled to an uncharacterized flavoprotein *in vivo*. In contrast, the *R. nubinhibens* DmdC3 was active with free FAD (17). Activity with free flavins is not common for acyl-CoA dehydrogenases (19), so it is difficult to compare this activity with that of the *R. pomeroyi* enzyme.

The response of RPO_DmdC1 dehydrogenase to pH was examined in the range of 6 to 8. Depending upon the buffer, activity was either indifferent to the pH or increased at the lower pHs in this range (Figure 3-3). Because the cation concentration and ionic strength also varied with pH, their effects were also tested (Figure S3-2). Both the chloride and acetate salts of the monovalent cations of lithium, sodium, potassium, and ammonium yielded about 40% inhibition at a concentration of 0.4 M. The lack of specificity for the salt suggested that activity was responding to the ionic strength of the buffer. Likewise, 0.4 M $CaCl_2$ and $MgCl_2$ both yielded 80% inhibition and had a much higher ionic strength. Thus, the small response to pH in the range of 6 to 8 was probably due to changes in the ionic strength of the buffers and not a direct effect of pH. In contrast, the pH optimum of the *R. nubinhibens* DmdC dehydrogenase was 9.0 (17). However, over the pH range of 6-8, activity only increased by about 20 % and did not differ greatly from the response of RPO_DmdC1 dehydrogenase. Importantly, a direct comparison of the pH responses of these two enzymes is difficult because the electron acceptors were different.

RPO_DmdC1 dehydrogenase was insensitive to potential effectors that might regulate the demethylation pathway (Figure S3-3). DMSP, MMPA, FMN, ADP, and ATP had little effect on activity. While FAD stimulated activity by 20%, this result was not surprising for a flavoprotein and was unlikely to denote a regulatory capacity.

Substrate specificity of RPO_DmdC1 dehydrogenase. The RPO_DmdC1 dehydrogenase possessed a broad substrate specificity with good activity towards MMPA-CoA and straight-chain C_4-C_8 acyl-CoA substrates (Table 3-1). Very low activity was detected with isobutyryl-CoA, but no activity was found with the longer branched-chain acyl-CoA substrates tested. Similarly, the activity with 3-mercaptopropionyl-CoA was below the limit of detection. Thus, its specificity was typical for a short-chain acyl-CoA dehydrogenase (19).

Conclusions

The structure and mechanism of the *R. nubinhibens* DmdC dehydrogenase closely resembles those of other short-chain acyl-CoA dehydrogenases (17). The low K_m and high catalytic efficiency of the RPO_DmdC1 for MMPA-CoA as well as the C_4-C_8 acyl-CoAs reported here support the hypothesis that this enzyme is closely related to short-chain acyl-CoA dehydrogenases as well as the proposed kinetic regulation of the demethylation pathway (17). The major modification seems to be the decrease in substrate specificity to include MMPA-CoA. No evidence was found for acquisition of regulatory functions related to DMSP demethylation, such as the inhibition of DmdB by DMSP (18). Thus, compared to the other enzymes of the DMSP demethylation pathway, DmdC has only minimal adaptations for DMSP metabolism.

Materials and Methods

Plasmid construction and expression of recombinant protein. The RPO_DmdC1 gene (SPO3804) of 1,767 bp was cloned from the *Ruegeria pomeroyi* DSS-3 genome and inserted into

the expression vector pET101, yielding pET101-*SPO3804*. *Escherichia coli* BL21 (DE3) cells bearing pET101-*SPO3804* were grown at 30 °C in 500 ml of Luria-Bertani broth with 100 µg ml^{-1} ampicillin. Expression of RPO_DmdC1 was induced by supplementation with 200 µM isopropyl-β-D-1-thiogalactopyranoside (IPTG) when the culture reached an optical density at 600 nm (OD_{600}) of 0.6-0.8, and then the culture was incubated at 30 °C overnight. Cells were harvested by centrifugation at 4 °C (5,000 ×g, 15 min), washed with 10 ml of 50 mM Tris-HCl (pH 7.5) and then resuspended in the same buffer. Cells were lysed by sonication with a W-380 sonicator (Heat Systems-Ultrasonics, Inc.) for 5 minutes of 5-s bursts with the output set at 5 and the duty cycle set at 40%. The lysed cell suspension was centrifuged at 17,000 ×g for 3 min to remove the cell debris from the supernatant.

Purification of RPO_DmdC1 dehydrogenase. The resulting supernatant was filtered (Whatman 0.2 µm PES Filter) to remove small particles and remaining bacterial cells. The filtrate was then loaded onto a Q-Sepharose HP (GE Healthcare) column (1.6 by 7.0 cm) in a AKTA purifier system (GE Healthcare) equilibrated with 50 mM Tris-HCl (pH 7.5), and proteins were eluted with a linear gradient from 0 to 1 M NaCl at a flow rate of 2 ml min^{-1}. Fractions containing RPO_DmdC1 dehydrogenase were identified by enzymatic assay, pooled, and further purified on the same Q-Sepharose HP column. Active fractions were pooled, and $(NH_4)_2SO_4$ was added to 1.7 M before loading onto a phenyl-Superose (GE Healthcare) column (1.0 by 10.0 cm) equilibrated with 50 mM Tris-HCl (pH 7.5) containing 1.7 M $(NH_4)_2SO_4$ and eluting with a linear gradient from 1.7 to 0 M $(NH_4)_2SO_4$ at a flow rate of 1 ml min^{-1}. Active fractions were pooled and concentrated using the Amicon Ultra-4 10K centrifugal filter (Millipore). Finally, 1 ml of enzyme containing 30% (vol/vol) glycerol, 1 mM DTT, and 0.1 mM EDTA was stored at -20 °C.

Enzyme assays. Unless specified differently, enzyme activity of RPO_DmdC1 dehydrogenase was assayed at room temperature (25 ºC) for 5 min in a reaction mixture containing 200 µM MMPA-CoA, the intermediate and terminal electron acceptors 50 µM phenazine methosulfate (PMS) and 200 µM 2,6-dichloroindophenol sodium (DCPIP), respectively, and 1.12 µg enzyme in 100 mM HEPES-NaOH buffer (pH 6.5) with a volume of 200 µl (7). The reaction was quenched by addition of concentrated H_3PO_4 acid to a final concentration of 10% (vol/vol) and centrifuged to remove denatured proteins. MTA-CoA formation was analyzed by high-performance liquid chromatography (Agilent 1260 Infinity) using a ZORBAX Eclipse Plus C_{18} column (3.5 µm, 4.6 by 100 mm; Agilent) and developed with a linear gradient of 2 to 20% acetonitrile in 50 mM ammonium acetate buffer (pH 6.0) over 10 min at a flow rate of 1 ml min^{-1}. The product was detected by its absorbance at 254 nm (7) and quantified with standard CoA samples analyzed with the same procedure (20). One unit was defined as the amount of enzyme producing 1 µmol of MTA-CoA per min, and the specific activity was defined as 1 U per mg of protein.

Apparent Michaelis-Menten kinetic constants were calculated by varying MMPA-CoA or fatty acid-CoAs in the standard assay. MMPA-CoA was varied over the range of 0.025 mM to 0.2 mM, butyryl-CoA over the range of 0.025 mM to 0.4 mM, caproyl-CoA over the range of 0.0074 mM to 0.059 mM, caprylyl-CoA over the range of 0.010 mM to 0.076 mM, isobutyryl-CoA over the range of 0.010 mM to 0.164 mM, and valeryl-CoA over the range of 0.011 mM to 0.087 mM. Kinetic data and statistical analyses were performed using SigmaPlot 12.5 (Systat Software Inc.).

Protein quantification. Protein concentrations were determined using either the Bio-Rad protein assay dye reagent concentrate or the bicinchoninic acid protein assay kit (Thermo Scientific)

with bovine serum albumin as the standard. Both the methods yielded similar results (21, 22).

SDS-PAGE. SDS-PAGE was accomplished using 4 to15% Mini-PROTEAN TGX precast gels (Bio-Rad). Gels were stained using Simply Blue safe stain (Invitrogen). Gel Pro Analyzer program version 4.0 (Media Cybernetics, L.P.) was used to assess the protein purity based upon images of the stained SDS-PAGE gels.

Native Molecular Mass. The native molecular mass of RPO_DmdC1 was determined as previously described (18). Briefly, a Sephacryl S200 HR (GE Healthcare) column (1.6 by 34 cm) equilibrated with 50 mM Tris-HCl (pH 7.5) and 250 mM NaCl was used, and proteins were eluted in the same buffer at a flow rate of 0.75 ml min^{-1}. β-Amylase (200 kDa), alcohol dehydrogenase (150 kDa), bovine albumin (66 kDa), carbonic anhydrase (29 kDa), and cytochrome c (12.4 kDa) served as molecular mass standards.

Substrate synthesis. MMPA-CoA was synthesized enzymatically using purified recombinant DmdB as previously described (7). After resuspension, MMPA-CoA was aliquoted and stored at -20 ºC for several months. Other substrates were synthesized with the acyl coenzyme A (acyl-CoA) synthetase as described by Crosby and Escalante-Semerena 2014 (23).

Phylogenetic analysis. The DmdC1 (SPO3804), DmdC2 (SPO0298), DmdC3 (SPO2915) from *R. pomeroyi* DSS-3 and DmdC (ISM) from *R. nubinhibens* ISM were used as query sequences for a BLASTp search against their respective genomes (24). All detected sequences aligned using the MUSCLE algorithm in MEGA 11(25). A maximum-likelihood tree was constructed with the best model (LG+G+I+F) identified by MEGA 11 and 100 bootstrap replicates.

Acknowledgements

This work was supported in part by a National Science Foundation Dimensions of Biodiversity grant (OCE-1342694).

References

1. Curson AR, Liu J, Martínez AB, Green RT, Chan Y, Carrión O, Williams BT, Zhang SH, Yang GP, Page PCB. 2017. Dimethylsulfoniopropionate biosynthesis in marine bacteria and identification of the key gene in this process. Nat Microbiol 2:17009.
2. Reisch CR, Moran MA, Whitman WB. 2011. Bacterial catabolism of dimethylsulfoniopropionate (DMSP). Front Microbiol 2:172.
3. Raina JB, Tapiolas D, Forêt S, Lutz A, Abrego D, Ceh J, Seneca FO, Clode PL, Bourne DG, Willis BL. 2013. DMSP biosynthesis by an animal and its role in coral thermal stress response. Nature 502:677-680.
4. Otte ML, Wilson G, Morris JT, Moran BM. 2004. Dimethylsulphoniopropionate (DMSP) and related compounds in higher plants. J Exp Bot 55:1919-1925.
5. Kiene RP, Linn LJ, Gonzalez J, Moran MA, Bruton JA. 1999. Dimethylsulfoniopropionate and methanethiol are important precursors of methionine and protein-sulfur in marine bacterioplankton. Appl Environ Microbiol65:4549-4558.
6. Charlson RJ, Lovelock JE, Andreae MO, Warren SG. 1987. Oceanic phytoplankton, atmospheric sulphur, cloud albedo and climate. Nature 326:655-661.
7. Reisch CR, Stoudemayer MJ, Varaljay VA, Amster IJ, Moran MA, Whitman WB. 2011. Novel pathway for assimilation of dimethylsulphoniopropionate widespread in marine bacteria. Nature 473:208-211.
8. Thume K, Gebser B, Chen L, Meyer N, Kieber DJ, Pohnert G. 2018. The metabolite dimethylsulfoxonium propionate extends the marine organosulfur cycle. Nature 563:412-415.

9. Bullock HA, Luo H, Whitman WB. 2017. Evolution of dimethylsulfoniopropionate metabolism in marine phytoplankton and bacteria. Front Microbiol 8:637.

10. Johnston AW, Green RT, Todd JD. 2016. Enzymatic breakage of dimethylsulfoniopropionate-a signature molecule for life at sea. Curr Opin Chem Biol 31:58-65.

11. Wirth JS, Wang T, Huang Q, White RH, Whitman WB. 2020. Dimethylsulfoniopropionate sulfur and methyl carbon assimilation in *Ruegeria* Species. mBio 11:e00329-20.

12. Keller MD. 1989. Dimethyl sulfide production and marine phytoplankton: the importance of species composition and cell size. Biol Oceanogr 6:375-382.

13. Luo H, Moran MA. 2014. Evolutionary ecology of the marine *Roseobacter* clade. Microbiol Mol Biol Rev 78:573-87.

14. Schuller DJ, Reisch CR, Moran MA, Whitman WB, Lanzilotta WN. 2012. Structures of dimethylsulfoniopropionate-dependent demethylase from the marine organism *Pelagabacter ubique*. Protein Sci 21:289-298.

15. Reisch CR, Moran MA, Whitman WB. 2008. Dimethylsulfoniopropionate-dependent demethylase (DmdA) from *Pelagibacter ubique* and *Silicibacter pomeroyi*. J Bacteriol 190:8018-8024.

16. Tan D, Crabb WM, Whitman WB, Tong L. 2013. Crystal structure of DmdD, a crotonase superfamily enzyme that catalyzes the hydration and hydrolysis of methylthioacryloyl-CoA. PLoS One 8:e63870.

17. Shao X, Cao HY, Zhao F, Peng M, Wang P, Li CY, Shi WL, Wei TD, Yuan Z, Zhang XH. 2019. Mechanistic insight into 3-methylmercaptopropionate metabolism and

kinetical regulation of demethylation pathway in marine dimethylsulfoniopropionate-catabolizing bacteria. Mol Microbiol 111:1057-1073.

18. Bullock HA, Reisch CR, Burns AS, Moran MA, Whitman WB. 2014. Regulatory and Functional diversity of methylmercaptopropionate coenzyme A ligases from the dimethylsulfoniopropionate demethylation pathway in *Ruegeria pomeroyi* DSS-3 and other proteobacteria. J Bacteriol 196:1275-1285.
19. Ghisla S, Thorpe C. 2004. Acyl-CoA dehydrogenases. Eur J Biochem 271:494-508.
20. Shimazu M, Vetcher L, Galazzo JL, Licari P, Santi DV. 2004. A sensitive and robust method for quantification of intracellular short-chain coenzyme A esters. Anal Biochem 328:51-59.
21. Bradford MM. 1976. A rapid and sensitive method for the quantitation of microgram quantities of protein utilizing the principle of protein-dye binding. Anal Biochem 72:248-254.
22. Smith Pe, Krohn RI, Hermanson GT, Mallia AK, Gartner FH, Provenzano M, Fujimoto EK, Goeke NM, Olson BJ, Klenk D. 1985. Measurement of protein using bicinchoninic acid. Anal Biochem 150:76-85.
23. Crosby HA, Escalante-Semerena JC. 2014. The acetylation motif in AMP-forming acyl coenzyme A synthetases contains residues critical for acetylation and recognition by the protein acetyltransferase Pat of *Rhodopseudomonas palustris*. J Bacteriol 196:1496-1504.
24. Altschul SF, Gish W, Miller W, Myers EW, Lipman DJ. 1990. Basic local alignment search tool. J Mol Biol 215:403-410.
25. Tamura K, Stecher G, Kumar S. 2021. MEGA11: molecular evolutionary genetics analysis version 11. Mol Biol Evol 38:3022-3027.

Table 3-1. Substrate specificity and apparent kinetic constants for recombinant RPO_DmdC1 dehydrogenase[a].

Substrates	K_m (μM)	V_{max} (μmol min^{-1} mg^{-1})	k_{cat} (s^{-1})	k_{cat}/K_m (s^{-1} mM^{-1})
MMPA-CoA	34±8	1.37±0.09	1.44±0.09	42
Butyryl-CoA	19±3	0.37±0.01	0.39±0.01	21
Valeryl-CoA	7.1±0.7	0.47±0.01	0.48±0.01	67
Caproyl-CoA	11.6±0.9	0.72±0.02	0.75±0.02	65
Heptanoyl-CoA	23±3	0.48±0.02	0.50±0.02	22
Caprylyl-CoA	21±5	0.28±0.02	0.29±0.02	13
Isobutyryl-CoA	280±36	0.16±0.01	0.17±0.01	0.61
3-Mercaptopropionyl-CoA		<0.005[b]		
2-Methylbutyryl-CoA		<0.005		
Isovaleryl-CoA		<0.005		

[a]Assayed under the standard conditions at pH 7.0. Values are based on duplicate assays at five concentrations of substrate and reported ± the standard errors.

[b]Limit of detection.

Figure 3-1. Demethylation pathway in *R. pomeroyi* DSS-3. The four Dmd enzymes and their locus numbers in *R. pomeroyi* DSS-3. Abbreviations: MMPA, 3-methylmercaptopropionic acid; MTA-CoA; 3-methylthioacryloyl-CoA; HS-CoA, coenzyme A.

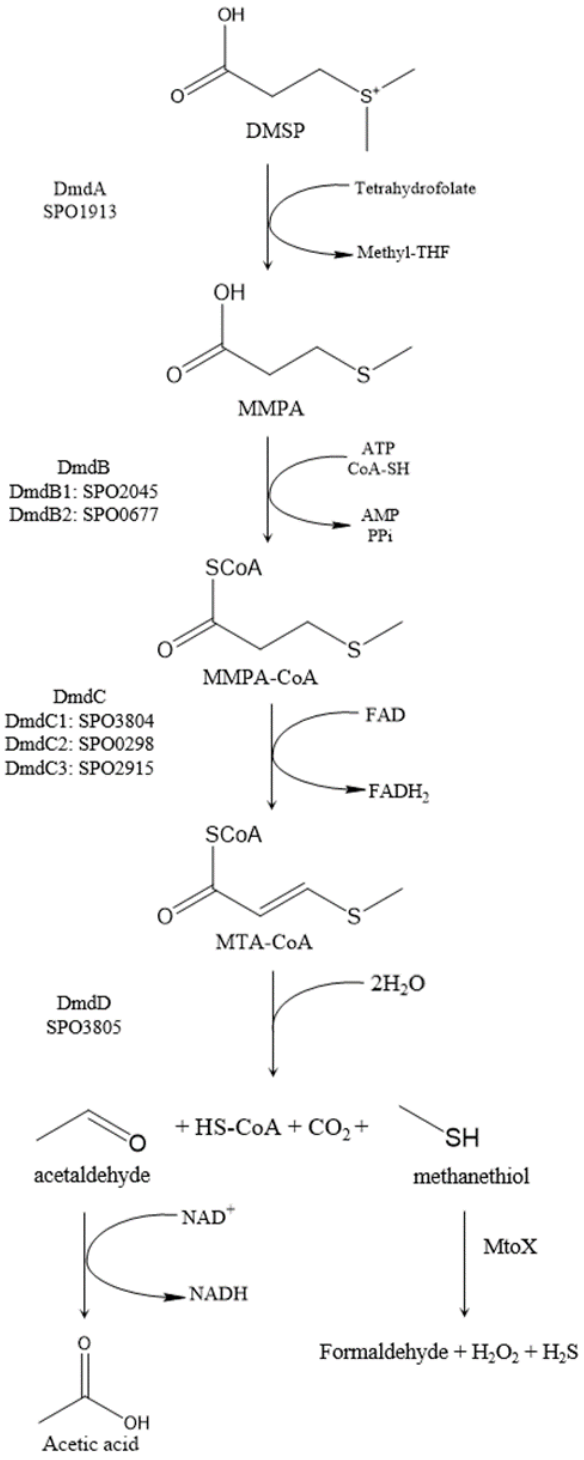

Figure 3-2. Phylogeny of DmdC homologues from *R. pomeroyi* DSS-3 and *R. nubinhibens* ISM. The maximum-likelihood tree shows that the DmdCs form a distinct clade within the other acyl-CoA dehydrogenase family genes encoded in the genomes of *R. pomeroyi* DSS-3 and *R. nubinhibens* ISM. Annotated clades are labeled. Numbers at the nodes are bootstrap percentages derived from 100 replications. Locus tags correspond to organisms as follows: *R. pomeroyi* (SPO) and *R. nubinhibens* ISM (ISM). The scale bar indicates the number of substitutions per site.

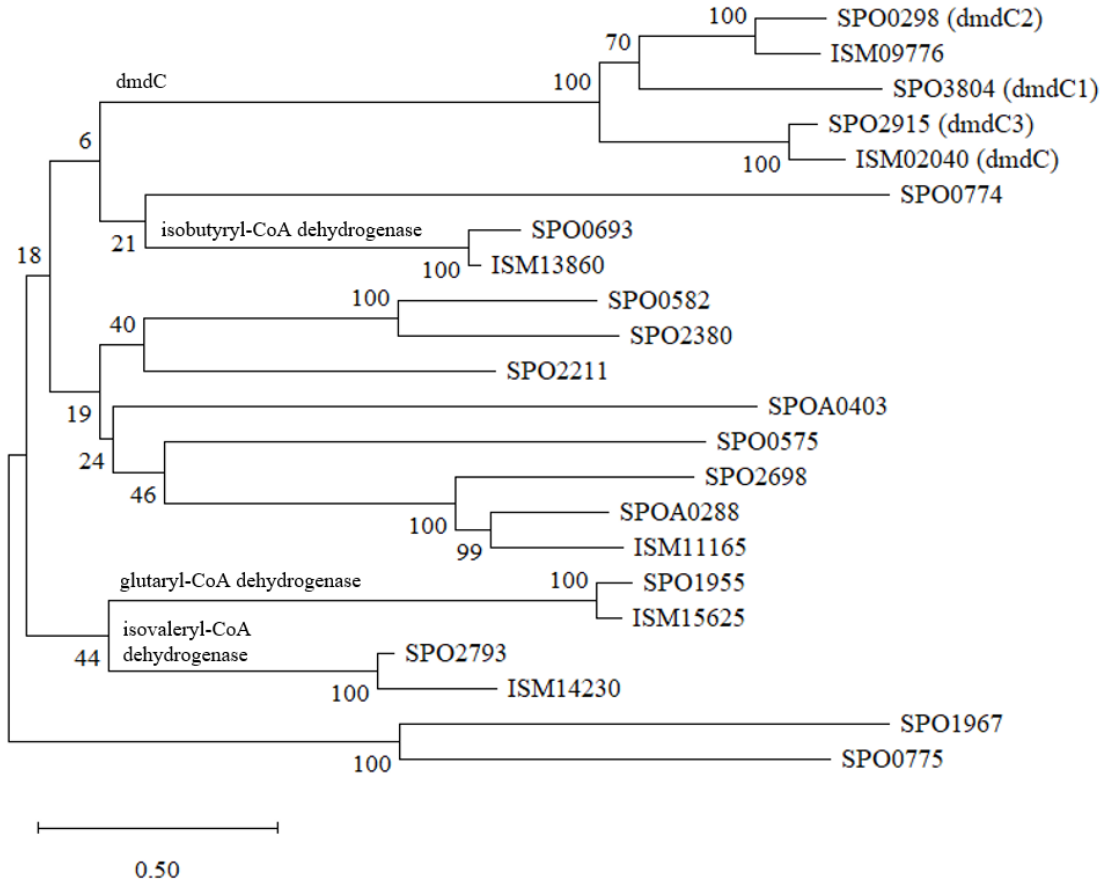

Figure 3-3. Response of the recombinant RPO_DmdC1 dehydrogenase to pH.

RPO_DmdC1 enzyme activity was tested in the standard enzymatic assay with 200 µM MMPA-CoA and 100 mM buffer of the designated pH. Results are averages of two replicates. Error bars are not shown because the duplicates were very close.

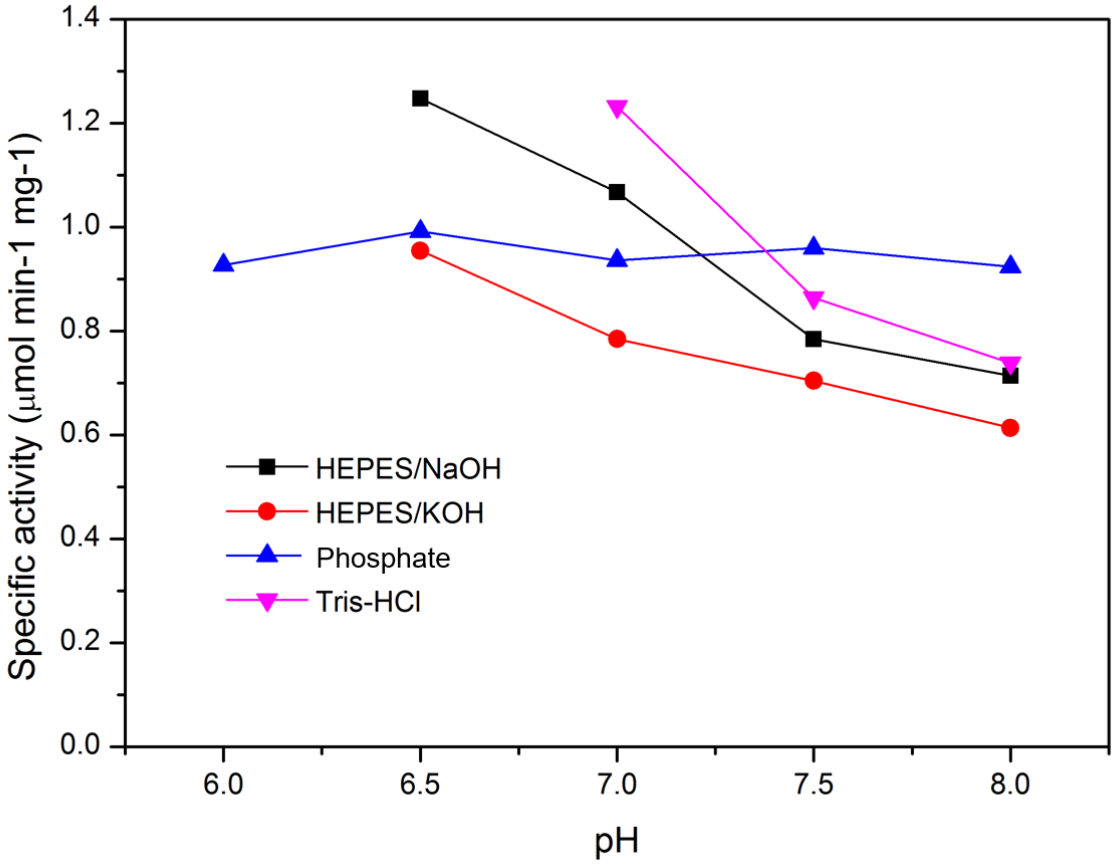

CHAPTER 4

THE GENUS *LOKTANELLA*[1]

[1]Wang T, Wirth JS, Whitman WB 2021. In *Bergey's Manual of Systematics of Archaea and Bacteria* (eds Trujillo ME, Dedysh S, DeVos P, Hedlund B, Kämpfer P, Rainey FA and Whitman WB).

Abstract

Gram-negative staining, aerobic, non-spore-forming, catalase- and oxidase-positive, cocci, ovoids, or rods. Halophilic or moderately halotolerant. Optimal growth typically occurs at 25 ˚C and pH 7.5-8. Capable of utilizing a large variety of organic carbon compounds. The majority of strains produce acids from sugars and are non-motile. The major fatty acid is $C_{18:1}\omega 7c$. The major quinone is ubiquinone 10 (Q-10). Species have been isolated globally from seawater and microbial mats from marine environments. Members of the family *Rhodobacteraceae*. The type species is *Loktanella salsilacus*.

Etymology

Lok.tan.el′la. N.L. fem. n. *Loktanella* named after Tjhing-Lok Tan from the Alfred Wegener Institute in Bremerhaven, who contributed to our understanding of marine and polar bacteriology and ecology.

Description

Rod-shaped, Gram-negative staining, non-spore-forming, and lacking flagella, except for *Loktanella atrilutea*, which possesses a polar flagellum. Motility was not observed except in *L. atrilutea*. All species are aerobes. Positive for catalase and oxidase. Ability to reduce nitrate to nitrite, depends on the species. Growth temperatures range from 5 to 37 ˚C, but optimal growth occurs at 25˚C. Grows at NaCl concentrations from 0% to 10% (w/v). All species have an optimal pH between 7.5 and 8, but growth occurs between pH 6 and pH 10.

Capable of degrading a variety of carbon compounds including carbohydrates and carboxylic acids. However, reports of the substrate specificity are incomplete for many species. The major quinone is ubiquinone 10 (Q-10). The polar lipids observed in at least one species comprise diphosphatidylglycerol, phosphatidylethanolamine, phosphatidylglycerol, and phosphatidylcholine. The major fatty acid is $C_{18:1}\omega 7c$. The other fatty acids observed with ≥ 1.0 % of the total fatty acids in at least one species comprise $C_{14:0}$, $C_{15:0,}$ $C_{16:0}$, $C_{17:0}$, $C_{18:0}$, $C_{18:2}$, $C_{16:1}\omega 8c$, $C_{18:1}\omega 9c$, $C_{19:1}cy$, 11-methyl $C_{18:1}\omega 7c$, $C_{10:0}$ 3-OH, summed feature 2 ($C_{12:0}$ aldehyde, iso-$C_{16:1}$ I, and $C_{14:0}$ 3-OH and/or unknown 10.928), summed feature 3 (iso-$C_{15:0}$ 2-OH and/or $C_{16:1}\omega 7c$), and summed feature 7 ($C_{19:1}\omega 6c$ and/or $C_{19:0}\omega 10c$ cyclo and/or unknown ELC 18.846).

Species are globally distributed in marine or salty water environments. Species have been isolated from seawater and microbial mats. Members of the family *Rhodobacteraceae*. The type

species is *Loktanella salsilacus*.

DNA G + C content (mol %): 60-66.3.

Type species: Loktanella salsilacus Van Trappen et al. 2004[VP].

Number of species with validated names: 4.

Further Descriptive Information

Cell morphology. The cells of all species in *Loktanella* are Gram-negative staining rods (1-3). For a summary of morphological characters, see Table 4-1. Cell length varies from 0.9 µm to 4 µm, and cell width ranges from 0.5 µm to 1 µm. All the species except *L. atrilutea* lack flagella and are nonmotile. *L. atrilutea* is motile by means of a polar flagellum. Some species, including *L. salsilacus* and *Loktanella fryxellensis*, often occur in pairs or form short chains of cells.

Colonial and cultural characteristics. On plates, colonies can typically be observed after 2-7 days. Colonies can be up to 3 mm in diameter. Colonies of *Loktanella agnita* are whitish, round, regular, convex, smooth, and 1-3 mm in diameter after incubation for 2-3 days on marine agar 2216 (MA, Difco) (2). Colonies of *L. atrilutea* are beige and round (3). Older colonies turn dark orange. Colonies of *L. fryxellensis* are pale pink to beige, convex, translucent, and 1.0 mm in diameter after incubation for 7 days at 25 ºC on MA (1). Colonies of *L. salsilacus* are beige, convex, translucent, and 1.0-2.0 mm in diameter after 2 days at 25 ºC on MA. Colonies of *L. salsilacus* and *L. fryxellensis* do not adhere to the agar.

Nutritional, growth conditions and biochemical characteristics. Data of *Loktanella* growth range and optimum conditions is incomplete. All the species tested grow optimally at 25 ºC. Additional information is listed in Table 4-1.

The ability to utilize various sole carbon sources has only been reported for *L. salsilacus* and *L. agnita*. Both species utilize cellobiose, D-fructose, D-galactose, D-glucose, and D-mannose but not L-arabinose, benzoate, citrate, formate, L-glutamate, salicin, sucrose, or

trehalose. All of the *Loktanella* species hydrolyze aesculin (no data for *L. atrilutea*) but not agar, casein, gelatin, or starch.

All species tested are negative for acetoin, hydrogen sulfide, and indole production. In assays with the API ZYM system, all the species are positive or weakly positive for acid phosphatase, alkaline phosphatase, esterase lipase (C8), and leucine arylamidase and negative for α-chymotrypsin, cystine arylamidase, α-fucosidase, *N*-acetyl-β-glucosaminidase, lipase (C14), and α-mannosidase.

Loktanella species are susceptible to a variety of antibiotics, but not all species have been tested for the same antibiotics. There are no data for antibiotic susceptibility of *L. atrilutea* and *L. fryxellensis*. All the species tested are susceptible to cephalothin, chloramphenicol, gentamicin, kanamycin, neomycin, novobiocin, oleandomycin, streptomycin, and tetracycline but resistant to ampicillin and lincomycin.

The characters that can be used to distinguish the *Loktanella* species from one another are listed in Table 4-2.

Chemotaxonomic characteristics. The major fatty acid in *Loktanella* is $C_{18:1}\omega 7c$. Every species possesses $C_{18:1}\omega 7c$, but its percentage ranges from 74.4% to 87.7%. The following fatty acids have also been observed in all *Loktanella* species: $C_{16:0}$, $C_{18:0}$ and $C_{10:0}$ 3-OH. For a summary of the fatty acids in the *Loktanella* species, see Table 4-3. All *Loktanella* species tested for polar lipids possess phosphatidylglycerol and phosphatidylcholine.

Genome features. Except for *L. agnita***,** whole genome sequences are publicly available for the type strains of the remaining *Loktanella* species. The detailed information of the whole-genome sequences is summarized in Table 4-4. So far, a genetics system for *Loktanella* has not been reported.

Ecology. *Loktanella* species are found in aerobic, marine environments. Except *L. salsilacus* and *L. fryxellensis*, which were originally isolated from Antarctica lakes, the remaining species were isolated from seas of Japan. Potential *Loktanella* species have been identified by 16S rRNA gene sequencing of environmental DNA sampled from saltwater lakes, seawater, marine sediment, algae, and corals from around the world. The wide range of growth temperature, salinity, and carbon sources of *Loktanella* species may help to explain their presence in such a wide variety of environments.

Enrichment and Isolation Procedures

All the *Loktanella* species were isolating by dilution plating. *L. salsilacus* and *L. fryxellensis* were isolated by plating dilutions of microbial mat samples from Ace Lake and Organic Lake, Vestfold Hills, Antarctica and Lake Fryxell, Antarctica, respectively, homogenized in sterile physiological water [0.86% (w/v) NaCl] (4). Plates were then incubated in aerobic conditions at 4 or 20 ºC. *L. agnita* was isolated by plating seawater collected from the first meter below the surface in Chazma Bay, Sea of Japan, Pacific Ocean on MA or medium B and incubating aerobically for 5-10 days at room temperature (2, 5). Medium B consists of 0.2% (w/v) peptone, 0.2% (w/v) casein hydrolysate, 0.2% (w/v) yeast extract, 0.1% (w/v) glucose, 0.02% (w/v) KH_2PO_4, 0.005% (w/v) $MgSO_4 \cdot 7H_2O$, and 1.5% (w/v) agar in 50% seawater with pH 7.8. *L. atrilutea* was isolated by plating seawater from off the Sanriku coast, Japan, on a modified gelatin agar and incubating at 25 ºC for one week (3).

Maintenance Procedures

Strains of *Loktanella* can be maintained on solid media or in liquid cultures. Because all *Loktanella* species are aerobes, shaking is recommended for liquid cultures in order to increase the oxygenation of the media.

Several types of rich media have been used to cultivate the *Loktanella* species. The most common medium is marine agar/broth 2216 (MA/MB, Difco). All the species are routinely cultivated on MA or MB. R2A agar was also used to cultivate *L. salsilacus*, *L. atrilutea* and *L. fryxellensis*. None of the tested species grow on Tryptic Soy Agar (TSA) or Nutrient Agar (NA).

The modified gelatin agar used for isolating *L. atrilutea* contains 0.75× artificial seawater (3% NaCl, 0.07% KCl, 1.08% $MgCl_2 \cdot 6H_2O$, 0.54% $MgSO_4 \cdot 7H_2O$ and 0.1% $CaCl_2 \cdot 2H_2O$), 0.4% gelatin, 0.025% peptone, 0.025% yeast extract, 0.001% $FeSO_4 \cdot 7H_2O$, 0.001% Na_2HPO_4 and 1% agar (3).

Differentiation of the genus *Loktanella* from other genera

Although many phenotypic and chemotaxonomic characters have been examined, many characteristics have not been tested for all the species. As a result, no clear characters except gelatin hydrolysis have been identified that distinguish *Loktanella* from the closely related genera *Flavimaricola*, *Cognatiyoonia*, *Yoonia*, and *Limimaricola*. So far, the most reliable way to distinguish *Loktanella* species from those of other genera is comparison of the whole-genome sequences. RpoC protein sequence is also proposed to serve as a reliable phylogenetic marker if the whole-genome is not available (6). In contrast, the 16S rRNA sequence similarity is not a reliable marker in this group (see below).

Taxonomic comments

The genus *Loktanella* was first proposed by Van Trappen *et al.* in 2004 to describe a distinct phylogenetic group (based on 16S rRNA gene sequence) of chemoheterotrophic, nonmotile, and oxidase-, catalase-, and β-galactosidase positive bacteria of the *Rhodobacter* group with three species, *L. salsilacus* (type), *L. fryxellensis* and *Loktanella vestfoldensis*. Since then, 19 species have been isolated and added to the genus *Loktanella* (listed in order of publication): *Loktanella*

hongkongensis, L. agnita, Loktanella rosea, Loktanella koreensis, Loktanella maricola, L. atrilutea, Loktanella pyoseonensis, Loktanella tamlensis, Loktanella litorea, Loktanella cinnabarina, Loktanella sediminilitoris, Loktanella soesokkakensis, Loktanella. aestuariicola, Loktanella maritima, Loktanella variabilis, Loktanella ponticola, Loktanella sediminum, Loktanella marina and *Loktanella acticola* (2, 3, 7-21). In many cases, the classification of these species within *Loktanella* was bases upon a high similarity of the 16S rRNA genes with the type species *L. salsilacus* (Figure 4-1). However, when genome sequences became available, the genus *Loktanella* proved to be polyphyletic.

After an extensive taxonomic reevaluation based on whole-genome sequences, core-gene average amino acid identity, percent of conserved proteins, and phenotypic data, most species were moved out of *Loktanella* (6). *L. hongkongensis, L. cinnabarina, L. pyoseonensis* and *L. soesokkakensis* were reclassified in the novel genus *Limimaricola* with *Limimaricola hongkongensis* as type. *L. marina* was reclassified in the novel genus *Flavimaricola*. *L. vestfoldensis, L. litorea, L. maricola, L. maritima, L. rosea, L. sediminilitoris* and *L. tamlensis* were reclassified in the novel genus *Yoonia* with *Yoonia vestfoldensis* as the type. *L. koreensis* and *L. sediminum* were reclassified in the novel genus *Cognatiyoonia* with *Cognatiyoonia koreensis* as type. At that time, genome sequences were not available for *L. aestuariicola, L. variabilis, L. agnita* and *L. ponticola*. *L. aestuariicola* and *L. variabilis* were moved into *Limimaricola* because of their high 16S rRNA sequence similarity with the other *Limimaricola* species and the phenotypic differences between these species and the remaining species in the genus *Loktanella*. *L. ponticola* and *L. agnita* were left in the genus *Loktanella* as there is no clear support from 16S rRNA and phenotype to move them into other genera. Subsequently, the genome sequence of *L. ponticola* became available. Reanalysis of its phylogeny suggested that it

was a deep lineage associated with *Yoonia* (Figure 4-2). However, neither the phylogenetic nor phenotype data clearly indicated whether or not it should be reclassified into the genus *Yoonia* or into a novel genus. Until this ambiguity is removed, the species is retained here in *Yoonia*. Lastly, *L. acticola* was described while Wirth and Whitman (2018) was in press, and its classification was not considered by them. It shares high 16S rRNA sequence similarity with most of the species reclassified as *Yoonia* compared to the similarity of the sequences of the type strains of other *Loktanella* species (94.0-96.3%) (21). It also has 8-25% DNA-DNA hybridization with *Yoonia* species. Thus, *L. acticola* should be reclassified into the genus *Yoonia* and is not considered a species of *Loktanella* here.

Currently, there are only 4 species remained in *Loktanella*. By comparing the 16S rRNA sequence similarity among them, *L. agnita* has the lowest similarity to the other three species, with a similarity of 94.25, 94.50, and 94.93% to *L. atrilutea, L. fryxellensis* and *L. salsilacus*, respectively (Figure 4-1). When the genome sequence of *L. agnita* is available, it may be reclassified into another genus.

List of species of the genus *Loktanella*

1. *Loktanella agnita* Ivanova *et al*. 2005 [VP]

ag.ni′ta. L. fem. part. adj. *agnita* recognized.

Description as for the genus and Tables 4-1 and 4-2 (2, 20). Na^+ or seawater is required for growth. Weakly reduces nitrate to nitrite. Hydrolyzes aesculin, hypoxanthine, Tweens 20, 40, and 60, and L-tyrosine but not agar, casein, chitin, DNA, gelatin, laminarin, starch, urea, or xanthine. There are conflicting results for Tween 80 hydrolysis. In assays with Biolog GN Microplates, exhibits only a limited ability to utilize carbon sources including glycyl L-glutamic acid, alaninamide, and glycyl L-aspartic acid. On basal medium (BM) (22), utilizes acetate,

cellobiose, D-fructose, D-galactose, D-glucose, L-malate, D-mannose, pyruvate, succinate, and D-xylose as sole carbon and energy sources but not L-arabinose, benzoate, citrate, formate, L-glutamate, maltose, salicin, sucrose, or trehalose. Negative for arginine dihydrolase, hemolysis, lysine decarboxylase, and ornithine decarboxylase. In assays with the API ZYM system, the reactions are positive for alkaline phosphatase, esterase lipase (C8), leucine arylamidase, and trypsin and weakly positive for acid phosphatase. The reactions are negative for α-chymotrypsin, cystine arylamidase, esterase (C4), α-fucosidase, α-galactosidase, β-galactosidase, α-glucosidase, β-glucuronidase, β-glucosidase, lipase (C14), α-mannosidase, *N*-acetyl-β-glucosaminidase, naphthol-AS-BI-phosphohydrolase, and valine arylamidase. Susceptible to carbenicillin, cephalothin, chloramphenicol, gentamicin, kanamycin, neomycin, novobiocin, oleandomycin, streptomycin, and tetracycline but resistant to ampicillin, lincomycin, penicillin G, and polymyxin B.

DNA G + C content (mol %): 59.1 (T_m).

Type strain: R10SW5 (=KMM 3788=CIP 107883).

GenBank accession (16S rRNA gene): AY682198.

GenBank accession (genome): not available.

2. *Loktanella atrilutea* Hosoya and Yokota 2007[VP]

at.ri.luˈte.a. L. adj. *ater -tra -trum* dark; L. adj. *luteus -a-um* orange; N.L. fem. adj. *atrilutea* dark orange.

Description as for the genus and Tables 4-1 and 4-2 (3). Grows on R2A agar but not on NA or TSA. Hydrolyzes Tweens 20, 40, 60, and 80 but not agar, alginate, casein, DNA, gelatin, starch, L-tyrosine, or urea. In marine oxidation fermentation (MOF) medium comprising 0.1% (w/v) casitone, 0.01% (w/v) yeast extract, 0.05% (w/v) ammonium sulfate, 0.05% (w/v) Tris buffer,

0.3% (w/v) agar, 0.001% (w/v) phenol red, and 0.5-1% (w/v) carbohydrate in half strength artificial seawater, pH 7.5 (23), produces acids from L-arabinose, cellobiose, D-fructose, D-galactose, D-glucose, lactose, maltose, D-mannose, raffinose, L-rhamnose, D-sorbitol, sucrose, and D-xylose but not dulcitol, glycerol, inositol, D-mannitol, or trehalose. Negative for production of acetoin, hydrogen sulfide, and indole. Negative for arginine dihydrolase, lysine decarboxylase, ornithine decarboxylase, and tryptophan deaminase. In assays with the API ZYM system, the reactions are positive for acid phosphatase, alkaline phosphatase, esterase (C4), esterase lipase (C8), α-galactosidase, α-glucosidase, β-glucuronidase, leucine arylamidase, and naphthol-AS-BI-phosphohydrolase. The reactions are negative for α-chymotrypsin, cystine arylamidase, α-fucosidase, β-galactosidase, β-glucosidase, lipase (C4), α-mannosidase, *N*-acetyl-β-glucosaminidase, trypsin, and valine arylamidase. The susceptibilities and resistances to antibiotics have not been reported.

DNA G + C content (mol %): 64.9 (genome).

Type strain: IG8 (=IAM 15450=NCIMB 14280=DSM 29326=JCM 23210).

GenBank accession (16S rRNA gene): AB246747.

GenBank accession (genome): GCA_ 900128995.

3. *Loktanella fryxellensis* Van Trappen et al. 2004[VP]

fry.xell.en′sis N.L. fem. adj. *fryxellensis* referring to the isolation source, Lake Fryxell, Antarctica.

Description as for the genus and Tables 4-1 and 4-2 (1, 3). Growth was observed on R2A agar but not on NA or TSA. Hydrolyzes aesculin, citrate, and Tween 80 but not agar, casein, DNA, gelatin, starch, L-tyrosine, or urea. In MOF medium, produces acids from D-fructose, D-galactose, D-glucose, inositol, lactose, maltose, D-mannose, raffinose, L-rhamnose, D-sorbitol,

sucrose, trehalose, and D-xylose but not L-arabinose, cellobiose, dulcitol, glycerol, or D-mannitol. In assays with the API 20E system, the reactions are negative for arginine dihydrolase, lysine decarboxylase, ornithine decarboxylase, and tryptophan deaminase. In assays with the API 20NE system, growth on carbohydrates is not observed, and acids from carbohydrates are not produced. In assays with the API ZYM system, the reactions are positive for alkaline phosphatase, esterase (C4), esterase lipase (C8), β-galactosidase, β-glucosidase, and leucine arylamidase and weakly positive for acid phosphatase, α-glucosidase, naphthol-AS-BI-phosphohydrolase, and valine arylamidase. The reactions are negative for α-chymotrypsin, β-glucuronidase, cystine arylamidase, α-fucosidase, α-galactosidase, *N*-acetyl-β-glucosaminidase, lipase (C14), α-mannosidase, and trypsin. The susceptibilities and resistances to antibiotics have not been reported.

DNA G + C content (mol %): 66.3 (genome).

Type strain: LMG 22007 (=CIP 108323=DSM 16213).

GenBank accession (16S rRNA gene): AJ582225.

GenBank accession (genome): GCA_ 900110065.

4. *Loktanella salsilacus* Van Trappen et al. 2004[VP]

sal.si.la′cus. L. adj. *salsus* salt, salty; L. gen. n. *lacus* of a lake; N.L. gen. n. *salsilacus* of a salt lake, referring to the isolation source, Ace Lake and Organic Lake, Vestfold Hills, Antarctica. Description as for the genus and Tables 4-1 and 4-2 (1, 3, 20). Growth was observed on R2A agar but not on NA or TSA. Hydrolyzes aesculin, citrate, hypoxanthine, and Tweens (20, 40, 60, and 80) but not agar, casein, DNA, gelatin, starch, or xanthine. There are conflicting results for urea hydrolysis, L-tyrosine hydrolysis, and nitrate reduction. Negative for production of acetoin, hydrogen sulfide, and indole. On BM, utilizes cellobiose, D-galactose, D-glucose, maltose, D-

mannose, and D-fructose as sole carbon and energy sources but not acetate, L-arabinose, benzoate, citrate, formate, L-glutamate, L-malate, pyruvate, salicin, succinate, sucrose, trehalose, or D-xylose. In MOF medium, produces acid from L-arabinose, cellobiose, D-fructose, D-galactose, D-glucose, glycerol, inositol, lactose, maltose, D-mannose, raffinose, sucrose, trehalose, and D-xylose but not dulcitol, D-mannitol, L-rhamnose, or D-sorbitol. In assays with the API 20E system, the reactions are negative for arginine dihydrolase, lysine decarboxylase, ornithine decarboxylase, and tryptophan deaminase. In assays with the API 20NE system, growth on carbohydrates is not observed, and acids from carbohydrates are not produced. In assays with the API ZYM system, the reactions are positive for esterase (C4), esterase lipase (C8), and leucine arylamidase and weakly positive for acid phosphatase, alkaline phosphatase, α-glucosidase, and naphthol-AS-BI-phosphohydrolase. The reactions are negative for α-chymotrypsin, cystine arylamidase, α-fucosidase, *N*-acetyl-β-glucosaminidase, β-glucuronidase, lipase (C14), α-mannosidase, and valine arylamidase. There are conflicting results for α-galactosidase, β-galactosidase, β-glucosidase, and trypsin. Susceptible to carbenicillin, cephalothin, chloramphenicol, gentamicin, kanamycin, neomycin, novobiocin, oleandomycin, penicillin G, polymyxin B, streptomycin, and tetracycline but resistant to ampicillin and lincomycin.

DNA G + C content (mol %): 60 (genome).

Type strain: LMG 21507 (=CIP 108322=DSM 16199).

GenBank accession (16S rRNA gene): AJ440997.

GenBank accession (genome): GCA_900114485.

Reference

1. Van Trappen S, Mergaert J, Swings J. 2004. *Loktanella salsilacus* gen. nov., sp. nov., *Loktanella fryxellensis* sp. nov. and *Loktanella vestfoldensis* sp. nov., new members of the *Rhodobacter* group, isolated from microbial mats in Antarctic lakes. Int J Syst Evol Microbiol 54:1263-1269.
2. Ivanova EP, Zhukova NV, Lysenko AM, Gorshkova NM, Sergeev AF, Mikhailov VV, Bowman JP. 2005. *Loktanella agnita* sp. nov. and *Loktanella rosea* sp. nov., from the north-west Pacific Ocean. Int J Syst Evol Microbiol 55:2203-2207.
3. Hosoya S, Yokota A. 2007. *Loktanella atrilutea* sp. nov., isolated from seawater in Japan. Int J Syst Evol Microbiol 57:1966-1969.
4. Van Trappen S, Mergaert J, Van Eygen S, Dawyndt P, Cnockaert MC, Swings J. 2002. Diversity of 746 heterotrophic bacteria isolated from microbial mats from ten Antarctic lakes. Syst and Appl Microbiol 25:603-610.
5. Ivanova EP, Nedashkovskaya OI, Sawabe T, Zhukova NV, Frolova GM, Nicolau DV, Mikhailov VV, Bowman JP. 2004. *Shewanella affinis* sp. nov., isolated from marine invertebrates. Int J Syst Evol Microbiol 54:1089-1093.
6. Wirth JS, Whitman WB. 2018. Phylogenomic analyses of a clade within the roseobacter group suggest taxonomic reassignments of species of the genera *Aestuariivita*, *Citreicella*, *Loktanella*, *Nautella*, *Pelagibaca*, *Ruegeria*, *Thalassobius*, *Thiobacimonas* and *Tropicibacter*, and the proposal of six novel genera. Int J Syst Evol Microbiol 68:2393-2411.
7. Lau SC, Tsoi MM, Li X, Plakhotnikova I, Wu M, Wong PK, Qian PY. 2004. *Loktanella hongkongensis* sp. nov., a novel member of the *alpha-Proteobacteria* originating from

marine biofilms in Hong Kong waters. Int J Syst Evol Microbiol 54:2281-2284.

8. Weon HY, Kim BY, Yoo SH, Kim JS, Kwon SW, Go SJ, Stackebrandt E. 2006. *Loktanella koreensis* sp. nov., isolated from sea sand in Korea. Int J Syst Evol Microbiol 56:2199-2202.

9. Yoon JH, Kang SJ, Lee SY, Oh TK. 2007. *Loktanella maricola* sp. nov., isolated from seawater of the East Sea in Korea. Int J Syst Evol Microbiol 57:1799-1802.

10. Moon YG, Seo SH, Lee SD, Heo MS. 2010. *Loktanella pyoseonensis* sp. nov., isolated from beach sand, and emended description of the genus *Loktanella*. Int J Syst Evol Microbiol 60:785-789.

11. Lee SD. 2012. *Loktanella tamlensis* sp. nov., isolated from seawater. Int J Syst Evol Microbiol 62:586-590.

12. Park S, Lee JS, Lee KC, Yoon JH. 2013. *Loktanella soesokkakensis* sp. nov., isolated from the junction between the North Pacific Ocean and a freshwater spring. Antonie Van Leeuwenhoek 104:397-404.

13. Park S, Jung YT, Yoon JH. 2013. *Loktanella sediminilitoris* sp. nov., isolated from tidal flat sediment. Int J Syst Evol Microbiol 63:4118-4123.

14. Yoon JH, Jung YT, Lee JS. 2013. *Loktanella litorea* sp. nov., isolated from seawater. Int J Syst Evol Microbiol 63:175-180.

15. Park S, Jung YT, Won SM, Park JM, Yoon JH. 2014. *Loktanella aestuariicola* sp. nov., an alphaproteobacterium isolated from a tidal flat. Antonie Van Leeuwenhoek 106:707-714.

16. Tanaka N, Romanenko LA, Kurilenko VV, Svetashev VI, Kalinovskaya NI, Mikhailov VV. 2014. *Loktanella maritima* sp. nov. isolated from shallow marine sediments. Int J

Syst Evol Microbiol 64:2370-2375.

17. Jung YT, Park S, Park JM, Yoon JH. 2014. *Loktanella ponticola* sp. nov., isolated from seawater. Int J Syst Evol Microbiol 64:3717-3723.

18. Park JM, Park S, Jung YT, Cho JY, Yoon JH. 2014. *Loktanella variabilis* sp. nov., isolated from a tidal flat. Int J Syst Evol Microbiol 64:2579-2585.

19. Liang J, Zhang Z, Liu Y, Wang M, Zhang XH. 2015. *Loktanella sediminum* sp. nov., isolated from marine surface sediment. Int J Syst Evol Microbiol 65:686-691.

20. Jung YT, Park S, Lee JS, Yoon JH. 2016. *Loktanella marina* sp. nov., isolated from seawater. Int J Syst Evol Microbiol 66:2528-2533.

21. Park S, Choi SJ, Won SM, Yoon JH. 2017. *Loktanella acticola* sp. nov., isolated from seawater. Int J Syst Evol Microbiol 67:4175-4180.

22. Baumann P, Baumann L. 1981. The marine gram-negative eubacteria: genera *Photobacterium*, *Beneckea*, *Alteromonas*, *Pseudomonas*, and *Alcaligenes*, p1302-1331. *In* Starr MP, Stolp H, Trüper hg, Balows A, Schlegel (ed), The Prokaryotes. Springer, Verlag Berlin.

23. Leifson E. 1963. Determination of carbohydrate metabolism of marine bacteria. J Bacteriol 85:1183.

24. Cole JR, Wang Q, Fish JA, Chai B, McGarrell DM, Sun Y, Brown CT, Porras-Alfaro A, Kuske CR, Tiedje JM. 2013. Ribosomal Database Project: data and tools for high throughput rRNA analysis. Nucleic Acids Res 42:D633-D642.

25. Kalyaanamoorthy S, Minh BQ, Wong TK, von Haeseler A, Jermiin LS. 2017. ModelFinder: fast model selection for accurate phylogenetic estimates. Nat Methods 14:587-589.

26. Nguyen L-T, Schmidt HA, Von Haeseler A, Minh BQ. 2015. IQ-TREE: a fast and effective stochastic algorithm for estimating maximum-likelihood phylogenies. Mol Biol Evol 32:268-274.

Table 4-1. Selected characteristics of *Loktanella* species. Species: 1, *L. agnita*; 2, *L. atrilutea*; 3, *L. fryxellensis*; 4, *L. salsilacus*. "+" positive. "-" negative. "ND" no data available. "v" conflicting results were reported.

Characteristic	**1**	**2**	**3**	**4**
Morphology	rods	rods	short rods	short rods
Cell size (μm)	0.7-0.9 in diameter	0.5-1.0×1.8-2.0	<1×2.0-3.0	<1×3.0-4.0
Motility	-	+	-	-
Flagellation	-	polar	-	-
Carbon source[a]				
Carbohydrates	+	ND	ND	+
Amino acids	-	ND	ND	-
Carboxylic acids	+	ND	ND	-
Catalase	+	+	+	+
Oxidase	+	+	+	+
Growth conditions (optimum)				
Temperature (ºC)	8-35 (25)	8-35 (25-30)	5-35 (25)	5-37 (25)
Salinity (% w/v NaCl)	3-6	0-8	0-5	0-10
pH	6-10 (7.5-8)	6-8	ND	ND
Nitrate reduction	+	-	-	v
Polar lipids identified	+	-	+	+
Abundant fatty acids	$C_{18:1}\omega 7c$	$C_{18:1}\omega 7c$	$C_{18:1}\omega 7c$	$C_{18:1}\omega 7c$
Major quinone	Q-10	Q-10	Q-10	Q-10
API ZYM determined[b]	+	+	+	+
Isolation habitat	Seawater	seawater	microbial mats from salty lake	microbial mats from salty lake
References	2, 20	3	1	1, 20

[a]Results based on tests describe in detail in the species description.

[b]API ZYM results are given in the species descriptions.

Table 4-2. Selected characteristics distinguishing of *Loktanella* species. Species: 1, *L. agnita*; 2, *L. atrilutea*; 3, *L. fryxellensis*; 4, *L. salsilacus*. "+" positive or weakly positive. "-" negative. "ND" no data available. "v" conflicting results were reported.

Characteristic	**1**	**2**	**3**	**4**
Hydrolysis of				
L-tyrosine	+	-	-	v
Tween 80	v	+	+	+
urea	-	-	-	v
Produce acid from				
L-arabinose	ND	+	-	+
cellobiose	ND	+	-	+
dulcitol	ND	-	+	+
glycerol	ND	-	-	+
inositol	ND	-	+	+
L-rhamnose	ND	+	+	-
D-sorbitol	ND	+	+	-
trehalose	ND	-	+	+
D-xylose	ND	+	+	+
Polar lipids				
diphosphatidylglycerol	+	ND	-	-
phosphatidylethanolamine	+	ND	-	+
Enzyme activity				
esterase (C4)	-	+	+	+
α-galactosidase	-	+	-	v
β-galactosidase	-	-	+	v
α-glucosidase	-	+	+	+
β-glucosidase	-	-	+	v
β-glucuronidase	-	+	-	-
naphthol-AS-BI-phosphohydrolase	-	+	+	+
trypsin	+	-	-	v
valine arylamidase	-	-	+	-
Antibiotics susceptibility				
penicillin G	-	ND	ND	+
polymycin B	-	ND	ND	+
References	2, 20	3	1, 3	1, 3, 20

Table 4-3. Cellular fatty acids in the *Loktanella* species. Species: 1, *L. agnita*; 2, *L. atrilutea*; 3, *L. fryxellensis*; 4, *L. salsilacus*. "-" no data available or not detected.

Fatty acids	**1**	**2**	**3[a]**	**4[b]**
$C_{12:0}$	0.4	-	-	-
$C_{14:0}$	4.6	-	-	-
$C_{14:1}$	4.6	-	-	-
$C_{15:0}$	4.6	-	-	-
$C_{16:0}$	4.6	9.5	2.7±1.1	2.9±0.9
$C_{17:0}$	1.7	-	-	-
$C_{18:0}$	-	2.2	1.6±0.9	1.4±0.8
$C_{18:2}$	1.8	-	-	-
$C_{10:0}$ 3-OH	1.0	1.5	3.7±1.1	2.4±0.7
$C_{12:1}$ 3-OH	-	-	-	-
$C_{16:1}\omega 7c$	1.9	-	-	-
$C_{17:1}\omega 6c$	-	-	-	-
$C_{17:1}\omega 8c$	-	-	-	-
$C_{18:1}\omega 7c$	79	74.4	84.9±3.7	87.7±1.9
$C_{18:1}\omega 9c$	4.4	-	-	-
$C_{19:1}cy$	1.7	-	-	-
11-methyl $C_{18:1}\omega 7c$	-	6.3	-	<1
Summed feature 2[c]	-	3.8	1.7±0.7	<1
Summed feature 3[d]	-	-	-	2.8±0.9
Summed feature 7[e]	-	1.0	4.7±2.0	1.2±1.0
References	2	3	1	1

[a]Mean percentage of total fatty acids with corresponding standard deviation from 12 strains.

[b]Mean percentage of total fatty acids with corresponding standard deviation from 10 strains.

[c]Summed feature 2 comprises $C_{12:0}$ aldehyde, iso-$C_{16:1}$ I, $C_{14:0}$ 3-OH and/or unknown 10.928.

[d]Summed feature 3 comprises iso-$C_{15:0}$ 2-OH and/or $C_{16:1}\omega 7c$.

[e]Summed feature 7 comprises $C_{19:1}\omega 6c$ and/or $C_{19:0}\omega 10c$ cyclo and/or unknown ELC 18.846.

Table 4-4. Genome sequences for the *Loktanella* species. All genomes were downloaded from NCBI (https://www.ncbi.nlm.nih.gov). Genomes of *L. agnita* is currently not available.

Strain	Assembly level	Genome size (Mbp)	Number of PEG[a]	Number of REG[b]
L. atrilutea IG8^T	contig	4.21	3940	51
L. fryxellensis LMG 22007^T	scaffold	3.55	3288	50
L. salsilacus LMG 21507^T	contig	4.13	3810	57

Table 4-4 (continued).

Strain	Number of scaffolds	Number of contigs	GenBank assembly
L. atrilutea IG8^T	46	46	GCA_ 900128995
L. fryxellensis LMG 22007^T	74	75	GCA_900110065
L. salsilacus LMG 21507^T	77	77	GCA_900114485

[a]Predicted protein-encoding genes (PEG).

[b]Predicted stable RNA-encoding genes (REG).

Table 4-5. Characteristics distinguishing of *Loktanella* from other, closely related genera.

Genera: 1, *Loktanella*; 2, *Cognatiyoonia*; 3, *Flavimaricola*; 4, *Limimaricola*; 5, *Yoonia*. "+" all of the species are positive. "-" all of the species are negative. "d" one or more but not all of the species are positive.

Characteristic	**1**	**2**	**3**	**4**	**5**
API ZYM					
acid phosphatase	+	d	+	d	d
α-chymotrypsin	-	d	-	d	-
cystine arylamidase	-	d	-	d	-
lipase (C14)	-	-	-	d	-
leucine arylamidase	+	+	+	+	d
Hydrolyze					
aesculin	+*	+	+	d	d
gelatin	-	+	-	-	-
starch	-	-	-	-	d

*: No data available for *Loktanella atrilutea*.

Figure 4-1. 16S rRNA gene-based phylogenetic tree of *Loktanella* species and their relatives. Prior to the reclassification by Wirth and Whitman (2018), all species shown in the tree except *Ruegeria atlantica, Wenxinia marina, Roseobacter litoralis, Salipiger mucosus* and *Shimia marina* were classified in the genus *Loktanella*. In the tree, former *Loktanella* species are named according to their reclassification. Type species are bolded. 16S rRNA gene sequences were downloaded from NCBI and aligned using RDP aligner (https://rdp.cme/msu.edu) (24). The phylogenetic tree was constructed by maximum-likelihood analysis using IQTREE with 1000 non-parametric bootstrap replicates (25, 26). The scale bar indicates the number of substitutions per site.

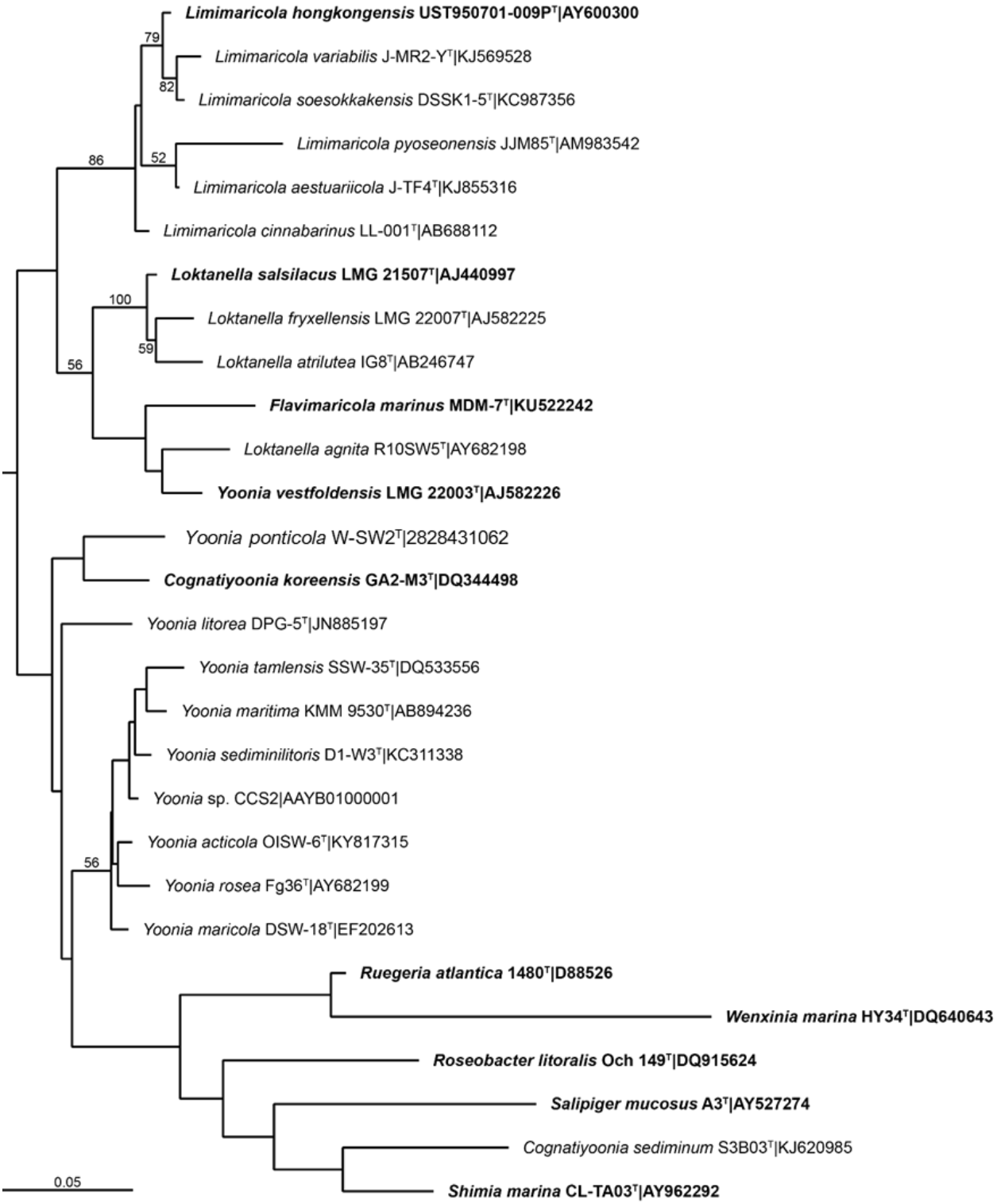
Limimaricola hongkongensis UST950701-009P^{T}|AY600300
Limimaricola variabilis J-MR2-Y^{T}|KJ569528
Limimaricola soesokkakensis DSSK1-5^{T}|KC987356
Limimaricola pyoseonensis JJM85^{T}|AM983542
Limimaricola aestuariicola J-TF4^{T}|KJ855316
Limimaricola cinnabarinus LL-001^{T}|AB688112
Loktanella salsilacus LMG 21507^{T}|AJ440997
Loktanella fryxellensis LMG 22007^{T}|AJ582225
Loktanella atrilutea IG8^{T}|AB246747
Flavimaricola marinus MDM-7^{T}|KU522242
Loktanella agnita R10SW5^{T}|AY682198
Yoonia vestfoldensis LMG 22003^{T}|AJ582226
Yoonia ponticola W-SW2^{T}|2828431062
Cognatiyoonia koreensis GA2-M3^{T}|DQ344498
Yoonia litorea DPG-5^{T}|JN885197
Yoonia tamlensis SSW-35^{T}|DQ533556
Yoonia maritima KMM 9530^{T}|AB894236
Yoonia sediminilitoris D1-W3^{T}|KC311338
Yoonia sp. CCS2|AAYB01000001
Yoonia acticola OISW-6^{T}|KY817315
Yoonia rosea Fg36^{T}|AY682199
Yoonia maricola DSW-18^{T}|EF202613
Ruegeria atlantica 1480^{T}|D88526
Wenxinia marina HY34^{T}|DQ640643
Roseobacter litoralis Och 149^{T}|DQ915624
Salipiger mucosus A3^{T}|AY527274
Cognatiyoonia sediminum S3B03^{T}|KJ620985
Shimia marina CL-TA03^{T}|AY962292
79
82
86
52
100
59
56
56
0.05

Figure 4-2. Core-gene-based phylogenetic tree of *Loktanella* species and its relatives. Bolded taxa indicate the type species of the genera. Note that *Limiamricola variabilis* and *Yoonia ponticola* were not included in the reclassification of Wirth and Whitman (2018). The whole-genome sequences were downloaded from NCBI (https://www.ncbi.nlm.nih.gov/) or IMG (https://img.jgi.doe.gov) and subjected to phylogenomic analyses as previously described (6). The maximum-likelihood tree was constructed using IQTree version 1.6.3 with the best model (LG+F+I+G4) identified by Bayesian information criterion and 100 bootstrap replicates (25, 26). The scale bar indicates the number of substitutions per site.

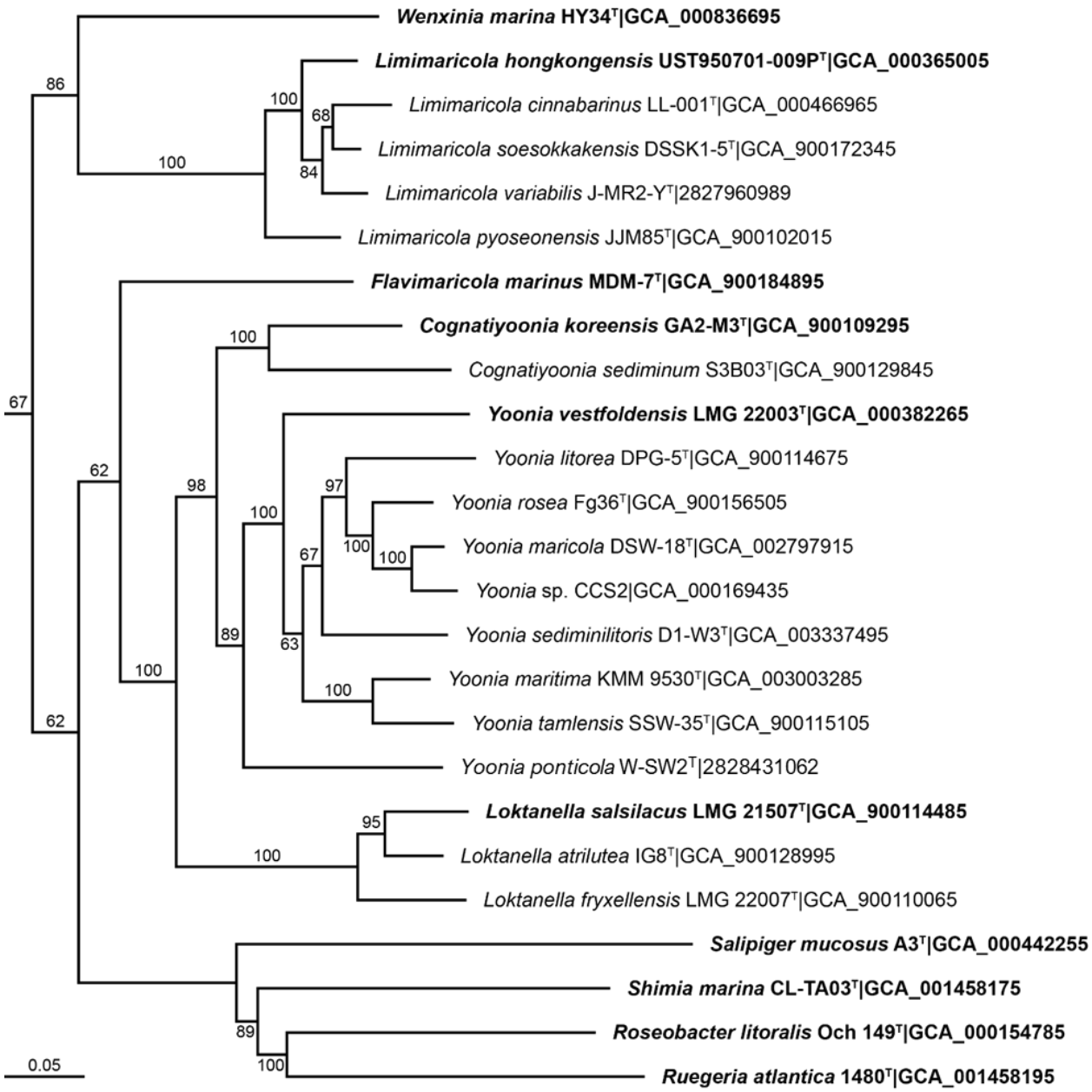
Wenxinia marina HY34T|GCA_000836695
Limimaricola hongkongensis UST950701-009PT|GCA_000365005
Limimaricola cinnabarinus LL-001T|GCA_000466965
Limimaricola soesokkakensis DSSK1-5T|GCA_900172345
Limimaricola variabilis J-MR2-YT|2827960989
Limimaricola pyoseonensis JJM85T|GCA_900102015
Flavimaricola marinus MDM-7T|GCA_900184895
Cognatiyoonia koreensis GA2-M3T|GCA_900109295
Cognatiyoonia sediminum S3B03T|GCA_900129845
Yoonia vestfoldensis LMG 22003T|GCA_000382265
Yoonia litorea DPG-5T|GCA_900114675
Yoonia rosea Fg36T|GCA_900156505
Yoonia maricola DSW-18T|GCA_002797915
Yoonia sp. CCS2|GCA_000169435
Yoonia sediminilitoris D1-W3T|GCA_003337495
Yoonia maritima KMM 9530T|GCA_003003285
Yoonia tamlensis SSW-35T|GCA_900115105
Yoonia ponticola W-SW2T|2828431062
Loktanella salsilacus LMG 21507T|GCA_900114485
Loktanella atrilutea IG8T|GCA_900128995
Loktanella fryxellensis LMG 22007T|GCA_900110065
Salipiger mucosus A3T|GCA_000442255
Shimia marina CL-TA03T|GCA_001458175
Roseobacter litoralis Och 149T|GCA_000154785
Ruegeria atlantica 1480T|GCA_001458195
0.05

CHAPTER 5

THE GENUS *YOONIA*[1]

[1]Wang T, Wirth JS, Chen C, Whitman WB. 2021. In *Bergey's Manual of Systematics of Archaea and Bacteria* (eds Trujillo ME, Dedysh S, DeVos P, Hedlund B, Kämpfer P, Rainey FA and Whitman WB).

Abstract

Gram-negative staining, aerobic, non-spore-forming, catalase- and oxidase-positive cocci, ovoids, or rods. Optimal growth typically occurs between 25 and 30 ˚C, 0-5 % (w/v) NaCl, and pH 6.5-8. Capable of utilizing a large variety of organic carbon compounds. All species tested can utilize acetate and L-malate as sole carbon and energy sources. The major fatty acid is $C_{18:1}\omega 7c$. The major quinone is ubiquinone 10 (Q-10). Species have been isolated globally from marine environments such as seawater, marine sediments, and microbial mats. Members of the family *Rhodobacteraceae*. The type species is *Yoonia vestfoldensis*.

Etymology

Yoo′ni.a. N.L. fem. n. *Yoonia* in honour of Jung-Hoon Yoon, for his contributions to the taxonomy of marine *Alphaproteobacteria*.

Description

Coccoid, ovoid, or rod shaped, Gram-negative staining, and non-spore-forming. Usually not flagellated. *Yoonia tamlensis* is the only flagellated species and possesses a polar flagellum. Motility was not observed in any species except *Y. tamlensis.* All species are aerobes. Positive for catalase and oxidase. Unable to reduce nitrate to nitrite. Growth temperatures range from 4 to 37 ˚C, but optimal growth occurs between 25 and 30 ˚C. Species including *Yoonia maricola*, *Yoonia maritima*, and *Yoonia rosea* require NaCl for growth. Optimal NaCl concentrations are between 0 and 5 % (w/v), but growth occurs between 0 % and 12 % (w/v) NaCl. All species have an optimal pH between 6.5 and 8, but growth occurs between pH 5.5 and pH 10.

Capable of degrading a variety of carbon compounds including carbohydrates and carboxylic acids. All species tested can utilize acetate, cellobiose, D-galactose, D-glucose, and L-malate as sole carbon and energy sources. None of the species tested can produce acids from D-glucose, lactose, maltose, melezitose, *myo*-inositol, raffinose, L-rhamnose, D-ribose, D-sorbitol, or trehalose. The major quinone is ubiquinone 10 (Q-10). The polar lipids in at least one species comprise diphosphatidylglycerol, phosphatidylethanolamine, phosphatidylcholine, phosphatidylglycerol, unidentified aminolipids, unidentified aminophospholipids, unidentified lipids, and unidentified phospholipids. The major fatty acid is $C_{18:1}\omega 7c$. The fatty acids ≥ 1.0 % of the total fatty acids in at least one species comprise $C_{16:0}$, $C_{17:0}$, $C_{18:0}$, $C_{18:2}$, $C_{17:1}\omega 8c$, $C_{18:1}\omega 7c$, 11-methyl $C_{18:1}\omega 7c$, $C_{10:0}$ 3-OH, $C_{12:1}$ 3-OH, iso-$C_{17:0}$ 3-OH, summed feature 3 (iso-$C_{15:0}$ 2-OH

and/or $C_{16:1}\omega 7c$), summed feature 7 ($C_{19:1}\omega 6c$ and/or $C_{19:0}\omega 10c$ cyclo and/or unknown ELC 18.846), and the unknown fatty acid ECL 11.799.

Species are globally distributed in marine environments. Species have been isolated from seawater, marine sediments, and microbial mats. Members of the family *Rhodobacteraceae*. The type species is *Yoonia vestfoldensis*.

DNA G + C content (mol %): 53.4-61.8.

Type species: Yoonia vestfoldensis Wirth and Whitman 2018^{VP} (*Loktanella vestfoldensis* Van Trappen et al. 2004^{VP}).

Number of species with validated names: 9.

Further Descriptive Information

Cell morphology. The cells of all species in *Yoonia* are Gram-negative staining cocci, ovoids, or rods (1-9). For a summary of morphological characters of the *Yoonia* species, see Table 5-1. Cell length varies from 0.4 to 7.0 µm and cell width varies from 0.2 to 1.2 µm. *Yoonia acticola* cells greater than 10 µm are also observed. Most species are nonmotile and not flagellated, but *Yoonia tamlensis* is motile by means of a polar flagellum (4). Some species, including *Y. tamlensis* and *Yoonia vestfoldensis*, can occur in pairs (2). *Y. vestfoldensis* can also form short chains.

Colonial and cultural characteristics. On plates, colonies can typically be observed after 2-7 days. Colonies can be up to 3 mm in diameter. Colonies of *Y. acticola* are greyish yellow, circular, slightly convex, glistening, smooth, and 0.5-1.0 mm in diameter after incubation for 7 days at 25 ºC on marine agar 2216 (MA, B.D.) (8). Colonies of *Yoonia litorea* are light orange-yellow, circular to slightly irregular, slightly convex, smooth, glistening, and 1.0-2.0 mm in diameter after 3 days at 30 ºC on MA (3). Colonies of *Y. maricola* are light orange, circular, slightly convex, glistening and 1.0-2.0 mm in diameter after 7 days at 25 ºC on MA (5). Colonies of *Y. maritima* are light beige-pigmented, shiny smooth with regular edges, and 2-3 mm in

diameter (1). Colonies of *Yoonia ponticola* are greyish-yellow, circular, slightly convex, smooth, glistening, and 1.0-2.0 mm in diameter after incubation for 7 days at 25 ºC on MA (9). Colonies of *Y. rosea* are pinkish, round, regular, convex, smooth, transparent, and 1-3 mm in diameter after 2-3 days on MA (7). Colonies of *Yoonia sediminilitoris* are greyish-yellow, circular, slightly convex, smooth, glistening and 0.5-1.0 mm in diameter after 7 days at 25 ºC (6). Colonies of *Y. tamlensis* are beige, circular, smooth, convex, translucent, and 1-3 mm in diameter on yeast extract-malt extract-seawater (YE-SW) agar after 3 days at 30 ºC (4). Colonies of *Y. vestfoldensis* are pale pink, convex, translucent with entire margins (2). The colonies are smaller than 1 mm in diameter after 2 days at 25 ºC on MA and do not adhere to the agar.

Nutrition and growth conditions. Reports on the *Yoonia* growth range and optimal conditions are incomplete (Table 5-1). All species tested grow optimally at pH 6.5-8.0 and 25-30 ºC. *Yoonia* species grow optimally at NaCl concentrations below 5 % (w/v), but *Y. rosea* and *Y. vestfoldensis* can tolerate more than 10% (w/v) NaCl.

Various carbon sources are utilized by *Yoonia* as sole sources of carbon and energy, but the data are not complete for *Y. acticola*, *Y. maritima*, *Y. ponticola*, and *Y. vestfoldensis* (Table 5-2 and species descriptions). All species tested can utilize acetate, cellobiose, D-galactose, D-glucose and L-malate but not benzoate, formate, L-glutamate, or salicin as sole carbon and energy sources. All species tested cannot produce acid from D-glucose, lactose, maltose, D-mannose, melezitose, *myo*-inositol, raffinose, L-rhamnose, D-ribose, D-sorbitol, or trehalose.

There are several characters that distinguish the *Yoonia* species from one another (Table 5-2). *Y. litorea* is the only species tested that is unable to utilize L-arabinose and D-fructose as sole sources of carbon and energy. *Y. maritima* is the only species tested that can produce acids from cellobiose and D-galactose and positive for valine arylamidase. *Y. ponticola* is the only

species that can hydrolyze xanthine. *Y. rosea* is the only species tested that can hydrolyze tyrosine, produce acid from D- fructose, and tolerate 12% (w/v) NaCl. *Y. sediminilitoris* is the only species tested that cannot utilize pyruvate or succinate as sole sources of carbon and energy. *Y. tamlensis* is the only species tested that can hydrolyze starch, produce acid from D-mannitol, and is positive for *N*-acetyl-β-glucosaminidase. *Y. vestfoldensis* is the only species tested that can hydrolyze urea and is positive for β-glucosidase.

In assays with the API ZYM system, all the species are positive or weakly positive for alkaline phosphatase, esterase (C4), and esterase lipase (C8). All the species are negative for α-chymotrypsin, cystine arylamidase, α-fucosidase, α-galactosidase, β-glucuronidase, lipase (C14), and α-mannosidase.

Yoonia species are susceptible to a variety of antibiotics, but not all species have been tested for the same antibiotics. The antibiotic susceptibility in *Y. vestfoldensis* has not been reported. The remaining species tested are susceptible to carbenicillin (no data for *Y. ponticola*), cephalothin, chloramphenicol, gentamicin, novobiocin, and oleandomycin. *Y. maricola*, *Y. maritima*, *Y. rosea*, *Y. sediminilitoris*, and *Y. tamlensis* are all susceptible to benzylpenicillin, cephazolin, cephalexin, erythromycin, oxacillin, ofloxacin, rifampicin, and vancomycin.

Chemotaxonomic characteristics. The major fatty acid in *Yoonia* is $C_{18:1}$ *ω7c*. It is present in every species with a range of 65-81 %. The following fatty acids have also been observed in all *Yoonia* species: $C_{16:0}$ and $C_{18:0}$. For a complete list of the fatty acids in the *Yoonia* species, see Table 5-3.

Although the polar lipid content of the type species *Y. vestfoldensis* has not been determined, all of the *Yoonia* species tested possess phosphatidylglycerol and phosphatidylcholine as major polar lipids (Table 5-2). All the *Yoonia* species tested except *Y.*

litorea and *Y. ponticola* also possess diphosphatidylglycerol as a major polar lipid. For a complete list of the polar lipids in the *Yoonia* species, see Table 5-2.

Genome features. Draft genome sequences are publicly available for the type strains of all of the *Yoonia* species except *Y. acticola*. By comparing the genomes of the type strains downloaded from NCBI, there are 721 core function genes shared in this genus. In addition, there is a complete genome sequence available for the reference strain of *Y. vestfoldensis*, strain SMR4r. This strain possesses 3 replicons: one chromosome of 3.84 Mbp and two small plasmids of 0.11 and 0.04 Mbp. Table 5-4 provides details of the whole-genome sequences of *Yoonia* species. A genetics system for the *Yoonia* species has not been published.

Ecology. *Yoonia* species are found in aerobic, saltwater environments (1-9). With the exception of *Y. vestfoldensis*, which was originally isolated from Antarctic lakes, all remaining species were isolated from seas around Korea, Japan, and Russia. *Yoonia* appears to be cosmopolitan, and closely related 16S rRNA genes have been identified in environmental samples from around the world, such as saltwater lakes, seawater, marine sediments, and algal or coral tissues. The wide range of growth temperatures, salinities, and carbon sources of *Yoonia* species may help to explain their presences in such a wide variety of environments.

Enrichment and Isolation Procedures

All of the *Yoonia* species were isolated by dilution plating (3-6, 8-12). *Y. acticola* was isolated by plating seawater collected near Oido, an island in the Yellow Sea, South Korea, on MA and incubating at 25 ºC for 10 days (8). *Y. maricola*, *Y. litorea*, and *Y. sediminilitoris* were isolated by standard dilution plating of seawater from the South Sea of Korea, the East Sea of Korea, and tidal sediment from Boseong in the South Sea of Korea, respectively, at 25 ºC on MA (3, 5, 6)**.** *Y. maritima* was isolated by serially diluting shallow sediment with sterile seawater, plating on MA,

and incubating for 7 days at 28 ºC (1). The sediment sample was collected from Peter the Great Bay, the Sea of Japan, Russia. *Y. ponticola*. was isolated by plating seawater from Wando in the South Sea of South Korea on MA and incubating at 25 ºC (9). *Y. rosea* was isolated from marine sediment from Chazhma Bay, Sea of Japan, Pacific Ocean, homogenized with sterile seawater (7, 13). Dilutions were then plated on MA or medium B. Medium B comprised 0.2% (w/v) peptone, 0.2% (w/v) casein hydrolysate, 0.2% (w/v) yeast extract, 0.1% (w/v) glucose, 0.02% (w/v) KH_2PO_4, 0.005% (w/v) $MgSO_4 \cdot 7H_2O$ and 1.5% (w/v) agar in 50% (v/v) seawater at pH 7.8. Plates were incubated aerobically for 7 days at room temperature. *Y. tamlensis* was isolated from surface seawater at Samyang Beach in Jeju, Republic of Korea, by directly diluting a water sample and plating onto YE-SW agar for 5 days at 30 ºC (4). *Y. vestfoldensis* was isolated by plating dilutions of homogenized microbial mat samples from lake Ace and Pendant, Vestfold Hills, Antarctica, in sterile physiological water [0.86% (w/v) NaCl] (1). Plates were then incubated in aerobic conditions at 4 ºC or 20 ºC.

Maintenance Procedures

Strains of *Yoonia* can be maintained on solid media or in liquid cultures. Because all *Yoonia* species are aerobes, shaking is recommended for liquid cultures in order to increase the oxygenation.

Several types of rich media have been used to cultivate the *Yoonia* species. The most common medium is marine agar/broth 2216 (MA/MB, B.D.). All species are routinely cultivated on MA or MB except *Y. tamlensis* (1-9). *Y. tamlensis* can also grow on MA but is routinely cultivated in YE-SW broth or agar. YE-SW broth comprises of 0.4% (w/v) yeast extract, 1% (w/v) malt extract, 0.4% (w/v) glucose in 60% (v/v) seawater, pH 7.2. This liquid medium can be solidified by adding 1.8% (w/v) agar. *Y. vestfoldensis* can also grow on R2A agar and grow

weakly on trypticase soy agar (TSA) and nutrient agar (NA). All other tested species cannot grow on either TSA or NA.

Several *Yoonia* species were cultivated in an artificial seawater-based medium (1, 3, 5, 6, 9). The artificial seawater contains 2.36% (w/v) NaCl, 0.064% (w/v) KCl, 0.453% (w/v) $MgCl_2 \cdot 6H_2O$, 0.594% (w/v) $MgSO_4 \cdot 7H_2O$, and 0.13% (w/v) $CaCl_2 \cdot 2H_2O$ (14). The amount of NaCl may vary depending on the desired salinity. A basal medium (BM) was also used to cultivate *Yoonia* species. It contains 200 mM NaCl, 50 mM $MgSO_4$, 10 mM KCl, 10 mM $CaCl_2$, 50-100 mM Tris HCl (pH 7.5), 19 mM NH_4Cl, 0.33 mM K_2HPO_4, and 0.1 mM $FeSO_4$ (15) with 2% (v/v) Hunter's mineral salts solution (16) and 1% (v/v) vitamin solution (3, 5, 6, 17). In addition, 0.02% (w/v) $NaNO_3$, 0.002% (w/v) yeast extract, and 1.5% (w/v) agar can be added when necessary (3). The sole carbon sources are typically added for a final concentration of 0.1% (w/v).

In order to store *Yoonia* species, cultures in rich media are mixed with a sterile glycerol solution for a final concentration of 20-30 % (v/v) glycerol. The freezer stock can then be stored at -20 ˚C or -80 ˚C for long-term preservation (1, 4, 6).

Differentiation of the genus Yoonia from other genera

Although many phenotypic and chemotaxonomic characters were examined for *Yoonia* and related genera, the data for many species are still not available, and many characteristics were not tested for all the species. Thus, only a few characters are known that distinguish *Yoonia* from the closely related genera *Cognatiyoonia*, *Flavimaricola*, *Limimaricola*, and *Loktanella*, Table 5-5. So far, the most reliable way to distinguish *Yoonia* species from other genera is via the comparisons of whole-genome sequences. RpoC protein sequences are also proposed to serve as a reliable phylogenetic marker to distinguish between various genera if whole-genomes are

unavailable (18). In contrast, the 16S rRNA sequence similarity is not a reliable marker in this group (see the following discussion).

Taxonomic comments

All the species of *Yoonia* were originally classified in the genus *Loktanella* because of the high similarity of the 16S rRNA gene sequences and biochemical properties (1-9). However, recent research indicated that 16S rRNA gene sequence similarity is a poor marker for the phylogeny of the roseobacter group, although it can still accurately assign members to this group (19, 20). After examining the core-gene phylogeny (Figure 5-1), core-gene average amino acid identity (cAAI), percent of conserved proteins (POPCs), and phenotypes, *Loktanella litorea*, *Loktanella maricola*, *Loktanella maritima***,** *Loktanella rosea*, *Loktanella sediminilitoris*, *Loktanella tamlensis*, and *Loktanella vestfoldensis* were reclassified into the novel genus *Yoonia* with *Yoonia vestfoldensis* as the type species (18). Similar conclusions were reached upon a phylogenomic analysis of the entire *Alphaproteobacteria* class (21). The genome of *Loktanella ponticola* was not available at that time, and it was left in the genus *Loktanella* in the absence of unambiguous evidence from the 16S rRNA and phenotype to move them into other genera. Recently, the genome sequence of *L. ponticola* became available. Reanalysis of its phylogeny suggested that it was a deep lineage associated with *Yoonia*, and it is reclassified to that genus (Figure 5-1). *Loktanella acticola* was described while Wirth and Whitman (2018) was in press, and its classification was not considered. It shares high 16S rRNA gene sequence similarity with most of the species reclassified as *Yoonia* (97.0-98.9%) compared to the similarity of the sequences of the type strains of other *Loktanella* species (94.0-96.3%) (8). It also has 8-25% DNA-DNA hybridization with *Yoonia* species. Thus, *L. acticola* was reclassified into the genus *Yoonia.*

Cognatiyoonia is a genus closely related to *Yoonia*. The core-genome phylogeny of these species indicates that they could be grouped into a single genus or two novel genera (18). They were split into two genera because of the lower cAAI and POCP value when combined. In addition, both the Cognatiyoonia species are positive for gelatinase and nitrate reduction, which none of the *Yoonia* species are. By pangenome analysis of *Yoonia* and *Cognatiyoonia* species, there are 1,317 core functional genes shared by all the species in these genera (Figure 5-2), which makes up more than 30% of the functional genes in each species.

List of species of the genus Yoonia

1. *Yoonia acticola* comb. nov., (*Loktanella acticola* Park et al. 2017)

ac.ti′co.la. L. n. *acta -ae* seaside, shore; L. suff. *-cola* (from L. n. *incola*) a dweller, inhabitant; N.L. fem. n. *acticola* a dweller of seaside.

Description as for the genus and Tables 5-1 and 5-2 (8). Mg^{2+} ions are not required for growth. Hydrolyzes aesculin, hypoxanthine, and Tween 80 but not agar, casein, gelatin, starch, L-tyrosine, urea, or xanthine. In marine oxidation fermentation (MOF) medium comprising 0.1% (w/v) Casitone, 0.01% (w/v) yeast extract, 0.05% (w/v) ammonium sulfate, 0.05% (w/v) Tris buffer, 0.3% (w/v) agar, 0.001% (w/v) phenol red, and 0.5-1% (w/v) carbohydrate in half strength artificial seawater, pH 7.5 (22), produces acids from D-fructose and D-mannitol but not L-arabinose, cellobiose, D-galactose, D-glucose, *myo*-inositol, lactose, maltose, D-mannose, melezitose, melibiose, raffinose, L-rhamnose, D-ribose, D-sorbitol, sucrose, trehalose, or D-xylose. In assays with API ZYM system, the reactions are positive for alkaline phosphatase, esterase (C4), esterase lipase (C8), leucine arylamidase, and naphthol-AS-BI-phosphohydrolase. The reactions are negative for acid phosphatase, α-chymotrypsin, cystine arylamidase, α-fucosidase, α-galactosidase, β-galactosidase, α-glucosidase, β-glucuronidase, β-glucosidase,

lipase (C4), α-mannosidase, *N*-acetyl-β-glucosaminidase, trypsin, and valine arylamidase. Susceptible to ampicillin, benzylpenicillin, cephalothin, chloramphenicol, gentamicin, kanamycin, neomycin, novobiocin, oleandomycin, penicillin G, streptomycin, and tetracycline but resistant to lincomycin and polymyxin B.

DNA G + C content (mol %): 57.3 (LC).

Type strain: OISW-6 (=KCTC 52837=NBRC 112781).

Basonym: *Loktanella acticola*.

GenBank accession (16S rRNA gene): KY817315.

GenBank accession (genome): not available.

2. *Yoonia litorea* Wirth and Whitman 2018^{VP} (*Loktanella litorea* Yoon et al. 2013^{VP}).

li.to′re.a. L. fem. adj. *litorea* of or belonging to the seashore.

Description as for the genus and Tables 5-1 and 5-2 (3). The properties are based on those of type strain and may not be typical for all members of the species. Hydrolyzes aesculin and hypoxanthine but not agar, casein, gelatin, starch, Tweens (20, 40, 60, and 80), L-tyrosine, urea, or xanthine. On BM agar, utilizes acetate, cellobiose, D-galactose, D-glucose, L-malate, maltose, D-mannose, pyruvate, sucrose, succinate, and trehalose (weakly) as sole carbon and energy sources but not L-arabinose, benzoate, citrate, formate, D-fructose, L-glutamate, salicin, and D-xylose. In MOF medium, produces acids from L-arabinose and melibiose but not from cellobiose, D-fructose, D-galactose, D-glucose, *myo*-inositol, lactose, maltose, D-mannitol, D-mannose, melezitose, raffinose, L-rhamnose, D-ribose, D-sorbitol, sucrose, trehalose, or D-xylose. In assays with the API ZYM system, the reactions are positive for acid phosphatase, alkaline phosphatase, esterase (C4), esterase lipase (C8), and naphthol-AS-BI-phosphohydrolase. The reactions are negative for α-chymotrypsin, cystine arylamidase, α-fucosidase, α-

galactosidase, β-galactosidase, *N*-acetyl-β-glucosaminidase, α-glucosidase, β-glucosidase, β-glucuronidase, leucine arylamidase, lipase (C14), α-mannosidase, trypsin, or valine arylamidase. Susceptible to carbenicillin, cephalothin, chloramphenicol, gentamicin, novobiocin, and oleandomycin but resistant to ampicillin, kanamycin, lincomycin, neomycin, penicillin G, polymyxin B, streptomycin, and tetracycline.

DNA G + C content (mol %): 57.5 (genome).

Type strain: DPG-5 (=KCTC 23883=CCUG 62113).

Basonym: *Loktanella litorea*.

GenBank accession (16S rRNA gene): JN885197.

GenBank accession (genome): GCA_900114675.

3. *Yoonia maricola* Wirth and Whitman 2018^{VP} (*Loktanella maricola* Yoon et al. 2007).

ma.ri′co.la. L. n. *mare* sea; L. suff. *-cola* (from L. n. *incola*) a dweller, inhabitant; N.L. n. *maricola* inhabitant of the sea.

Description as for the genus and Tables 5-1 and 5-2 (1, 3, 5). The properties are based on those of the type strain and may not be typical for all members of the species. Growth does not occur on TSA, NA, MacConkey agar, or in the absence of NaCl. Hydrolyzes hypoxanthine and Tweens 20, 40, and 60 but not agar, casein, chitin, DNA, gelatin, starch, L-tyrosine, urea, or xanthine. There are conflicting results for the hydrolysis of aesculin and Tween 80. Produces bacteriochlorophyll *a* aerobically in the dark but not hydrogen sulfide or indole. Negative for arginine dihydrolase, lysine decarboxylase, ornithine decarboxylase, and tryptophan deaminase. On BM, utilizes acetate, L-arabinose, cellobiose, citrate, D-galactose, D-glucose, D-fructose, L-malate, pyruvate, and succinate as energy and carbon sources but not benzoate, formate, L-glutamate, maltose, D-mannose, salicin, sucrose, trehalose, or D-xylose. In MOF medium, does

not produce acid from L-arabinose, cellobiose, D-fructose, D-galactose, D-glucose, *myo*-inositol, lactose, maltose, D-mannitol, D-mannose, melezitose, melibiose, raffinose, L-rhamnose, D-ribose, D-sorbitol, sucrose, trehalose, or D-xylose. In assays with the API ZYM system, the reactions are positive for alkaline phosphatase, esterase (C4), esterase lipase (C8), and naphthol-AS-BI-phosphohydrolase and weakly positive for acid phosphatase and leucine arylamidase. The reactions are negative for α-chymotrypsin, cystine arylamidase, α-fucosidase, α-galactosidase, β-galactosidase, *N*-acetyl-β-glucosaminidase, α-glucosidase, β-glucosidase, β-glucuronidase, lipase (C14), α-mannosidase, trypsin, and valine arylamidase. There are conflicting results for naphthol-AS-BI-phosphohydrolase. Susceptible to ampicillin, benzylpenicillin, carbenicillin, cephazolin, cephalothin, chloramphenicol, doxycycline, erythromycin, gentamycin, kanamycin, lincomycin, nalidixic acid, neomycin, novobiocin, oleandomycin, oxacillin, ofloxacin, penicillin G, rifampicin, streptomycin, tetracycline, and vancomycin but resistant to polymyxin B.

DNA G + C content (mol %): 56.2 (genome).

Type strain: DSW-18 (=KCTC 12863=JM 14564= DSM 29128).

Basonym: *Loktanella maricola*.

GenBank accession (16S rRNA gene): EF202613.

GenBank accession (genome): GCA_002797915.

4. *Yoonia maritima* Wirth and Whitman 2018^{VP} (*Loktanella maritima* Tanaka et al. 2014).

ma.ri′ti.ma. L. fem. adj. *maritima* maritime, marine.

Description as for the genus and Tables 5-1 and 5-2 (1, 8). The properties are based on those of type strain and may not be typical for all members of the species. Growth does not occur on TSA, NA, R2A agar, or in the absence of NaCl. Hydrolyzes aesculin and hypoxanthine but not casein, chitin, DNA, gelatin, starch, Tween 80, L-tyrosine, urea, or xanthine. Does not produce

bacteriochlorophyll *a* or hydrogen sulfide. In MOF medium, produces acids from cellobiose, D-galactose, sucrose, and D-xylose but not L-arabinose, D-fructose, D-glucose, *myo*-inositol, lactose, maltose, D-mannitol, D-mannose, melezitose, melibiose, raffinose, L-rhamnose, D-ribose, D-sorbitol, or trehalose. In assays with the API 20NE and API 20E system, only aesculin hydrolysis, *p*-nitrophenyl-β-D-galactopyranoside (PNPG) test, and citrate utilization are positive. Cannot assimilate any of the substrates in the ID32 GN gallery. In assays with the API ZYM system, the reactions are positive for acid phosphatase, alkaline phosphatase, esterase (C4), esterase lipase (C8), β-glucosidase, leucine arylamidase, and naphthol-AS-BI-phosphohydrolase and weakly positive for α-glucosidase and valine arylamidase. The reactions are negative for α-chymotrypsin, cystine arylamidase, α-fucosidase, α-galactosidase, β-galactosidase, *N*-acetyl-β-glucosaminidase, β-glucuronidase, lipase (C14), α-mannosidase, and trypsin. Susceptible to ampicillin, benzylpenicillin, carbenicillin, cephazolin, cephalothin, chloramphenicol, erythromycin, gentamycin, kanamycin, neomycin, novobiocin, oleandomycin, ofloxacin, oxacillin, penicillin G, rifampicin, streptomycin, and vancomycin but resistant to doxycycline, lincomycin, nalidixic acid, polymyxin B, and tetracycline.

DNA G + C content (mol %): 53.4 (genome).

Type strain: KMM 9530 (=NRIC 0919=JCM 19807= DSM 101533).

Basonym: *Loktanella maritima*.

GenBank accession (16S rRNA gene): AB894236.

GenBank accession (genome): GCA_003003285.

5. *Yoonia ponticola* comb. nov. (*Loktanella ponticola* Jung et al. 2014)

pon.ti′co.la. L. n. *pontus* the sea; L. suff. *-cola* (from L. n. *incola*) a dweller, inhabitant; N.L. fem. n. *ponticola* a dweller of sea

Description as for the genus and Tables 5-1 and 5-2 (9). Mg^{2+} ions are not required for growth. The predominant isoprenoid quinone is Q10. Minor amounts of Q-8 (3.5%) and Q-9 (4.2%) are also present. Hydrolyzes aesculin, hypoxanthine, L-tyrosine, and xanthine (weakly) but not agar, casein, gelatin, starch, Tween 80, or urea. Produces acids from L-arabinose (weakly), D-galactose, and D-mannitol but not cellobiose, D-fructose, D-glucose, *myo*-inositol, lactose, maltose, D-mannose, melezitose, melibiose, raffinose, L-rhamnose, D-ribose, D-sorbitol, sucrose, trehalose, or D-xylose. In assays with the API ZYM system, the reactions are positive for acid phosphatase, alkaline phosphatase, esterase (C4), esterase lipase (C8), and β-galactosidase and weakly positive for *N*-acetyl-β-glucosaminidase and leucine arylamidase. The reactions are negative for α-chymotrypsin, cystine arylamidase, α-fucosidase, α-galactosidase, α -glucosidase, β-glucosidase, β-glucuronidase, lipase (C14), α-mannosidase, naphthol-AS-BI-phosphohydrolase, trypsin, and valine arylamidase. Susceptible to ampicillin, benzylpenicillin, cephalothin, chloramphenicol, gentamicin, kanamycin, neomycin, novobiocin, oleandomycin, penicillin G, polymyxin B, streptomycin, and tetracycline but resistant to lincomycin.

DNA G + C content (mol %): 55.45 (LC).

Type strain: W-SW2 (=KCTC 42133=NBRC 110409).

GenBank accession (16S rRNA gene): KJ855314.

IMG accession (genome): 2828431062.

6. *Yoonia rosea* Wirth and Whitman 2018^{VP} (*Loktanella rosea* Ivanova et al. 2005).

ro.se′a. L. fem. adj. *rosea* rose-colored or rosy, referring to the pinkish color of the colonies.

Description as for the genus and Tables 5-1 and 5-2 (1, 3, 7). The properties are based on those of type strain and may not be typical for all members of the species. Na^{+} or seawater is required for growth. Growth does not occur on TSA or NA. Diffusible pigments have not been detected

on any of the media tested. Hydrolyzes aesculin and hypoxanthine but not agar, casein, chitin, DNA, gelatin, laminarin, starch, urea, or xanthine. There are conflicting results for Tween 80. Does not produce indole, hydrogen sulfide, poly-β-hydroxybutyrate, or acetoin. Negative for arginine dihydrolase, hemolysis, lysine decarboxylase, and ornithine decarboxylase. On BM agar, utilizes acetate, L-arabinose, alaninamide, L-alanylglycine, cellobiose, citrate, D-fructose, D-galactose, D-glucose, glucuronamide, L-malate, maltose, pyruvate, succinate, and D-xylose as sole energy and carbon sources but not benzoate, formate, L-glutamate, D-mannose, salicin, sucrose, or trehalose. In MOF medium, produces acids from L-arabinose and D-fructose, but not from cellobiose, D-galactose, D-glucose, *myo*-inositol, lactose, maltose, D-mannitol, D-mannose, melezitose, melibiose, raffinose, L-rhamnose, D-ribose, D-sorbitol, sucrose, trehalose, or D-xylose. In assays with the API ZYM system, the reactions are positive for alkaline phosphatase (weak), esterase (C4), esterase lipase (C8), β-glucosidase, leucine arylamidase, and naphthol-AS-BI-phosphohydrolase. The reactions are negative for α-chymotrypsin, cystine arylamidase, α-fucosidase, α-galactosidase, β-galactosidase, *N*-acetyl-β-glucosaminidase, α-glucosidase, β-glucuronidase, lipase (C14), α-mannosidase, trypsin, and valine arylamidase. There are conflicting results for acid phosphatase. Susceptible to ampicillin, benzylpenicillin, carbenicillin, cephazolin, cephalothin, chloramphenicol, doxycycline, erythromycin, gentamycin, kanamycin, nalidixic acid, neomycin, novobiocin, oleandomycin, oxacillin, ofloxacin, penicillin G, rifampicin, streptomycin, tetracycline, and vancomycin but resistant to lincomycin and polymyxin B.

DNA G + C content (mol %): 57.7 (genome).

Type strain: Fg36 (=DSM 29591=KMM 6003= CIP 107851= LMG 22534).

Basonym: *Loktanella rosea*.

GenBank accession (16S rRNA gene): AY682199.

GenBank accession (genome): GCA_900156505.

7. *Yoonia sediminilitoris* Wirth and Whitman 2018^{VP} (*Loktanella sediminilitoris* Park et al. 2013).

se.di.mi.ni.li′to.ris. L. neut. n. *sedimeninis*, -inis sediment; L. neut . n. *litus -oris* the seashore, beach; N.L. gen. n. *sediminilitoris* of sediment, of seashore.

Description as for the genus and Tables 5-1 and 5-2 (1, 6). The properties are based on those of the type strain and may not be typical for all members of the species. Mg^{2+} is required for growth. Hydrolyzes aesculin, DNA, and Tweens 20, 40, 60, and 80 but not agar, casein, chitin, gelatin, hypoxanthine, starch, L-tyrosine, urea, or xanthine. Produces hydrogen sulfide. On BM, utilizes acetate, L-arabinose, cellobiose, D-fructose, D-galactose, D-glucose, L-malate, D-mannose, sucrose, and D-xylose as sole energy and carbon sources but not benzoate, citrate, formate, L-glutamate, maltose, pyruvate, salicin, succinate, and trelahose. In MOF medium, does not produce acid from L-arabinose, cellobiose, D-fructose, D-galactose, D-glucose, *myo*-inositol, lactose, maltose, D-mannitol, D-mannose, melezitose, melibiose, raffinose, L-rhamnose, D-ribose, D-sorbitol, sucrose, trehalose, or D-xylose. In assays with the API ZYM system, the reactions are positive for alkaline phosphatase, esterase (C4), esterase lipase (C8), and trypsin. The reactions are negative for acid phosphatase, α-chymotrypsin, cystine arylamidase, α-fucosidase, α-galactosidase, β-galactosidase, *N*-acetyl-β-glucosaminidase, β-glucosidase, β-glucuronidase, leucine arylamidase, lipase (C14), α-mannosidase, naphthol-AS-BI-phosphohydrolase, and valine arylamidase. There are conflicting results for α-glucosidase. Susceptible to ampicillin, benzylpenicillin, carbenicillin, cephazolin, cephalothin, chloramphenicol, doxycycline, erythromycin, gentamycin, kanamycin, neomycin, novobiocin,

ofloxacin, oleandomycin, oxacillin, penicillin G, rifampicin, streptomycin, tetracycline, and vancomycin but resistant to lincomycin, nalidixic acid, and polymyxin B.

DNA G + C content (mol %): 57.2 (genome).

Type strain: D1-W3 (=KCTC 32383=CECT 8284=DSM 29955).

Basonym: *Loktanella sediminilitoris*.

GenBank accession (16S rRNA gene): KC311338.

GenBank accession (genome): GCA_003058085.

8. *Yoonia tamlensis* Wirth and Whitman 2018^{VP} (*Loktanella tamlensis* Lee 2012).

tam.len′sis. N.L. fem. adj. *tamlensis* of or belonging to Tamla, the old name of Jeju, Republic of Korea, referring to the site where the type strain was isolated.

Description as for the genus and Tables 5-1 and 5-2 (1, 4, 6). The properties are based on those of type strain and may not be typical for all members of the species. Motile by means of a polar flagellum. Growth does not occur on TSA, NA, or yeast extract-malt extract agar. Diffusible pigments have not been detected on any of the media tested. Hydrolyzes aesculin, carboxymethylcellulose, and starch but not chitin, DNA, gelatin, Tween 80, DL-tyrosine, urea, or xanthine. There are conflicting results for the hydrolysis of casein and hypoxanthine. On BM, utilizes acetate, L-arabinose, cellobiose, citrate, D-fructose, D-galactose, D-glucose, L-malate, maltose, D-mannose, pyruvate, succinate, sucrose, and D-xylose as sole energy and carbon sources but not benzoate, formate, L-glutamate, salicin, or trehalose. In MOF medium, produces acids from D-mannitol and sucrose but not from L-arabinose, cellobiose, D-fructose, D-galactose, D-glucose, *myo*-inositol, lactose, maltose, D-mannose, melezitose, melibiose, raffinose, L-rhamnose, D-ribose, D-sorbitol, trehalose, or D-xylose. In assays with API 20 NE, no growth is observed with any carbohydrates. In assays with API 50 CH, no acid is produced

from any substrate. In assays with the API ZYM system, the reactions are positive for acid phosphatase, alkaline phosphatase, esterase (C4), esterase lipase (C8), β-galactosidase, *N*-acetyl-β-glucosaminidase, and leucine arylamidase. The reactions are negative for α-chymotrypsin, cystine arylamidase, α-fucosidase, α-galactosidase, β-glucosidase, β-glucuronidase, lipase (C14), α-mannosidase, naphthol-AS-BI-phosphohydrolase, trypsin, and valine arylamidase. There are conflicting results for α-glucosidase and hydrogen sulfide production. Susceptible to ampicillin, benzylpenicillin, carbenicillin, cephazolin, cephalothin, chloramphenicol, doxycycline, erythromycin, gentamycin, kanamycin, lincomycin, nalidixic acid, neomycin, novobiocin, ofloxacin, oleandomycin, oxacillin, penicillin G, rifampicin, streptomycin, tetracycline, and vancomycin but resistant to polymyxin B.

DNA G + C content (mol %): 56.9 (genome).

Type strain: SSW-35 (=DSM 26879=KCTC 12722=JCM 14020).

Basonym: *Loktanella tamlensis*.

GenBank accession (16S rRNA gene): DQ533556.

GenBank accession (genome): GCA_900115105.

9. *Yoonia vestfoldensis* Wirth and Whitman 2018^{VP} (*Loktanella vestfoldensis* Van Trappen et al. 2004).

vest.fold.en′sis. N.L. fem. adj. *vestfoldensis* referring to the isolation source, lakes Ace and Pendant, Vestfold Hills, Antarctica.

Description as for the genus and Tables 5-1 and 5-2 (2, 5). Growth occurs on NA (weak), TSA (weak), and R2A agar. Hydrolyzes aesculin, Tween 80, and urea but not agar, casein, DNA, gelatin, starch, or L-tyrosine. In assays of API 20NE system, growth is not observed, and acids are not produced from any carbohydrate. The reactions are negative for gelatinase, hydrogen

sulfide production, indole production, nitrate reduction, and acetoin production. None of the strains show activity for arginine dihydrolase, lysine decarboxylase, ornithine decarboxylase, or tryptophan deaminase. In assays with the API ZYM system, reactions are positive for acid phosphatase, esterase (C4), esterase lipase (C8), and trypsin and weakly positive for alkaline phosphatase, β-galactosidase, α-glucosidase, β-glucosidase, leucine arylamidase, and naphthol-AS-BI-phosphohydrolase. The reactions are negative for α-chymotrypsin, cystine arylamidase, α-fucosidase, α-galactosidase, *N*-acetyl-β-glucosaminidase, β-glucuronidase, lipase (C14), α-mannosidase, and valine arylamidase. The susceptibilities and resistances to antibiotics have not been reported.

DNA G + C content (mol %): 61.8 (genome).

Type strain: LMG 22003 (=CIP 108321= DSM 16212= NBRC 102487).

Basonym: *Loktanella vestfoldensis*.

GenBank accession (16S rRNA gene): AJ582226.

GenBank accession (genome): GCA_000382265.

References

1. Tanaka N, Romanenko LA, Kurilenko VV, Svetashev VI, Kalinovskaya NI, Mikhailov VV. 2014. *Loktanella maritima* sp. nov. isolated from shallow marine sediments. Int J Syst Evol Microbiol 64:2370-2375.
2. Van Trappen S, Mergaert J, Swings J. 2004. *Loktanella salsilacus* gen. nov., sp. nov., *Loktanella fryxellensis* sp. nov. and *Loktanella vestfoldensis* sp. nov., new members of the *Rhodobacter* group, isolated from microbial mats in Antarctic lakes. Int J Syst Evol Microbiol 54:1263-1269.
3. Yoon JH, Jung YT, Lee JS. 2013. *Loktanella litorea* sp. nov., isolated from seawater. Int J Syst Evol Microbiol 63:175-180.
4. Lee SD. 2012. *Loktanella tamlensis* sp. nov., isolated from seawater. Int J Syst Evol Microbiol 62:586-590.
5. Yoon JH, Kang SJ, Lee SY, Oh TK. 2007. *Loktanella maricola* sp. nov., isolated from seawater of the East Sea in Korea. Int J Syst Evol Microbiol 57:1799-1802.
6. Park S, Jung YT, Yoon JH. 2013. *Loktanella sediminilitoris* sp. nov., isolated from tidal flat sediment. Int J Syst Evol Microbiol 63:4118-4123.
7. Ivanova EP, Zhukova NV, Lysenko AM, Gorshkova NM, Sergeev AF, Mikhailov VV, Bowman JP. 2005. *Loktanella agnita* sp. nov. and *Loktanella rosea* sp. nov., from the north-west Pacific Ocean Int J Syst Evol Microbiol 55:2203-2207.
8. Park S, Choi SJ, Won SM, Yoon JH. 2017. *Loktanella acticola* sp. nov., isolated from seawater. Int J Syst Evol Microbiol Microbiology 67:4175-4180.
9. Jung YT, Park S, Park JM, Yoon JH. 2014. *Loktanella ponticola* sp. nov., isolated from seawater. Int J Syst Evol Microbiol 64:3717-3723.

10. Van Trappen S, Mergaert J, Van Eygen S, Dawyndt P, Cnockaert MC, Swings J. 2002. Diversity of 746 heterotrophic bacteria isolated from microbial mats from ten Antarctic lakes. Syst Appl Microbiol 25:603-610.

11. Romanenko LA, Schumann P, Rohde M, Mikhailov VV, Stackebrandt E. 2004. *Reinekea marinisedimentorum* gen. nov., sp. nov., a novel *gamma-Proteobacterium* from marine coastal sediments. Int J Syst Evol Microbiol 54:669-673.

12. Ivanova EP, Kiprianova EA, Mikhailov VV, Levanova GF, Garagulya AD, Gorshkova NM, Yumoto N, Yoshikawa S. 1996. Characterization and identification of marine *Alteromonas nigrifaciens* strains and emendation of the description. Int J Syst Evol Microbiol 46:223-228.

13. Ivanova EP, Nedashkovskaya OI, Sawabe T, Zhukova NV, Frolova GM, Nicolau DV, Mikhailov VV, Bowman JP. 2004. *Shewanella affinis* sp. nov., isolated from marine invertebrates. Int J Syst Evol Microbiol 54:1089-1093.

14. Bruns A, Rohde M, Berthe-Corti L. 2001. *Muricauda ruestringensis* gen. nov., sp. nov., a facultatively anaerobic, appendaged bacterium from German North Sea intertidal sediment. Int J Syst Evol Microbiol 51:1997-2006.

15. Baumann P, Baumann L. 1981. The marine gram-negative eubacteria: genera *Photobacterium, Beneckea, Alteromonas, Pseudomonas,* and *Alcaligenes,* p1302-1331. *In* Starr MP, Stolp H, Trüper hg, Balows A, Schlegel (ed), The Prokaryotes. Springer, Verlag Berlin.

16. Cohen-Bazire G, Sistrom W, Stanier R. 1957. Kinetic studies of pigment synthesis by non-sulfur purple bacteria. J Cell Comp Physiol 49:25-68.

17. Staley JT. 1968. *Prosthecomicrobium* and *Ancalomicrobium*: new prosthecate freshwater bacteria. J Bacteriol 95:1921-1942.

18. Wirth JS, Whitman WB. 2018. Phylogenomic analyses of a clade within the roseobacter group suggest taxonomic reassignments of species of the genera *Aestuariivita*, *Citreicella*, *Loktanella*, *Nautella*, *Pelagibaca*, *Ruegeria*, *Thalassobius*, *Thiobacimonas* and *Tropicibacter*, and the proposal of six novel genera. Int J Syst Evol Microbiol 68:2393-2411.

19. Buchan A, González JM, Moran MA. 2005. Overview of the marine *Roseobacter* lineage. Appl Environ Microbiol 71:5665-5677.

20. Breider S, Scheuner C, Schumann P, Fiebig A, Petersen J, Pradella S, Klenk HP, Brinkhoff T, Goker M. 2014. Genome-scale data suggest reclassifications in the *Leisingera-Phaeobacter* cluster including proposals for *Sedimentitalea* gen. nov. and *Pseudophaeobacter* gen. nov. Front Microbiol 5:416.

21. Hördt A, López MG, Meier-Kolthoff JP, Schleuning M, Weinhold LM, Tindall BJ, Gronow S, Kyrpides N, Woyke T, Göker M. (2020) Analysis of 1,000+ type-strain genomes substantially improves taxonomic classification of *Alphaproteobacteria*. Front Microbiol 11: 468.

22. Leifson E. 1963. Determination of carbohydrate metabolism of marine bacteria. J Bacteriol 85:1183.

23. Nguyen L-T, Schmidt HA, Von Haeseler A, Minh BQ. 2015. IQ-TREE: a fast and effective stochastic algorithm for estimating maximum-likelihood phylogenies. Mol Biol Evol 32:268-274.

24. Kalyaanamoorthy S, Minh BQ, Wong TK, von Haeseler A, Jermiin LS. 2017. ModelFinder: fast model selection for accurate phylogenetic estimates. Nat Methods 14:587-589.

25. Arkin AP, Cottingham RW, Henry CS, Harris NL, Stevens RL, Maslov S, Dehal P, Ware D, Perez F, Canon S, Sneddon MW, Henderson ML, Riehl WJ, Murphy-Olson D, Chan SY, Kamimura RT, Kumari S, Drake MM, Brettin TS, Glass EM, Chivian D, Gunter D, Weston DJ, Allen BH, Baumohl J, Best AA, Bowen B, Brenner SE, Bun CC, Chandonia J-M, Chia J-M, Colasanti R, Conrad N, Davis JJ, Davison BH, Dejongh M, Devoid S, Dietrich E, Dubchak I, Edirisinghe JN, Fang G, Faria J, Frybarger PM, Gerlach W, Gerstein M, Greiner A, Gurtowski V, Haun HL, He F, Jain R, Joachimiak MP, Keegan KP, Kondo S, Kumar V, Land ML, Meyer F, Mills M, Novichkov PS, Oh T, Olsen GJ, Olson R, Parrello B, Pasternak S, Pearson E, Poon SS, Price GA, Ramakrishnan S, Ranjan P, Ronald PC, Schatz MC, Seaver SMD, Shukla M, Sutormin RA, Syed MH, Thomason J, Tintle NL, Wang D, Xia F, Yoo H, Yoo S, Yu D. 2018. KBase: the United States Department of energy systems biology knowledgebase. Nat Biotechnol 36: 566-569.

Table 5-1. Selected characteristics of *Yoonia* species. Species: 1, *Y. acticola*; 2, *Y. litorea*; 3, *Y. maricola*; 4, *Y. maritima*; 5, *Y. ponticola*; 6, *Y. rosea*; 7, *Y. sediminilitoris*; 8, *Y. tamlensis*; 9, *Y. vestfoldensis*. "+" positive. "-" negative. "ND" no data available.

Characteristic	**1**	**2**	**3**	**4**	**5**
Morphology	coccus, ovoids or rods	rods	rods	ovoids or short rods	coccus, ovoids or rods
Cell size (µm)	0.4-1.2×>0.4	0.4-0.8×0.8-5.5	0.3-0.6×0.8-3.0	0.6-0.8×1.6-2.0	0.2-0.7×0.4-7.0
Motility	-	-	-	-	-
Flagellation	-	-	-	-	-
Carbon source [a]					
Carbohydrates	ND	+	+	ND	ND
Carboxylic acids	ND	+	+	ND	BD
Catalase	+	+	+	+	+
Oxidase	+	+	+	+	+
Growth ranges (optimum)					
Temperature (ºC)	4-30 (25)	15-37 (30)	4-34 (25)	4-36 (28-30)	4-30 (25)
Salinity (% w/v NaCl)	0-8 (2-3)	0.5-6 (2)	0.5-7	2-8 (3-4)	0.5-6 (2)
pH	6-8 (7-8)	6-8 (7-8)	5.5-8 (7-8)	5.5-9 (6.5-7.5)	5.5-8 (7-8)
Nitrate reduction	-	-	-	-	-
Polar lipids identified	+	+	+	+	+
Major fatty acids	$C_{18:1}\omega 7c$	$C_{18:1}\omega 7c$	$C_{18:1}\omega 7c$	$C_{18:1}\omega 7c$	$C_{18:1}\omega 7c$
Major quinone	Q-10	Q-10	Q-10	Q-10	Q-10
API ZYM determined	+	+	+	+	+
Isolation habitat	seawater	seawater	seawater	shallow sediment	seawater
References	8	3	5	1	9

Table 5-1 (continued).

Characteristic	**6**	**7**	**8**	**9**
Morphology	rods	rods	short rods	short rods
Cell size (µm)	0.7-0.9 in diameter	0.4-0.8×0.9-4.0	0.7×1.1-1.7	<1×3-4
Motility	-	-	+	-
Flagellation	-	-	polar	-

Carbon source [a]				
Carbohydrates	+	+	+	ND
Carboxylic acids	+	+	+	ND
Catalase	+	+	+	+
Oxidase	+	+	+	+
Growth ranges (optimum)				
Temperature (ºC)	4-35 (25)	10-35 (25)	4-30 (25-30)	5-37 (25)
Salinity (% w/v NaCl)	1-12	0-5 (2)	1-6	0-10 (0-5)
pH	6-10 (7.5-8)	5.5-8 (7-8)	7-10 (7-8)	ND
Nitrate reduction	-	-	-	-
Polar lipids identified	+	+	+	-
Major fatty acids	$C_{18:1}\omega 7c$	$C_{18:1}\omega 7c$	$C_{18:1}\omega 7c$	$C_{18:1}\omega 7c$
Major quinone	Q-10	Q-10	Q-10	Q-10
API ZYM determined	+	+	+	+
Isolation habitat	marine sediment	tidal flat sediment	surface seawater	microbial mat
References	3, 7	6	1, 4, 6	2

[a]Results based upon tests described in detail in the species descriptions.

Table 5-2. Selected characteristics distinguishing of *Yoonia* species. Species: 1, *Y. acticola*; 2, *Y. litorea*; 3, *Y. maricola*; 4, *Y. maritima*; 5, *Y. ponticola*; 6, *Y. rosea*; 7, *Y. sediminilitoris*; 8, *Y. tamlensis*; 9, *Y. vestfoldensis*. "+" positive or weakly positive. "-" negative. "ND" no data available. "v" conflicting results were reported.

Characteristic	**1**	**2**	**3**	**4**	**5**
Hydrolysis of					
aesculin	+	+	v	+	+
agar	-	-	-	ND	-
casein	-	-	-	-	-
DNA	ND	ND	-	-	ND
hypoxanthine	+	+	+	+	ND
starch	-	-	-	-	-
tyrosine	-	-	-	-	+
Tween 80	+	-	v	-	-
xanthine	-	-	-	-	+
urea	-	-	-	-	-
Utilization of					
L-arabinose	ND	-	+	ND	ND
citrate	ND	-	+	ND	ND
D-fructose	ND	-	+	ND	ND
maltose	ND	+	-	ND	ND
D-mannose	ND	+	-	ND	ND
pyruvate	ND	+	+	ND	ND
succinate	ND	+	+	ND	ND
sucrose	ND	+	-	ND	ND
trehalose	ND	+	-	ND	ND
D-xylose	ND	-	-	ND	ND
Acid production from					
L-arabinose	-	+	-	-	+
cellobiose	-	-	-	+	-
D-fructose	+	-	-	-	-
D-galactose	-	-	-	+	+
D-mannitol	+	-	-	-	+
melibiose	-	+	-	-	-
sucrose	-	-	-	+	-
D-xylose	-	-	-	+	-
Polar lipids					

diphosphatidylglycerol	+	-	+	+	+
phosphatidylethanolamine	-	+	-	-	-
unidentified phospholipid	+	-	-	+	+
unidentified aminolipid	+	-	-	+	+
unidentified lipid	-	-	-	+	+
unidentified aminophospholipid	-	-	-	-	-
Enzyme activity					
acid phosphatase	-	+	+	+	+
β-galactosidase	-	-	-	-	+
N-acetyl-β-glucosaminidase	-	-	-	-	+
α-glucosidase	-	-	-	+	-
β-glucosidase	-	-	-	-	-
leucine arylamidase	+	-	+	+	+
naphthol-AS-BI-phosphohydrolase	+	+	v	+	-
trypsin	-	-	-	-	-
valine arylamidase	-	-	-	+	-
Antibiotics susceptibility					
ampicillin	+	-	+	+	+
doxycycline	ND	ND	+	-	ND
kanamycin	+	-	+	+	+
lincomycin	-	-	+	-	-
nalidixic acid	ND	ND	+	-	ND
neomycin	+	-	+	+	+
penicillin G	+	-	+	+	+
polymyxin B	-	-	-	-	+
streptomycin	+	-	+	+	+
tetracycline	+	-	+	-	+
References	8	3	1, 3, 5	1, 8	9

Table 5-2 (continued).

Characteristic	**6**	**7**	**8**	**9**
Hydrolysis of				
aesculin	+	+	v	+
agar	-	-	+	-
casein	-	-	v	-
DNA	-	+	-	-
hypoxanthine	+	-	v	ND
starch	-	-	+	-
tyrosine	+	-	-	-

Tween 80	v	+	-	+
xanthine	-	-	-	-
urea	-	-	-	+
Utilization of				
L-arabinose	+	+	+	ND
citrate	+	-	+	ND
D-fructose	+	+	+	ND
maltose	+	-	+	ND
D-mannose	-	+	+	ND
pyruvate	+	-	+	ND
succinate	+	-	+	ND
sucrose	-	+	+	ND
trehalose	-	-	-	ND
D-xylose	+	+	+	ND
Acid production from				
L-arabinose	+	-	-	ND
cellobiose	-	-	-	ND
D-fructose	+	-	-	ND
D-galactose	-	-	-	ND
D-mannitol	-	-	+	ND
melibiose	-	-	-	ND
sucrose	-	-	+	ND
D-xylose	-	-	-	ND
Polar lipids				
diphosphatidylglycerol	+	+	+	ND
phosphatidylethanolamine	+	+	+	ND
unidentified phospholipid	+	+	+	ND
unidentified aminolipid	+	+	-	ND
unidentified lipid	+	+	+	ND
unidentified aminophospholipid	-	+	-	ND
Enzyme activity				
acid phosphatase	v	-	+	+
β-galactosidase	-	-	+	+
N-acetyl-β-glucosaminidase	-	-	+	-
α-glucosidase	-	v	v	+
β-glucosidase	-	-	-	+
leucine arylamidase	+	-	+	+
naphthol-AS-BI-phosphohydrolase	+	-	-	+
trypsin	-	+	-	+
valine arylamidase	-	-	-	-

Antibiotics susceptibility				
ampicillin	+	+	+	ND
doxycycline	+	+	+	ND
kanamycin	+	+	+	ND
lincomycin	-	-	+	ND
nalidixic acid	+	-	+	ND
neomycin	+	+	+	ND
penicillin G	+	+	+	ND
polymyxin B	-	-	-	ND
streptomycin	+	+	+	ND
tetracycline	+	+	+	ND
References	1, 3, 7	1, 6	1, 4, 6	2, 5

Table 5-3. Cellular fatty acids in the *Yoonia* species. Species: 1, *Y. acticola*; 2, *Y. litorea*; 3, *Y. maricola*; 4, *Y. maritima*; 5, *Y. ponticola*; 6, *Y. rosea*; 7, *Y. sediminilitoris*; 8, *Y. tamlensis*; 9, *Y. vestfoldensis*. Values for *Y. vestfoldensis* are the averages of four strains. The remaining values are for the type strains. "-" no data available or not detected.

Fatty acids	**1**[a]	**2**	**3**	**4**	**5**
$C_{16:0}$	6.5	5.3	3.9	5.8	4.6
$C_{17:0}$	<0.5	0.8	0.7	2.3	<0.5
$C_{18:0}$	1.9	2.4	2.9	1.4	<0.5
$C_{18:2}$	-	-	-	3.4	-
iso-$C_{17:0}$ 3-OH	-	-	1.3	-	-
iso-$C_{20:0}$	-	0.8	-	-	-
$C_{10:0}$ 3-OH	1.7	2.8	-	3.1	1.2
$C_{12:1}$ 3-OH	3.4	-	2.9	2.5	3.6
$C_{16:1}\omega 7c$	-	-	-	0.5	-
$C_{17:1}\omega 6c$	<0.5	-	-	-	-
$C_{17:1}\omega 8c$	<0.5	0.4		1.1	-
$C_{18:1}\omega 7c$	73.6	67.5	75.9	77.0	79.1
$C_{18:1}\omega 9c$	0.7	-	-	-	-
11-methyl $C_{18:1}\omega 7c$	8.7	17.2	10.2	2.6	2.4
Summed feature 3[b]	1.2	1.1		-	-
Summed feature 7[c]	1.1	1.4	-	-	<0.5
Unknown 11.799	-	-	-	-	-
References	8	3	5	1	9

Table 5-3 (continued).

Fatty acids	**6**	**7**	**8**	**9**
$C_{16:0}$	7.9	13.6	6.98	2.9±0.7
$C_{17:0}$	0.9	-	0.55	-
$C_{18:0}$	2.3	8.2	1.25	1.8±0.3
$C_{18:2}$	-	-	1.65	-
iso-$C_{17:0}$ 3-OH	-	-	-	-
iso-$C_{20:0}$	-	-	-	-
$C_{10:0}$ 3-OH	2.1	3.0	3.29	6.1±1.5
$C_{12:1}$ 3-OH	4.4	5.8	1.95	5.6±1.4
$C_{16:1}\omega 7c$	-	-	1.92	-
$C_{17:1}\omega 6c$	-	-	-	-
$C_{17:1}\omega 8c$	-	-	-	-

$C_{18:1}\omega 7c$	81.2	69.3	75.21	74.1±3.1
$C_{18:1}\omega 9c$	-	-	-	-
11-methyl $C_{18:1}\omega 7c$	13.5	-	4.56	1.9±0.8
Summed feature 3[b]	1.0	-	-	-
Summed feature 7[c]	-	-	-	4.7±0.7
Unknown 11.799	-	-	-	2.3±1.2
References	3	6	1	2

[a]Data from cells cultivated for 5 days.

[b]Summed feature 3 comprises iso-$C_{15:0}$ 2-OH and/or $C_{16:1}\omega 7c$.

[c]Summed feature 7 comprises $C_{19:1}\omega 6c$ and/or $C_{19:0}\omega 10c$ cyclo and/or unknown ELC 18.846.

Table 5-4. Genome sequences for the *Yoonia* species. All genomes were downloaded from NCBI (https://www.ncbi.nlm.nih.gov) or IMG (https://img.jgi.doe.gov).

Strain	Assembly level	Genome size (Mbp)	Number of PEG[a]	Number of REG[b]
Y. litorea DPG-5^T	Contig	3.32	3252	47
Y. maricola DSW-18^T	Contig	3.80	3727	46
Y. maritima KMM 9530^T	Scaffold	3.68	3544	48
Y. ponticola W-SW2^T	Scaffold	3.73	3705	53
Y. rosea Fg36^T	Contig	3.51	3471	48
Y. sediminilitoris D1-W3^T	Scaffold	4.67	4328	49
Y. tamlensis SSW-35^T	Scaffold	3.19	3161	51
Y. vestfoldensis LMG 2200 3^T	Scaffold	3.72	3654	60
Y. vestfoldensis SKA53	Complete	3.99	3856	53

Table 5-4 (continued).

Strain	Number of scaffolds	Number of contigs	GenBank assembly
Y. litorea DPG-5^T	8	8	GCA_900114675
Y. maricola DSW-18^T	7	7	GCA_002797915
Y. maritima KMM 9530^T	26	27	GCA_003003285
Y. ponticola W-SW2^T	30	NR[c]	2828431062[d]
Y. rosea Fg36^T	5	5	GCA_900156505
Y. sediminilitoris D1-W3^T	49	50	GCA_003058085
Y. tamlensis SSW-35^T	7	9	GCA_900115105
Y. vestfoldensis LMG 2200 3^T	45	49	GCA_000382265
Y. vestfoldensis SKA53	3	3	GCA_002158905

[a]Predicted protein-encoding genes (PEG).

[b]Predicted stable RNA-encoding genes (REG).

[d]Not reported.

[e]IMG identification number.

Table 5-5. Characteristics distinguishing of *Yoonia* from closely related genera. Genera: 1, *Yoonia*; 2, *Cognatiyoonia*; 3, *Flavimaricola*; 4, *Limimaricola*; 5, *Loktanella*. "+" all species are positive or weakly positive. "-" all species are negative. "d" one or more but not all of the species are positive or weakly positive.

Characteristic	**1**	**2**	**3**	**4**	**5**
Nitrate reduction	-	d	+	d	d
API ZYM					
α-chymotrypsin	-	d	-	d	-
cystine arylamidase	-	d	-	d	-
esterase (C4)	+	+	+	+	d
α-galactosidase	-	-	+	d	d
β-glucuronidase	-	-	-	-	d
lipase (C14)	-	-	-	d	-
Hydrolyze					
gelatin	-	+	-	-	-

Figure 5-1. Phylogeny of *Yoonia* and *Cognatiyoonia species.* Whole genome sequences were downloaded from NCBI (https://www.ncbi.nlm.nih.gov/) or IMG (https://img.jgi.doe.gov) and subjected to phylogenomic analyses as previously described (18). The maximum-likelihood tree was constructed based on the core-genes using IQTree version 1.6.3 with the best model (LG+F+I+G4) identified by Bayesian information criterion and 100 bootstrap replicates (23, 24). The root is the other genomes of the related roseobacters. The genome of *Y. acticola* is not available and not included in the tree. Bolded taxa indicate the type species of the genera *Yoonia* and *Cognatiyoonia*. The scale bar indicates the number of substitutions per site.

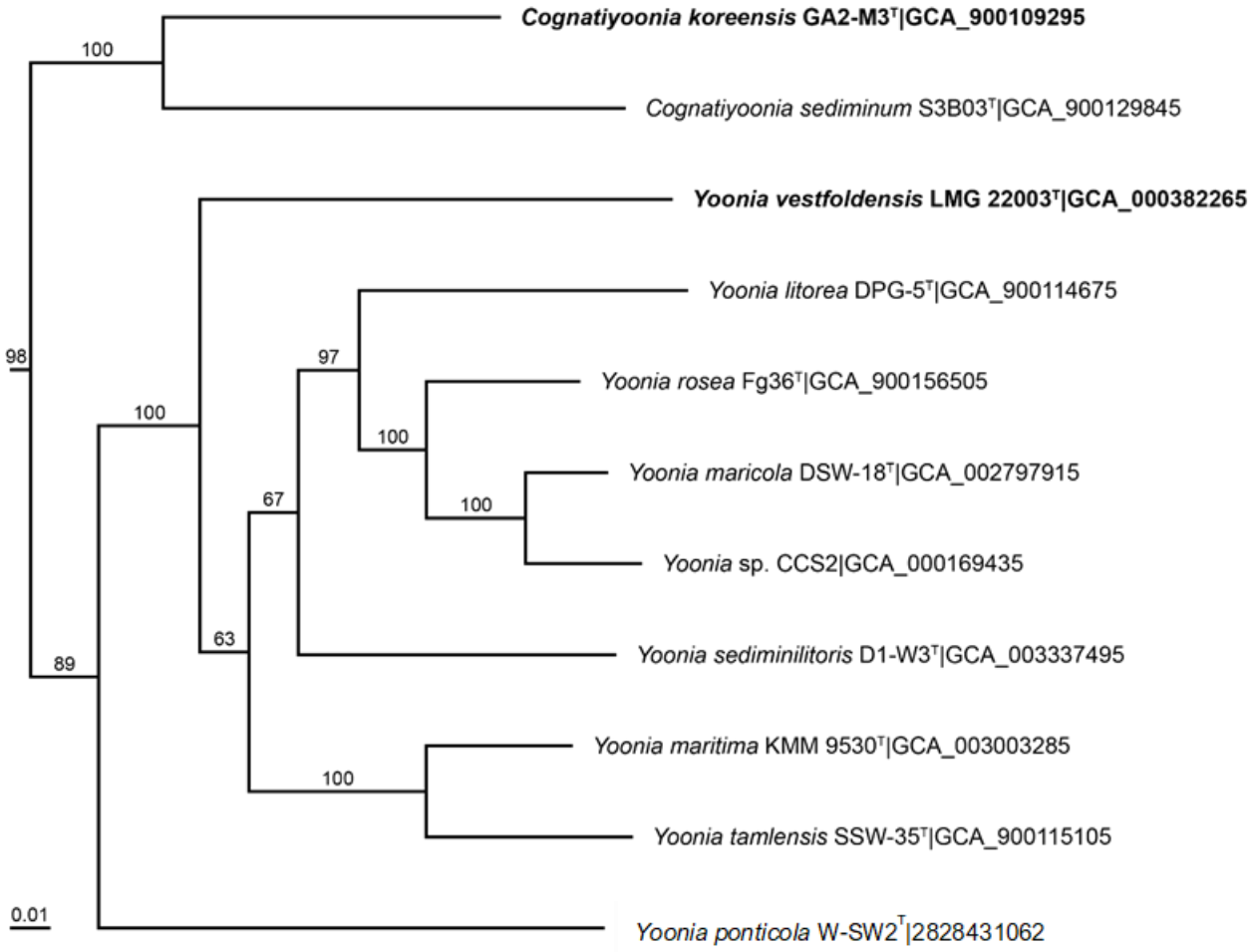

Figure 5-2. Pangenome analysis of *Yoonia* and *Cognatiyoonia species.* The pangenome analysis was performed with KBase platform, by using Genome Comparison SDK version 0.07 and kb_phylogenomics version 1.4.0 for core, partial pangenome and singleton genes calculation (26). The phylogenetic tree in Figure 5-1 was pruned to remove *Yoonia* sp. CCS2 which was not included in this analysis. The node number in the tree indicates the corresponding set of species involved in each set. Core, ortholog sets whose members are found in all the collected genome. Partial pangenome, ortholog clusters present in more than one genome and fewer than all. Singleton, genes with no sequence homology in any other genomes.

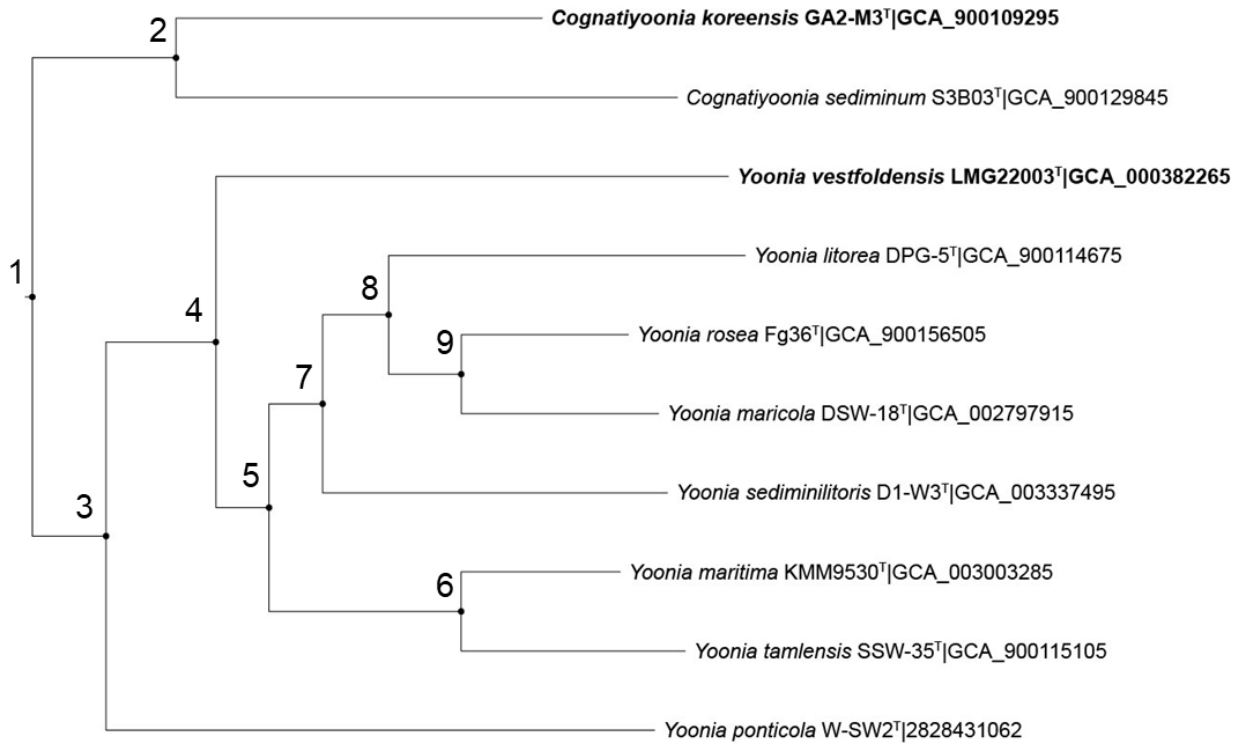

Node number	1	2	3	4	5	6	7	8	9
Core	1317	1912	1436	1568	1621	2287	1879	2067	2456
Partial pangenome	2989	0	2512	2221	2003	0	1113	612	0
Singleton	8984	2823	7340	6194	5381	2013	4254	2828	2155

CHAPTER 6

CONCLUSIONS

1. DMSP acts as an antioxidant in *R. pomeroyi*.

The antioxidant role of DMSP has been reported for about 20 years and tested in algae, corals, and higher plants. To my best knowledge, prior to our experiments in Chapter 2, there was no similar study done in bacteria with direct treatment of ROS. With the modified chemostat system, we can constantly and continuously treat *R. pomeroyi* wild-type and a catalase deletion mutant, *ΔkatG* strain, with H_2O_2 and minimize the abiotic degradation caused by the medium components.

For wild-type, catalase is a powerful tool to resist H_2O_2, whose activity was quickly upregulated after exposure. As a result, no H_2O_2 was detected in the outflow throughout the experiment. The original catalase activity was lower when DMSP was available in the absence of added H_2O_2, suggesting DMSP alleviated the oxidative stress faced. When catalase is deleted, the *ΔkatG* strain faces inherent oxidative stress as the poor growth ability and high expression level of repair genes showed. When *ΔkatG* strain was treated by 0.1 mM H_2O_2, one tenth of the concentration for wild-type, there was about 5% of H_2O_2 remaining in the outflow, confirming the presence of strong oxidative stress. But when DMSP was added, the H_2O_2 in outflow dropped back to background level. All these results confirm the antioxidant role of DMSP is present in bacteria as well.

2. The interaction between the two DMSP catabolic pathways in *R. pomeroyi*.

Unlike other DMSP producers or consumers, bacteria are the only known group of organisms that can utilize DMSP via both the cleavage and demethylation pathway. The widespread MeSH oxidase MtoX plays an important role in sulfur assimilation as it coverts MeSH to sulfide. But this process also produces H_2O_2, resulting in oxidative stress. As DMSP cleavage is reported to be an antioxidant system, the production of H_2O_2 should lead to the upregulation of the cleavage pathway. Although in Chapter 2, no significant difference in DMS and MeSH production was detected before and after adding H_2O_2, the transcriptional analysis showed the upregulation of *dddW* and *dddD*, and downregulation of *dmdA*, *dmdC1*, *dmdD*, and *mtoX* in both strains. Similarly, higher expression of *dddD* and *dddW*, and lower expression of *mtoX* were observed when comparing *ΔkatG* strain to the wild-type without treatment with H_2O_2. These results confirmed that under oxidative stress, *R. pomeroyi* lowers demethylation pathway activity to avoid the further production of H_2O_2 but increases the cleavage pathway activity to produce more DMS and acrylate.

Acryloyl-CoA is a strong electrophilic compound produced downstream of the cleavage pathway, and has to be converted to other compounds such as propionyl-CoA to avoid cellular toxicity. In the *R. pomeroyi* genome, the acryloyl-CoA reductase gene *acuI* is located right downstream of *dmdA* and these two genes are co-regulated. Previous studies and our data have reported that acrylate treatment will lead to a stimulus of MeSH production, indicating that high activity of cleavage pathway causes increased activity of demethylation pathway. Thus, both DMSP catabolic pathways produce harmful products, which will upregulate the other pathway for detoxification. As a result, the two pathways are likely to drive a positive feedback and keep both pathways upregulated with increasing DMSP concentrations.

3. DMSP is the preferred sulfur source compared to sulfate for *R. pomeroyi*.

In our previous experiment studying the assimilation of DMSP sulfur, it was found that even when the available DMSP concentration was only about 1 µM, more than 90% of cellular sulfur was assimilated from DMSP rather than sulfate, whose concentration was about 14 mM in the medium. In Chapter 2, the significant downregulation of sulfate reduction genes *cysH* and *cysJI* when DMSP was present also supported findings that DMSP was the preferred sulfur source compared to sulfate. In addition, under this condition, *mtoX* was one of the most upregulated genes, which agreed with the previous result that more DMSP sulfur was assimilated in the form of sulfide rather than MeSH. When H_2O_2 was added, it restricted the expression of *dmdD* and *mtoX*, but the expression level of these two genes were still higher than during grow on glucose. The expression of *cysH* and *cysJI* remained low as well. These findings show that when there is oxidative stress, DMSP will still be demethylated for a sulfur source, even though this could lead to more H_2O_2.

4. DmdC1 has minimal adaptations for DMSP catabolism.

DmdC catalyzes the third step of the demethylation pathway, and it shares sequence and structural similarity to acyl-CoA dehydrogenases involved in fatty acid metabolism. It has been proposed that the steps of DMSP demethylation may have evolved about 250 million years ago, when DMSP likely first become abundant, by recruiting existing enzymes through specific adaptations. To address this question for DmdC, in Chapter 3, *dmdC1* gene was recombinantly expressed to study its substrate specificity and sensitivity to a variety of potential effectors. DmdC1 possessed a broad substrate specificity with good activity towards MMPA-CoA and straight-chain C4-C8 acyl-CoAs. However, DmdC1 was insensitive to DMSP, MMPA, ATP, and

ADP, which may regulate the demethylation pathway. Thus, DmdC1 is likely to be a short-chain acyl-CoA dehydrogenase with modification to decrease the substrate specificty to include MMPA-CoA. Compared to other enzymes of the demethylation pathway, DmdC1 has only minimal adapations to DMSP metabolism.

5. Reclassification of *Lotanella acticola* and *Loktanella ponticola* into the genus *Yoonia*.

Though the reclassification by Wirth et al., 16 species in the genus *Loktanella* were moved into novel genera including *Cognatiyoonia*, *Flavimaricola*, *Limimaricola*, and *Yoonia* based on whole-genome sequences, core-gene average amino acid identity, percent of conserved proteins and phenotypic data. *Loktanella acticola* and *Loktanella ponticola* were not included in this reclassification because they were isolated after this time or there was no genome sequence available, respectively (Chapter 4 and Chapter 5). *L. ponticola* remained in the genus *Loktanella* as there is no clear evidence supporting to move it into another genus. Recently, the genome for *L. ponticola* has become available. By reevaluating the phylogeny, *L. ponticola* was moved into the genus *Yoonia*, as it was a deep lineage associated with *Yoonia*, and no data clearly indicate it should be reclassified into a novel genus. Although there is no genome sequence for *L. acticola*, the high 16S rRNA sequence similarity and DNA-DNA hybridization percentage to *Yoonia* species supports the reclassification of it into the genus *Yoonia*. Currently, there are 4 and 9 species in the genus *Loktanella* and *Yoonia* respectively.

APPENDIX A

CHAPTER 2 SUPPLEMENTARY INFORMATION[1]

Table S2-1. Primers used for generating pCR2.1 deletion vector. Restriction sites are in bold.

Primers	Sequences
*tetAR*_F SpeI	5'-**ACTAGT**ACCGTATTACCGCCTTTGAGTGAG-3'
*tetAR*_R XhoI	5'-**CTCGAG**ACGCTGAGTGCGCTTCAAATCATC-3'
*katG*_Up_Fwd HindIII	5'-GACCATGATTACGCC**AAGCTT**GGACACCAACATGCCCAG-3'
*katG*_Up_Rev SpeI	5'-GGCGGTAATACGGT**ACTAGT**CAGCACCAGAAAGAACCGG-3'
*katG*_Down_Fwd XhoI	5'-AGCGCACTCAGCGT**CTCGAG**GACCTAGGCCGCGCGTCCCG-3'
*katG*_Down_Rev XbaI	5'-GGGCGAATTGGGCCC**TCTAGA**CTGGGCATGTTGGTGTCC-3'

Table S2-2. H_2O_2 stability in culture media[1]. The abiotic controls were setup following the routine chemostat procedure except that the chemostats were not inoculated. The maximum volume was 144 ml. The flowrates of medium and air were 0.1 and 3 ml min^{-1}, respectively.

H_2O_2 added	1000	1000	100	100
DMSP added[2]	0	250±16	0	250±16
H_2O_2 in outflow[3]	606±54	704±26	49±3	66±5
DMSP in outflow[4]	0	231±20	0	233±19

[1]All values are reported in micromolar.

[2]The DMSP concentration added was the average of 6 measurements at the beginning and the end of the experiment. The 95% confidence intervals are indicated.

[3]The concentration is the average detected from day 3 to day 5 after adding H_2O_2 (n=9), when the concentration was stable. The 95% confidence intervals are indicated. In the absence of added H_2O_2, the concentration measured was <0.5 µM.

[4]The amount of DMSP in outflow was measured in triplicates at the end of the experiment. The 95% confidence intervals are indicated.

Table S2-3. Summary of sequencing data including the number of reads and indicators of their quality. Sample abbreviations are defined in Figure 2-2, with the number indicating the replicate.

Sample	Raw reads (M)	Effective rate (%)	Q30 (%)	GC (%)	Overall alignment rate (%)
W1	9.706	98.10	94.27	62.64	98.06
W2	11.170	97.71	94.97	63.55	97.68
W3	11.967	96.85	95.07	63.02	95.21
WH1	9.569	97.19	96.13	63.00	99.63
WH2	9.977	96.76	95.90	63.13	99.62
WH3	9.705	97.28	95.91	62.81	98.64
WD1[1]	10.198	99.25	93.94	66.78	99.57
WD2	14.037	98.33	94.04	63.70	99.00
WD3	12.162	99.11	93.91	63.46	100.00
WDH1	11.159	98.77	93.62	65.39	98.93
WDH2	10.276	99.00	94.35	65.82	99.18
WDH3	12.441	98.95	93.70	63.61	98.28
K1	11.742	97.46	95.18	61.79	82.22
K2	13.889	95.36	95.15	63.72	99.12
K3	14.848	98.57	94.69	64.50	99.13
KH1	11.661	98.48	93.33	64.92	98.84
KH2	12.218	98.68	93.08	65.86	98.95
KH3	12.448	98.45	93.35	63.59	98.88
KD1[2]	10.688	99.07	95.05	64.93	99.40
KD2	13.053	99.20	93.68	64.24	99.07
KD3	11.926	99.31	93.81	63.16	98.60
KDH1	13.657	99.39	93.59	66.05	99.25
KDH2	14.674	99.30	93.36	65.31	99.37
KDH3	13.852	99.60	93.69	66.31	99.50

[1]Sample dropped during analysis.

[2]Data contained contaminating reads from *E.coli*, which were removed during the analysis.

Table S2-4. Comparison of replicates and determination of batch effects. To calculate the distance between samples, the counts were transformed by regularized-logarithm transformation (rlog). Sample abbreviations are defined in Figure 2-2, with the number indicating the replicate. NA: not applicable.

Sample	Chemostat batch	Sequencing batch	Distance to replicate 1	Distance to replicate 2
W1	A	5	NA	37
W2*	A’	5	37	NA
W3*	A’	5	43	24
WH1*	A	4	NA	12
WH2*	A	4	12	NA
WH3*	A	4	49	47
WD1	B	3	NA	65
WD2	B	3	65	NA
WD3	B	2	71	14
WDH1	B	3	NA	60
WDH2	B	3	60	NA
WDH3	B	2	37	47
K1*	C’	5	NA	15
K2*	C’	5	15	NA
K3	C	5	56	56
KH1	C	3	NA	43
KH2	C	3	43	NA
KH3	C	3	24	48
KD1	D	1	NA	39
KD2	D	2	39	NA
KD3	D	2	45	17
KDH1	D	2	NA	21
KDH2	D	2	21	NA
KDH3	D	2	11	28

*: sample cleaned by RNA Clean & Concentrator kit.

’: backup chemostat for makeup samples.

Table S2-5. Number of differentially expressed genes in each comparison with adjusted p values <0.1. Abbreviations for growth conditions are defined in Figure 2. Conditions in parentheses are controls for each comparison. The mean count for all genes under all conditions was 1 or greater.

	K(W)	WH(W)	KH(K)	WD(W)	KD(K)
Upregulated	73	65	360	634	775
Downregulated	20	97	422	793	862
Outlier[1]	52	24	26	8	19

Table S2-5 (continued).

	KD(WD)	WDH (WD)	KDH (KD)	WDH (WH)	KDH (KH)
Upregulated	668	869	543	1084	1551
Downregulated	248	325	1417	1055	1514
Outlier[1]	0	0	0	9	0

[1]Detected by Cook's distance.

Table S2-6. Full list of genes selected for analyzing sulfur metabolism and oxidative stress.

Locus tag	Genes	Annotations
		Oxidative stress genes (84)
SPO_RS10675		hydrogen peroxide-inducible genes activator (*oxyR* homologue)
SPO_RS11345		hydrogen peroxide-inducible genes activator (*oxyR* homologue)
SPO_RS20080	*katG*	catalase/peroxidase HPI
SPO_RS00535	*yaaA*	peroxide stress protein YaaA
SPO_RS19660	*trxA*	thioredoxin
SPO_RS17330	*trxA*	thioredoxin
SPO_RS04550	*trxB*	thioredoxin-disulfide reductase
SPO_RS13145		thioredoxin domain-containing protein
SPO_RS04995	*soxW*	thioredoxin family protein
SPO_RS02235		thiol reductase thioredoxin
SPO_RS10235		SufD family Fe-S cluster assembly protein
SPO_RS10240	*sufC*	Fe-S cluster assembly ATPase SufC
SPO_RS10265	*sufB*	Fe-S cluster assembly protein SufB
SPO_RS13285		SUF system Fe-S cluster assembly protein
SPO_RS13290		iron-sulfur cluster assembly accessory protein
SPO_RS06770	gor	glutathione-disulfide reductase
SPO_RS03235		carboxymuconolactone decarboxylase family protein/alkylhydroperoxidase AhpD family core domain protein
SPO_RS03835		carboxymuconolactone decarboxylase family protein/alkylhydroperoxidase AhpD family protein
SPO_RS06395		peroxidase-related enzyme
SPO_RS07105		carboxymuconolactone decarboxylase family protein/alkylhydroperoxidase AhpD family protein
SPO_RS19070		peroxidase-related enzyme
SPO_RS19230		carboxymuconolactone decarboxylase family protein/alkylhydroperoxidase AhpD family protein
SPO_RS00370	*hemH*	protoporphyrin/coproporphyrin ferrochelatase
SPO_RS01680	*ccpA*	cytochrome-c peroxidase
SPO_RS03770		peroxidase
SPO_RS04325		cytochrome-c peroxidase
SPO_RS18990		glutathione peroxidase
SPO_RS20600		di-heme cytochrome c peroxidase family protein/hypothetical protein
SPO_RS21190		methylamine utilization protein MauG/c-type cytochrome
SPO_RS22125		vanadium-dependent haloperoxidase
SPO_RS20725		LysR family transcriptional regulator
SPO_RS04195		LysR family transcriptional regulator
SPO_RS17675		LysR family transcriptional regulator
SPO_RS07845		LysR family transcriptional regulator

SPO_RS16785		hydrogen peroxide-inducible genes activator
SPO_RS21470		LysR family transcriptional regulator
SPO_RS21795		LysR family transcriptional regulator
SPO_RS20665		LysR family transcriptional regulator
SPO_RS01230		LysR family transcriptional regulator
SPO_RS20010	*pcaQ*	pca operon transcription factor PcaQ
SPO_RS12080		LysR family transcriptional regulator
SPO_RS10920	*lexA*	transcriptional repressor LexA,in the response to DNA damage (SOS response)
SPO_RS18960		peroxiredoxin
SPO_RS01605	*soxR*	redox-sensitive transcriptional activator SoxR
SPO_RS04980	*soxR*	winged helix-turn-helix transcriptional regulator
SPO_RS04985	*soxS*	regulatory protein
SPO_RS11860	*sodB*	superoxide dismutase
SPO_RS00070	*msrA*	peptide-methionine (S)-S-oxide reductase MsrA
SPO_RS18980	*msrA*	peptide-methionine (S)-S-oxide reductase MsrA
SPO_RS18985	*msrB*	peptide-methionine (R)-S-oxide reductase MsrB
SPO_RS16560	*msrQ*	protein-methionine-sulfoxide reductase heme-binding subunit MsrQ
SPO_RS16565	*msrP*	protein-methionine-sulfoxide reductase catalytic subunit MsrP
SPO_RS10320	*recA*	recombinase RecA
SPO_RS00775	*recF*	DNA replication/repair protein RecF
SPO_RS08535	*recG*	ATP-dependent DNA helicase RecG
SPO_RS08815	*recJ*	single-stranded-DNA-specific exonuclease RecJ
SPO_RS16190	*recO*	DNA repair protein RecO
SPO_RS18080	*recR*	recombination protein RecR
SPO_RS15785	*ruvB*	Holliday junction branch migration DNA helicase RuvB
SPO_RS15790	*ruvA*	Holliday junction branch migration protein RuvA
SPO_RS15795	*ruvC*	crossover junction endodeoxyribonuclease RuvC
SPO_RS15845	*priA*	primosomal protein N'
SPO_RS19505	*polA*	DNA polymerase I
SPO_RS11250	*uvrA*	excinuclease ABC subunit UvrA
SPO_RS02750	*uvrB*	excinuclease ABC subunit UvrB
SPO_RS18425	*uvrC*	excinuclease ABC subunit UvrC
SPO_RS05950	*uvrD*	UvrD-helicase domain-containing protein
SPO_RS08530	*ligA*	NAD-dependent DNA ligase LigA
SPO_RS10520	mfd	transcription-repair coupling factor
SPO_RS07205		DNA modification methyltransferase
SPO_RS00750	*mutM*	bifunctional DNA-formamidopyrimidine glycosylase/DNA-(apurinic or apyrimidinic site) lyase
SPO_RS17455	*mutY*	A/G-specific adenine glycosylase
SPO_RS00305	*mutT*	8-oxo-dGTP diphosphatase MutT

SPO_RS00055	*mutS*	DNA mismatch repair protein MutS
SPO_RS17030	*mutL*	DNA mismatch repair endonuclease MutL
SPO_RS18140	nth	endonuclease III
SPO_RS12740	xth	exodeoxyribonuclease III
SPO_RS09650	tag	DNA-3-methyladenine glycosylase I
SPO_RS01465	*udgA*	uracil-DNA glycosylase
SPO_RS10785		DNA-3-methyladenine glycosylase 2 family protein
SPO_RS06850	xseA	exodeoxyribonuclease VII large subunit
SPO_RS01270	xseB	exodeoxyribonuclease VII small subunit
SPO_RS10390	zwf	glucose-6-phosphate dehydrogenase
SPO_RS15375	zwf	glucose-6-phosphate dehydrogenase
		Sulfur metabolism genes (39)
SPO_RS00195	*cysQ*	3'(2'),5'-bisphosphate nucleotidase CysQ
SPO_RS11395	*cysK*	pyridoxal-phosphate dependent cysteine synthase A
SPO_RS11400	*cysE*	serine O-acetyltransferase
SPO_RS13360	*cysJI*	nitrite/sulfite reductase
SPO_RS13365	*cysH*	phosphoadenylyl-sulfate reductase
SPO_RS04535	sat	bifunctional sulfate adenylyltransferase/adenylylsulfate kinase
SPO_RS04990	*soxV*	cytochrome C biogenesis protein CcdA
SPO_RS04995	*soxW*	thioredoxin family protein
SPO_RS05000	*soxX*	sulfur oxidation c-type cytochrome SoxX
SPO_RS05005	*soxY*	thiosulfate oxidation carrier protein SoxY
SPO_RS05010	*soxZ*	thiosulfate oxidation carrier complex protein SoxZ
SPO_RS05015	*soxA*	sulfur oxidation c-type cytochrome SoxA
SPO_RS05020	*soxB*	thiosulfohydrolase SoxB
SPO_RS05025	*soxC*	sulfite dehydrogenase, sulfur oxidation molybdopterin C protein
SPO_RS05030	*soxD*	c-type cytochrome
SPO_RS05035	*soxE*	c-type cytochrome
SPO_RS05040	*soxF*	FAD-dependent oxidoreductase
SPO_RS07755	*soxY*	quinoprotein dehydrogenase-associated SoxYZ-like carrier
SPO_RS14335	*soxH*	MBL fold metallo-hydrolase
SPO_RS17005	*soeC*	LysR family transcriptional regulator/membrane-bound sulfite dehydrogenase soeABC
SPO_RS17010	*soeB*	serine/threonine protein phosphatase/membrane-bound sulfite dehydrogenase soeABC
SPO_RS17015	*soeA*	L-threonine 3-dehydrogenase/membrane-bound sulfite dehydrogenase soeABC
SPO_RS18875	*sseA*	3-mercaptopyruvate sulfurtransferase
SPO_RS03405	*tauA*	ABC transporter substrate-binding protein/taurine transporter
SPO_RS03410	*tauB*	ABC transporter ATP-binding protein/taurine transporter
SPO_RS03415	*tauC*	ABC transporter permease subunit/taurine transporter

SPO_RS09100		sulfate/tungstate uptake family ABC transporter, permease protein
SPO_RS09105		ATP-binding cassette domain-containing protein/sulfate/tungstate uptake family ABC transporter
SPO_RS09110		extracellular solute-binding protein/sulfate/tungstate uptake family ABC transporter
SPO_RS09930	*sulP*	sulfate permease
SPO_RS15495	*sulP*	SulP family inorganic anion transporter
SPO_RS09750		cysteine synthase A
SPO_RS08200		NAD(P)/FAD-dependent oxidoreductase/sulfide:quinone oxidoreductase
SPO_RS08800	*metA*	homoserine O-succinyltransferase
SPO_RS06880	*metZ*	O-succinylhomoserine sulfhydrylase
SPO_RS21430	*megL*	methionine gamma-lyase
SPO_RS08355		selenium-binding protein
SPO_RS07295	*metY*	O-acetylhomoserine aminocarboxypropyltransferase/cysteine synthase
SPO_RS09575	bmt	5-methyltetrahydrofolate--homocysteine methyltransferase

Figure S2-1. Chemostat design for H_2O_2 additions. One of the reservoirs contained 160 mM HEPES (pH 6.8), 0.01 mM Fe(III)EDTA, 0.2 % (v/v) trace mineral solution, and 0.2 % (v/v) vitamin solution in general salts solution with carbon sources. The other reservoir contained 1.16 mM KH_2PO_4 solution with the desired H_2O_2 concentration. The stir bars in reservoirs and the culture are not shown.

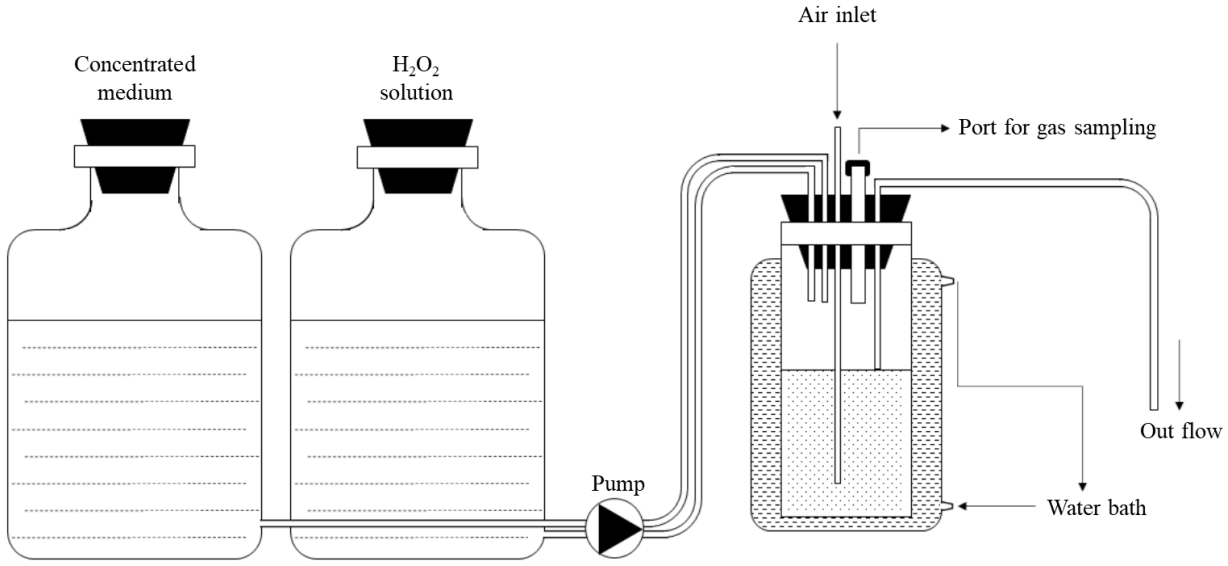

Figure S2-2. Identification of oxidative stress responsive genes. Heatmap of genes likely to play a role in the oxidative stress response in *R. pomeroyi* based upon their annotation and homology to oxidative stress responsive genes in other proteobacteria. Abbreviations are defined in Figure 2-2.

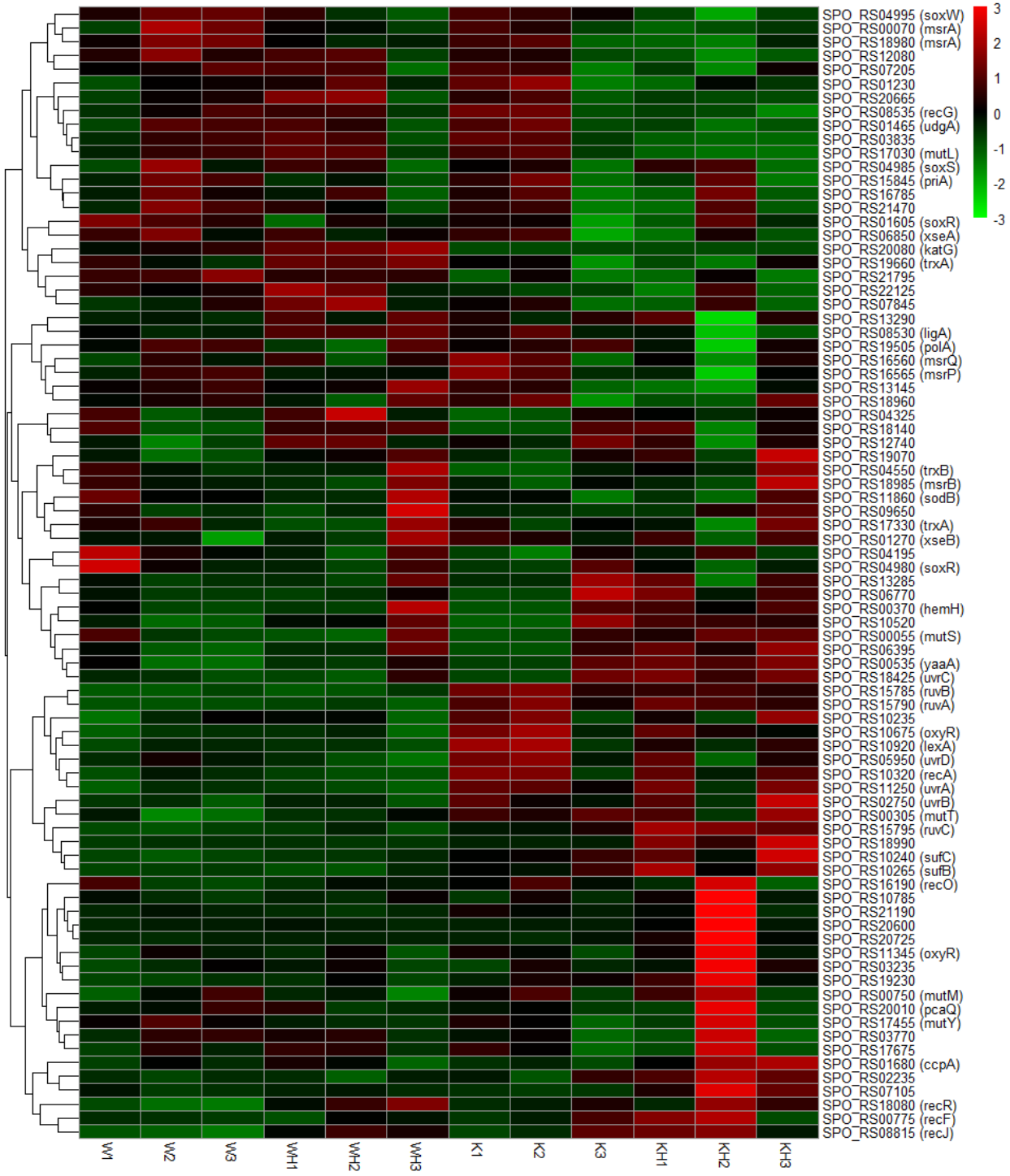
SPO_RS04995 (soxW)
SPO_RS00070 (msrA)
SPO_RS18980 (msrA)
SPO_RS12080
SPO_RS07205
SPO_RS01230
SPO_RS20665
SPO_RS08535 (recG)
SPO_RS01465 (udgA)
SPO_RS03835
SPO_RS17030 (mutL)
SPO_RS04985 (soxS)
SPO_RS15845 (priA)
SPO_RS16785
SPO_RS21470
SPO_RS01605 (soxR)
SPO_RS06850 (xseA)
SPO_RS20080 (katG)
SPO_RS19660 (trxA)
SPO_RS21795
SPO_RS22125
SPO_RS07845
SPO_RS13290
SPO_RS08530 (ligA)
SPO_RS19505 (polA)
SPO_RS16560 (msrQ)
SPO_RS16565 (msrP)
SPO_RS13145
SPO_RS18960
SPO_RS04325
SPO_RS18140
SPO_RS12740
SPO_RS19070
SPO_RS04550 (trxB)
SPO_RS18985 (msrB)
SPO_RS11860 (sodB)
SPO_RS09650
SPO_RS17330 (trxA)
SPO_RS01270 (xseB)
SPO_RS04195
SPO_RS04980 (soxR)
SPO_RS13285
SPO_RS06770
SPO_RS00370 (hemH)
SPO_RS10520
SPO_RS00055 (mutS)
SPO_RS06395
SPO_RS00535 (yaaA)
SPO_RS18425 (uvrC)
SPO_RS15785 (ruvB)
SPO_RS15790 (ruvA)
SPO_RS10235
SPO_RS10675 (oxyR)
SPO_RS10920 (lexA)
SPO_RS05950 (uvrD)
SPO_RS10320 (recA)
SPO_RS11250 (uvrA)
SPO_RS02750 (uvrB)
SPO_RS00305 (mutT)
SPO_RS15795 (ruvC)
SPO_RS18990
SPO_RS10240 (sufC)
SPO_RS10265 (sufB)
SPO_RS16190 (recO)
SPO_RS10785
SPO_RS21190
SPO_RS20600
SPO_RS20725
SPO_RS11345 (oxyR)
SPO_RS03235
SPO_RS19230
SPO_RS00750 (mutM)
SPO_RS20010 (pcaQ)
SPO_RS17455 (mutY)
SPO_RS03770
SPO_RS17675
SPO_RS01680 (ccpA)
SPO_RS02235
SPO_RS07105
SPO_RS18080 (recR)
SPO_RS00775 (recF)
SPO_RS08815 (recJ)
WT1
WT2
WT3
WTH1
WTH2
WTH3
K1
K2
K3
KH1
KH2
KH3
3
2
1
0
-1
-2
-3

APPENDIX B

CHAPTER 3 SUPPLEMENTARY INFORMATION[1]

[1]Wang T, Shi H and Whitman W.B. 2021. *Applied and Environmental Microbiology*. AEM. 01729-21.

Reprinted here with permission of the publisher.

Table S3-1. Purification of the recombinant *R. pomeroyi* DSS-3 DmdC dehydrogenase from *E. coli* BL21(DE3) cells.

Step	Protein (mg)	Activity[a] (μmol min^{-1})	Specific activity (μmol min^{-1} mg^{-1})	Purification fold	Yield (%)
Cell extract	40.6	3.95	0.0973	1	100
Q-Sepharose[b]	1.82	1.39	0.765	7.86	35.2
Phenyl Superose	1.01	0.593	0.587	6.03	15.0
Centrifuge filter	0.896	0.703	0.785	8.69	17.8

[a]Enzyme activity was determined in the standard assay at pH 7.5.

[b]Results after the second Q-Sepharose column.

Table S3-2. Electron acceptors of recombinant RPO_DmdC1 dehydrogenase[a].

Electron acceptors	Specific activity (μmol min^{-1} mg^{-1})
PMS+DCPIP	1.15±0.11
PMS+INT	0.84±0.04
DCPIP	<0.05[b]
FAD	<0.05
FMN	<0.05
NADP	<0.05

[a]Cofactor specificity was determined in the standard assay at pH 7.0 by replacing PMS plus 2,6-dichlorophenol indophenol (DCPIP) with 50 μM PMS plus 200 μM iodonitrotetrazolium violet (INT), 200 μM DCPIP alone, and 200 μM each of FAD, FMN or NADP. Values are the standard deviation calculated from two replicates.

[b]Limits of detection.

Figure S3-1. Purification of the recombinant RPO_DmdC1 expressed in *E. coli* BL21(DE3). SDS-PAGE of the cell extract and after each purification step. Lane 1: broad-range protein marker (New England Biolabs, Cat. No. P7702). Lane 2: cell lysate of *E. coli* BL21(DE3) harboring pET101 without RPO_*dmdC1*. Lane 3: cell lysate of recombinant strain with RPO_DmdC1 induced. Lane 4: RPO_DmdC1 following the first Q-Sepharose column. Lane 5: RPO_DmdC1 following the second Q-Sepharose column. Lane 6: RPO_DmdC1 following the Phenyl Superose column.

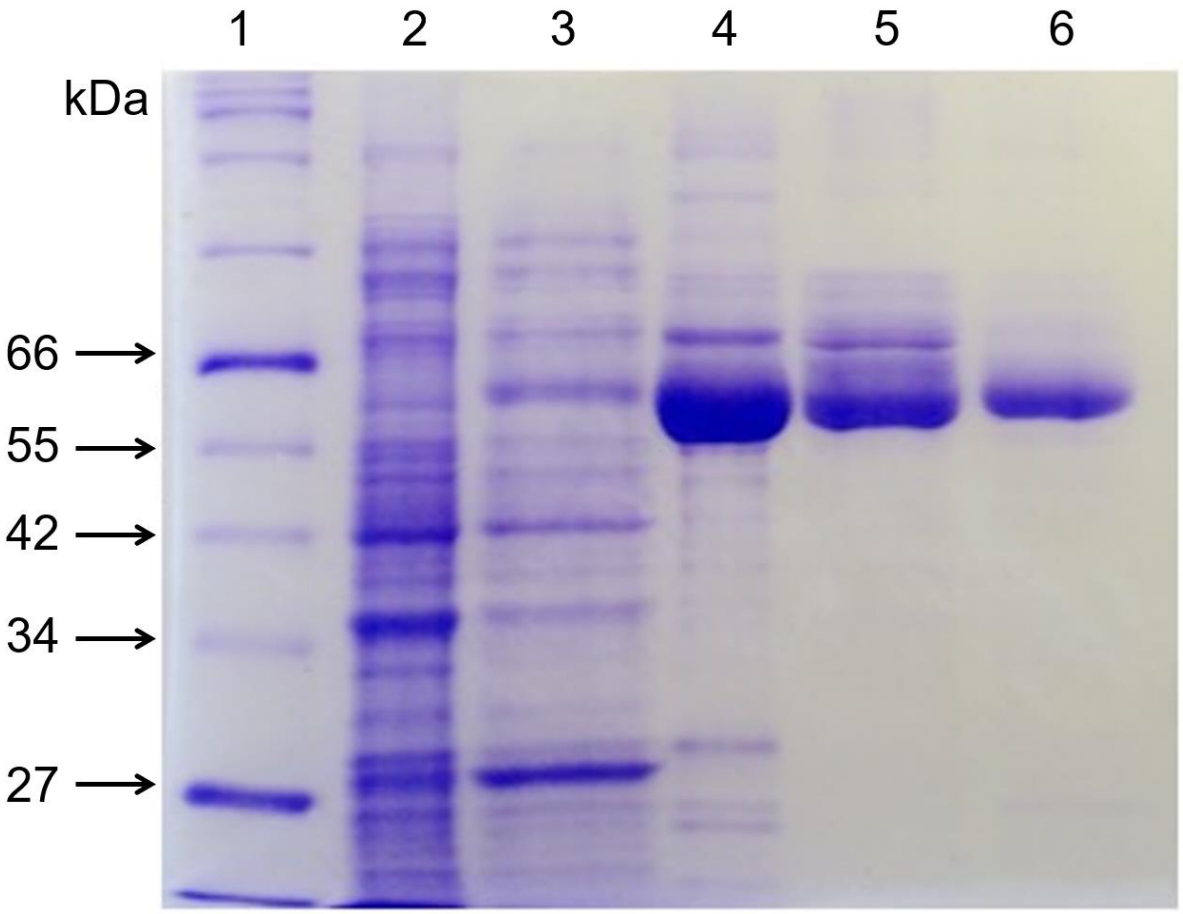

Figure S3-2. Inhibition of recombinant RPO_DmdC1 dehydrogenase activity by 0.4 M salts. The salt effect was tested in the standard assay with 100 mM HEPES-NaOH buffer (pH 6.5) plus addition of the designated salt. The control was without the addition of salt. Standard error bars are the ranges from two replicates.

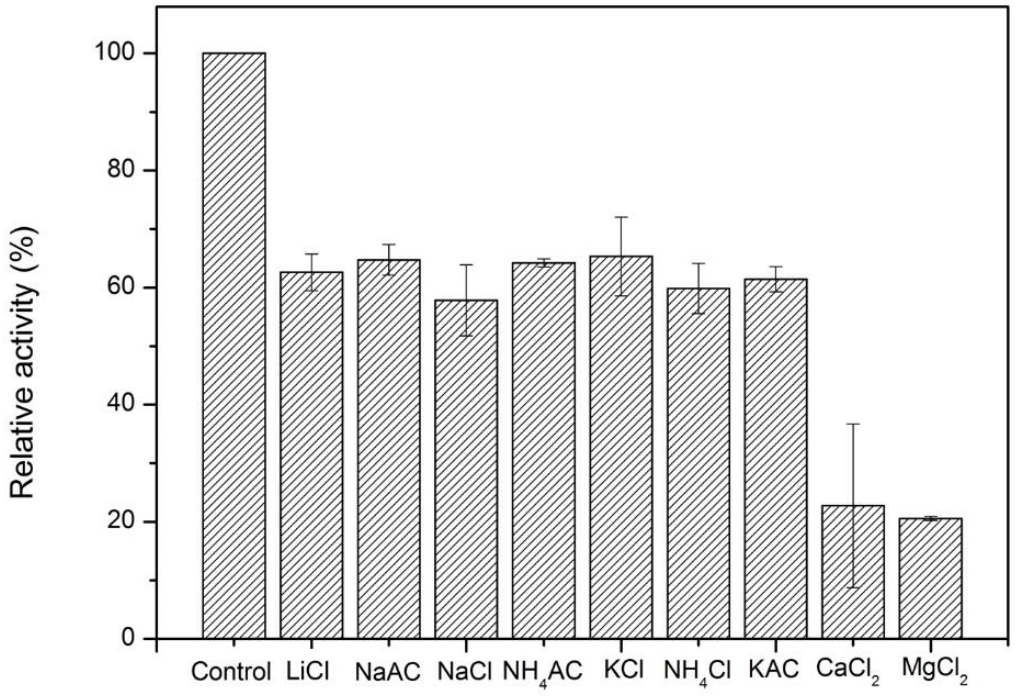

Figure S3-3. Role of potential effectors on RPO_DmdC dehydrogenase activity. Activity was tested in the standard assay at pH 7.0 with 150 µM MMPA-CoA. Standard error bars are the ranges from two replicates. The concentrations of FMN and FAD were 50 µM. The concentration of DMSP was 50 mM. The concentrations of the other compounds were 2 mM.